**Ministry of Higher Education & Scientific Research**
**Ninevah University**
**College of Electronics Engineering**
**Communication Engineering Department**

# Acoustic Tracking System Based on Microphones Array Technique

By

## Abbas Haider Suleiman

**M.Sc. Thesis**

**In**

**Communication Engineering**

**Supervised by**

## Asst. Prof. Dr. Mahmod A. Mahmod

**2022 A.D.**                                    **1443 A.H.**

**Ministry of Higher Education & Scientific Research**
**Ninevah University**
**College of Electronics Engineering**
**Communication Engineering Department**

# Acoustic Tracking System Based on Microphones Array Technique

A dissertation Submitted

By

## Abbas Haider Suleiman

To

The Council of the College of Electronic Engineering

Ninevah University

As a Partial Fulfillment of the Requirements

for the Degree of Master of Science

In

Communication Engineering

Supervised by

## Asst. Prof. Dr. Mahmod A. Mahmod

**2022 A.D.**                                   **1443 A.H.**

بِسْمِ اللهِ الرَّحْمَنِ الرَّحِيمِ

﴿ نَرْفَعُ دَرَجَاتٍ مَّن نَّشَاءُ ۗ وَفَوْقَ كُلِّ ذِي عِلْمٍ عَلِيمٌ ﴾

صَدَقَ اللهُ العَظِيمُ

سورة يوسف – اية76

# Acknowledgments

First and foremost all praise be to Allah who create everything in this world; without His Aid, this dissertation would never have been completed.

I would like to express my profound gratitude and thankfulness to my supervisor (Asst. Prof. Dr. Mahmod A. Mahmod) for his efforts and excellent guidance during the progress of the dissertation.

I should also thank the head of the Communication Engineering Department, all academic, staff, and all postgraduate students for their help and support.

I would also like to thank the Dean of the Electronics Engineering College and his two assistants for their efforts in making the scientific process a success.

Finally, special thanks must go to my family, for their love and unconditional support.

# ABSTRACT

Recently, acoustic source tracking systems have a wide interest. These systems have been used in all applications that can benefit from the audio signal in order to achieve tracking, making them the most important issues in the signal processing and communications fields. The communications systems are recently dependent on the electronic scanning of the radiating lobe, this can be done by the microphones array beamforming system.

In this study, the lobe switching tracking technique was design to achieve an acoustic tracking system. An electronic beam scanning system based on the microphone array is required for this system. With the proposed architecture, a microphone array beamscanning system with fifty seven uniform distance microphones (seven groups of linear array elements) has been designed. An amplitude weighting based on the binomial distribution technique was used to achieve the beanscanning system of the radiation lobe which has no sidelobes component.

The proposed beamscanning system has achieved a scanning span between 30 to 150 degrees with two degrees intervals at a scanning angle of about 20 degrees in each case. This proposed beamscaning system was a main part in implementing the acoustic tracking system using MATLAB (ver. 2019) software. The proposed acoustic tracking system achieved tracking, with deviation from the center of the scan zone in the range of 0 to 5%. Due to the use of the amplitude weighting technique in the implementation of the beamscanning system.  This deviation appeared because the two sides of the scanning lobes were not identical.

# TABLE OF CONTENTS

# LIST OF FIGURES

# LIST OF TABLES

# LIST OF ABBREVIATIONS

| Abbreviation | Name |
|---|---|
| 5G | Fifth Generation of Communications |
| AEP | Array Element Pattern |
| AF | Array Factor |
| CFDBF | Conventional Frequency Domain Beamforming |

| EHR–CLEAN–SC | Enhanced High-Resolution CLEAN–SC |
|---|---|
| FUNBF | Functional Beamforming |
| GA | Genetic Algorithms |
| GIBF | Generalized Inverse Beamforming |
| GSC | Generalized Sidelobe Canceller |
| HPBW | Half-Power Beamwidth |
| LCMV | Linearly Constrained Minimum Variance |
| LOS | Line of Sight |
| MVDR | Minimum Variance Distortionless Response beamformer |
| SLL | Side Lobe Level |

# LIST OF SYMBOLS

| Symbol | Description |
|---|---|
| $\lambda$ | Wavelength |
| $\nu$ | velocity of sound |
| $f$ | frequency |
| $p(x,t)$ | Sound pressure |
| $p_0$ | Wave amplitude |
| k | Propagation constant |
| $\omega$ | Radial frequency |
| $EP$ | Element Pattern |
| $AF$ | Array Factor |
| $E_\theta$ | Electric field |
| r | The distance from any point on the source to the far point |
| N | Number of array elements |
| $\varphi$ | Phase difference between the elements |
| $\theta$ | Azimuth Angle |
| d | Distance between the array elements |
| $\psi$ | Relative phase |
| m | Number of Radiating Sources |
| HPBW | Half Power Beam Width |
| $D_0$ | Directivity |
| $a_n$ | Excitation amplitude |
| $R_0$ | Sidelobe Ratio |
| P | Integer equal to one less than the number of array elements |

# Chapter One
# Introduction

## 1.1 Background

Acoustics is a branch of science that relates to the topics of mechanical waves in liquids, solids, and gases. It also relates to the transmission, control, and reception of sound. The areas of this branch of science may include sound, infrasound, ultrasound, and vibration. The applications of acoustics vary such as atmosphere, geologic, underwater phenomena, and many aspects of modern society [1].

Acoustics tracking has noticeably become a common tool that is used in detecting moving objects. It is also in the early tracking systems for tracking the movements of marine organisms. This kind of tracking system constitutes equipping individual animals with acoustic transmitters. Then, it is deployed in an underwater array of acoustic receivers aiming at detecting whether an object is in the area. Recently, acoustic tracking systems are used in a variety of applications such as drones, vehicle tracking systems, and tracking sound sources (i.e., lecturer voice tracking in class or with for video recording or tracking for singer or actor in theater for the same purpose, etc. [2].

Tracking of moving objects is typically achieved by using acoustic receivers in certain arrays forms called microphones arrays. Furthermore, a microphone array is an array that includes a number of microphones positioned in specific locations to extract the sound signals in a specific direction and neglect the other unwanted signals in the other directions.

In the context of the working of antennas arrays in wireless communications, the beamforming technique has the ability to capture information in a direction of interest and neglects the information in the other directions [3].

## 1.2    Beamforming Technique

Beamforming is a common technique in the field of signal processing. It is utilized in sensor arrays for performing particular radiation patterns. Achieving spatial selectivity can be performed using beamforming since it is used in receivers or /and transmitters. It is also used in directing the radiation electromagnetic signal to a particular direction of interest. This is done by combining elements in an antenna array in a way that guarantees signals at particular angles experience constructive interference, while others experience destructive interference [4].

The patterns of radiation and lobe direction can be controlled using the radio signals that are applied to antenna elements in the array, where each microphones is fed with the same transmitted signal but the phase and amplitude of the signal fed to each element are adjusted, steering the beam in the desired direction.

It should be mentioned that the beamforming technique is utilized in dealing with sound waves and radio for a variety of purposes. For instance, in the applications of wireless communications, sonar systems, radar systems, astronomy, biomedicine, and seismology.

## 1.3    Beam Steering

It is a technique in which the direction of the main lobe of a radiation pattern changes. This is accomplished by switching the antenna elements or by changing the (phases or amplitude) excitation of the RF signals of the elements.

In the state-of-the-art, the beamsteering technique has significantly contributed to the 5G communication, and this is due to the quasi optic nature of the 5G communication frequencies.

In acoustics, beamsteering is used to extract the signals from the audio source in a specific direction. This is done by changing the (amplitude and/or phase) coefficients for the microphones array installed for this purpose [5].

In the context of antennas, when an array is scanned electrically, it is referred to as a phased array. Beamscanning technique can be performed on this kind of array through using different phases of a) frequency scanning, or b) elements excitations. These two techniques struggled with many implementation issues. Furthermore, beamscanning can be applied through varying the magnitudes of the element's excitations [6].

## 1.4 Literature Review

The literature contains many studies that investigated the topic considered in this dissertation. These studies vary in terms of the problems and issues they consider. The literature tries to address most of the introduced issues and challenges.

One of the oldest studies was performed by Soderman and Noble in 1975, who utilized the end-fire microphone array with digital time delays. In their study, they concentrated on the sources of noise intending to remove the background noise and reverberations in the NASA Ames (40x80) ft. wind tunnel [7].

A year later, Billingsley and Kinns in 1976 study on The Acoustic Telescope. Their design of a telescope comprises a microphone array. It also includes a digital computer for processing the signals and output source distributions. Their study took into considerations position and frequency [8].

About nine years later, Brooks et al. in 1987 investigated a particular issue in a helicopter. In their study, the square array frequency domain beamforming was placed in the helicopter rotor sweep area [9].

Later on, Gramann and Mocio in 1995 studied the issue of adaptive versus conventional beamforming. The purpose of the study was for aeroacoustic measurements in wind tunnels [10].

Furthermore, the beginning of the current century witnessed a lot of works and contributions in this field. Huge signs of progress happened and sophisticated techniques were introduced. The study of Dam et al. in 2003 suggested a new adaptive beamforming employing recursively updated soft constraints for acoustic speech enhancement. In the new approach, the authors operated the beamformer in a subband structure. The reason for this was to consequently permit a time-frequency operation(s) for each channel [11].

Hou and Jia, in the same year developed new recursive soft constrained beamformer with a new adaptive beamforming as well as an exact Finite Impulse Response structure. The proposed adaptive beamformer significantly improves the speech quality while maintaining high noise suppression levels up to 17 dB for real car data [12].

In the same context, three years later, Abad and Javier, in 2007 suggested a Generalized Sidelobe Canceller (GSC) with adaptive beamforming that involved a Wiener filter [13]. Moreover, Qi and Moir in 2007 suggested a new approach that was based on merging three microphones. Also, the noise-canceling system was deeply investigated for the purpose of improving the capabilities of speech recognition in a car driving environment [14].

In addition to the aforementioned studies, Sayidmarie and Jasim in 2007 [15] presented a method of array beamscanning. Their method was based on performing a variation of amplitude excitation. Their approach was applied to an array of three elements. The findings demonstrated a maximum scan angle of (±20˚). Then, in [16] the same authors developed an approach

in linear antennas arrays of amplitude based on beamscanning. Their technique was applied to an array of seven elements and reflected a maximum scan angle of (±13°). They also proved that the Half power beam width (HPBW) of the main beam was increased as long as the beam was scanned far away from the broadside.

Warsitz et al., 2008 developed a new blocking matrix. Their approach depended on a concept that generalizes an eigenvalue problem. The solution of such a problem is considered as an indirect estimation of the transfer functions between a source and sensors [17].

Souden et al. in 2010 investigated the Linearly Constrained Minimum Variance (LCMV) and Minimum Variance Distortionless Response Beamformer (MVDR) Noise Reduction Filters. They used the beamformer to eliminate the interference, preserve the target signal, and decrease the overall mixture energy [18].

Comminiello et al., in 2011 developed an efficient adaptive beamforming technique. The goal of this approach was to enhance the performance of speech applications. Also, the approach was proved as a reliable approach and robust to non-stationary interfering sources in noisy environments [19].

Suleiman et al. in 2011 implemented a real-time noise cancellation for speech signal using least mean square algorithm as well as TMS320C6713 DSP kit for the adaptive filter [20].

The study of Sayidmarie and Saghurchy in 2011 developed an array beamscanning by variation of elements amplitude-only excitations and benchmarked it with the frequency scanning technique [21].

In 2012 Jafar and Sayidmarie suggested an efficient method that was able to cancel the sidelobe aiming at involving the addition of two elements.

One of the elements was at the end of the Monopulse antenna array. The purpose behind this was to produce a cosine pattern that is, in turn, utilized in providing wide-angular nulls [22].

Another study performed by Omar in 2012 who developed a technique based on MATLAB programming and TMS320C6713DSK KIT for implementing an adaptive noise cancellation in a speech signal [23].

In a different study by Tronc et al. in 2013, the authors presented methods for involving beamforming in mobile satellite systems. The study also focused on evaluating the possible advantages and disadvantages of onboard beamforming compared to on-ground beamforming approaches [24].

Bodhe et al. in 2014 utilized rectangular array structure in the beamforming technique that are used in smart antenna applications [25]. In the same context, the researchers Younis et al. in 2015 involved beamforming techniques in radar system applications [26].

Sayidmarie and Abdul-Rahman Shakeeb in 2017 investigate the array beam scanning and switching by varying the amplitude excitations. Their results using two half-wave diploe elements show that the main beam can be scanned $\pm$ 30˚ with the mainbeam magnitude less than 1.8dB [27]. Also in the same authors in 2018 investigate a simple technique to vary the coverage of the base station. Two conventional antennas were used deviating by a certain angle and fed by the same signal but with amplitude varying. It is demonstrated that when varying the excitation of the two antenna elements, the field across the one half of the covered sector can be increased gradually while at the other half is reduced [28].

Other studies dealt with the problem of differential beamforming and microphone arrays of arbitrary planar geometry Huang in 2018. Then, using Jacobi-Anger expansion for estimating the beampattern, an algorithm was

developed to create a frequency-invariant beampattern. The approach also involved a microphone array of planar geometry. In the approach, the coordinates of the sensors were provided as well as the distances among neighboring sensors which were smaller than the minimum wavelength [29].

The most recent studies in the literature such as Grondin et al. in 2019 who studied the interactions between a robot and human in regular environments. Investigating this kind of interaction requires filtering out the different sources of sounds. Performing such an ability requires using microphone arrays in order to track, localize, and differentiate sources of sounds. Multimicrophone signal processing techniques are considered an efficient approach for enhancing the performance towards the noise. However, the cost can be increased in an exponential way due to the microphones used, which are not cheap. The measurement in the work was response time that should be minimized [30].

Another recent study performed by Merino-Martineza et al. in 2020 who evaluated the efficiency of acoustic imaging approaches namely, Functional Beamforming (FUNBF), Conventional Frequency Domain Beamforming (CFDBF), Generalized Inverse Beamforming (GIBF), and Enhanced High-Resolution CLEAN–SC (EHR–CLEAN–SC). The performance was benchmarked the four approaches in terms of accuracy and variability [31].

Finally, Khatami and Jamalabadi in 2021 studied an optimized-microphone array configuration. The study was based on using a bio-inspired method such as the Genetic Algorithm (GA) aiming at enhancing the map resolution of the beamforming output [32].

7

## 1.5 The Aims of the Dissertation

1. Studying the acoustic tracking system using microphones array.
2. Realizing a MATLAB simulation of acoustic tracking system using microphones array.

## 1.6 Research Methodology

The research method followed in this study can be summarized according to the following steps:

**Step_1:  Study and Analysis**

This step includes a study and reviewed the literature and the state-of-the-art topics considered in this thesis including array antennas, microphone array beamforming, and the characteristics of sound.

**Step_2: Simulations**

This step is divided into two portions as follows:

**Part_1**: Simulating the microphone array beam scanning system using MATLAB.

**Part_2**: Simulating the two-dimension acoustic tracking system depending on the designed microphone array beam scanning system using MATLAB.

**Step_3**: Analyzing the obtained results and concluding them.

## 1.7 Dissertation Organization

This dissertation is organized as follows:

- **Chapter One:** Presents an introduction, reviews the literature, the aims, research method steps, and the dissertation organization.
- **Chapter Two:** Provides the required theoretical background of all the topics considered in this dissertation including microphone array beamforming and tracking techniques.

8

- **<u>Chapter Three</u>:** Describes the detailed steps of the design of microphone array beamforming using MATLAB.

- **<u>Chapter Four</u>:** Presents the acoustic tracking system implementation based on microphone array using MATLAB.

- **<u>Chapter Five</u>:** Contains the conclusions and future study suggestions.

# Chapter Two

## Theoretical Background

### 2.1 Overview

In this chapter, theoretical concepts about the topics considered in this thesis have been provided. Also, the required equations and figures that are needed for illustrating the theoretical concepts corresponding to this work such as acoustic, antennas array, beamforming, microphone array beamforming, and tracking systems have been listed.

### 2.2 Sound and Acoustic Waves

The sound signals can be defined as the wave created by the vibrations (within the sound frequency range) of a surface in contact with a flexible medium. These expansions and compressions are then passed to the next layer and so forth, therefore these expansion and compression waves of the medium will surround the area of the vibrating plane. These compressions and expansions of the medium caused the change of pressure at a given spot which creates the sound signal at this given time.

A single tone is heard when the pressure changes in a single sinusoidal fashion. The wavelength of pure sinusoidal sound is the distance between successive crests or troughs of the sinusoid. A sound signal's wavelength is the distance it travels in one cycle of a sinusoid. The following formula can be used to calculate the wavelength of any signal [33]:

$$\lambda = \frac{v}{f} \tag{2.1}$$

Where $\lambda$ is the wavelength in meters, $v$ reflects the velocity of sound in m/s, and $f$ is the frequency of the signal in $Hz$.

Sound velocity is a function of the medium parameters (e.g., temperature, density, steady-state pressure, or other parameters). Sound

travels slowest through the air and the fastest through solids. The sound has a velocity of 344 meters per second in the air at 20°C and 101 kPa normal atmospheric pressure. The amplitude of the signal is another significant feature of sound. For one tone, this is the greatest variation in pressure from the steady-state value. A collection of sinusoids with different frequencies, amplitudes, and phases makes up the sound signals.

A single-tone sound wave may travels in one direction of propagation, this path can be taken in the x-axis' positive direction, while a plane wave is one in which all of the points of equal pressure in the wave are joined to form a plane as shown in Figure (2.1). Plane waves can only be generated in controlled conditions, such as small tubes, and even then, only as a rough approximation. The majority of genuine waves are spherical waves, in which sound waves radiate from the source in all directions. Getting a sphere for such a wave by combining the sites of equal pressure. Also, the curvature of the wave-front is estimated or approximated by a plane, a plane wave can be approximated as a small part of a spherical wave that has traveled over a distance that is sufficient.
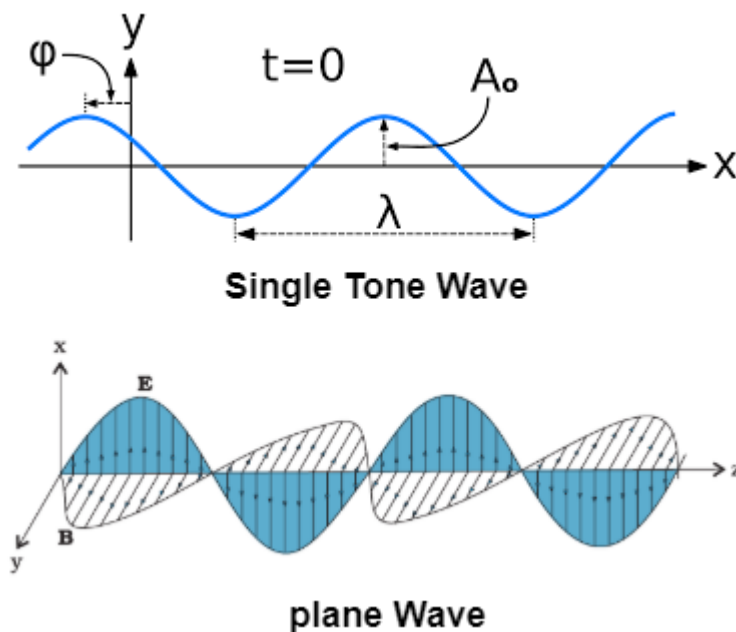


**Figure (2.1):** Single-Tone and plane waves [33].

11

For a plane sound wave, the wave equation is as follows:

$$p(x,t) = p_0 \cos(wt - kx) \tag{2.2}$$

Where $p(x, t)$ represents the sound pressure, which is a function of both time that is denoted by $t$ and spatial locations that is referred by $x$. Also, $\omega$ refers to the radial frequency ($2\pi f$), $p_0$ denotes the amplitude of the wave, and $K$ is the propagation constant given by the following equation [34]:

$$k = \frac{\omega}{v} \tag{2.3}$$

Based on both; Equation (2.1) and Equation (2.3), the relation between the wavelength and propagation constant is described based on the following equation.

$$\lambda = \frac{2\pi}{k} \tag{2.4}$$

## 2.3 Antenna Arrays

Antennas can be organized in a particular pattern of interest such as plane, circle, line, etc. aiming at creating another radiation pattern. Antenna arrays are obtained by configuring more than one antenna (called elements). These elements are arranged and organized to provide a specific radiation pattern. For designing array pattern, numerous array design variables can be adjusted. These variables include the following parameters; element spacing, excitation amplitude and phase, pattern, and a general shape of the element.

Given that we have an array as described above, its pattern of radiation can be obtained based on the pattern multiplication theorem, which can be described as follows: [35]

$$Array\ Pattern = Element\ Pattern(EP) \times Array\ Factor(AF)$$
$$\tag{2.5}$$

Where, EP: the pattern of individual array elements, AF: function that depends on elements' excitation and array's geometry.

### 2.3.1 The Arrays of N-Element

The derivation of the array utilizes what is called Isotropic Radiators. At the origin, the electric field of an isotropic radiator can be expressed as follows [35]:

$$E_\theta = I_0 \frac{e^{-jkr}}{4\pi r} \tag{2.6}$$

Where, $I_0$ is maximum current, $E_\theta$, Electric field and r is the distance from any point on the source to the far field point.

Assuming the array elements that are uniformly-spaced with a separation distance of *d*.

The array elements magnitudes are considered equal. Also, the current on the elements of the array is positioned at the origin and used as the phase reference zero phases [35]:

$$I_1 = I_0 \quad I_2 = I_0 e^{j\varphi_2} \quad I_3 = I_0 e^{j\varphi_3} \quad \dots I_N = I_0 e^{j\varphi_N} \tag{2.7}$$

$$AF = \left[1 + e^{j(\varphi_2 + kd\cos\theta)} + e^{j(\varphi_3 + 2kd\cos\theta)} + \cdots + \right.$$
$$\left. e^{j[\varphi_N + (N-1)kd\cos\theta]}\right] \tag{2.8}$$

Equation (2.8) represents the array factor for an *N-element* linear array with uniform spacing). Where, φ is Phase difference between the elements and Θ is Azimuth Angle [35].

$$r_1 = r$$

$$r_2 \approx r - d \cos \theta$$

$$r_3 \approx r - 2d \cos \theta$$

$$\vdots$$

$$r_N \approx r - (N-1)d \cos \theta$$
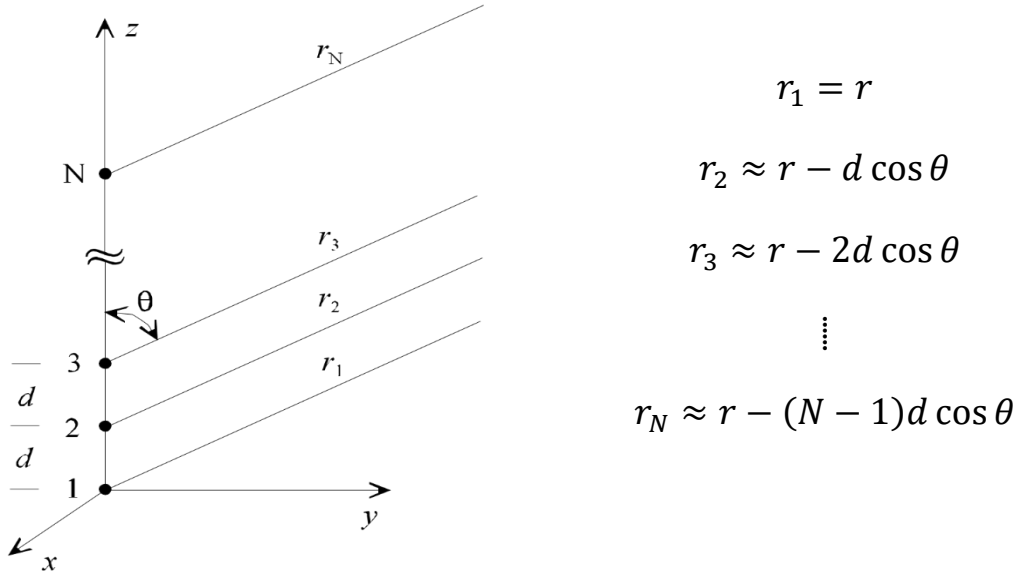
**Figure (2.2):** Far-field geometry of N-element array of isotropic sources positioned along the z-axis.

### 2.3.2 End-Fire/Broadside Arrays

In the case of the uniform linear array elements' phasing is set, if the main lobe of the array pattern is normal to the array axis, it is then called broadside array (main lobe at $\theta = 90°$). When it is along to the array axis, it is called End-fire (main lobe at $\theta = 0°$ or $180°$).

Now, the array factor reaches maximum when having zero for the function of the array phase [35]:

$$\psi = \varphi + kd \cos \theta = 0 \tag{2.9}$$

Where, $\psi$ the relative phase and d is is Distance between the array elements. For a broadside array, to satisfy the above formula with a value of $\theta$ is equal to $90°$, the phase angle should be zero. More precisely, array elements should be driven with the same phase. Also, when the value of $\theta = 0°$, the normalized array factor reduces to:

$$(AF)_n = \frac{1}{N} \frac{\sin\left(\frac{Nkd \cos \theta}{2}\right)}{\sin\left(\frac{kd}{2} \cos \theta\right)} \tag{2.10}$$

The end-fire arrays are constructed to concentrates the main beam in either the value of $\theta$ is $0^o$ or $180^o$ directions along the array axis. Given that the array factor reaches its maximum when: $\psi = \varphi + kd \cos\theta = 0$

To satisfy the above formula with $\theta$ is equal to $0^o$, the phase angle should be:

$$\varphi = -kd \tag{2.11}$$

As for $\theta$ is equal to $180^o$, the phase angle is set to be:

$$\varphi = +kd \tag{2.12}$$

The above description leads to the following formulas [35]:

$$\psi = kd(\cos\theta \mp 1) \qquad \theta = \left\{ \begin{matrix} 0^\circ \\ 180^\circ \end{matrix} \right\} \tag{2.13}$$

For the end-fire array, the normalized array factor becomes as follows [35]:

$$(AF)_n = \frac{1}{N} \frac{\sin\left[\frac{Nkd}{2}(\cos\theta \mp 1)\right]}{\sin\left[\frac{kd}{2}(\cos\theta \mp 1)\right]} \tag{2.14}$$

### 2.3.3 Equally-Spaced/Non-Uniformly Excited Arrays

When an array total length is increased the directivity is improved. This method produces a large number of minor lobes, which are undesirable for the applications of narrow beam. The number of minor lobes in the resultant pattern is increased in the case when (spacing between elements $> \lambda/2$). The highly-demand is to design an array of only main lobe, as per the desire of modern communication, where narrow beams (no minor lobes) are preferable. The ratio of the power density of the main lobe to the power density of the longest minor lobe is termed the side lobe ratio. Tapering, is an approach that can be utilized in decreasing side lobe level. The tapering

principle is most commonly used in broadside arrays, although it can also be used in end-fire arrays. A binomial array is an array of n-isotropic sources with non-equal amplitudes and is a common example of a tapering approach. Also, the amplitude of the radiating sources arc is organized based on the binomial expansion. In the case of minor lobes shown in the array and required to be neglected, the radiating sources should have current amplitudes proportional to the coefficient of binomial series as shown in the following example [35]:

$$(1 + x)^{m-1} = 1 + (m - 1)x + \frac{(m-1)(m-2)}{2!}x^2 + \frac{(m-1)(m-2)(m-3)}{3!}x^3 \pm \cdots \qquad (2.15)$$

Where the number of radiating sources are denoted by *m*.

The aforementioned relationship is equivalent to Pascal's Triangle as shown in figure (2.3). For instance, for the array of 1 to 10 radiating sources, the relative amplitudes can be [35]:

| No. of sources | | | | | Pascal's triangle | | | | | |
|---|---|---|---|---|---|---|---|---|---|---|
| n = 1 | | | | | | 1 | | | | |
| n = 2 | | | | | 1 | | 1 | | | |
| n = 3 | | | | | 1 | 2 | 1 | | | |
| n = 4 | | | | 1 | 3 | | 3 | 1 | | |
| n = 5 | | | 1 | 4 | 6 | | 4 | 1 | | |
| n = 6 | | 1 | 5 | 10 | | 10 | 5 | 1 | | |
| n = 7 | 1 | 6 | 15 | 20 | | 15 | 6 | 1 | | |
| n = 8 | 1 | 7 | 21 | 35 | 35 | 21 | 7 | 1 | | |
| n = 9 | 1 | 8 | 28 | 56 | 70 | 56 | 28 | 8 | 1 | |
| n = 10 | 1 | 9 | 36 | 84 | 126 | 126 | 84 | 36 | 9 | 1 |
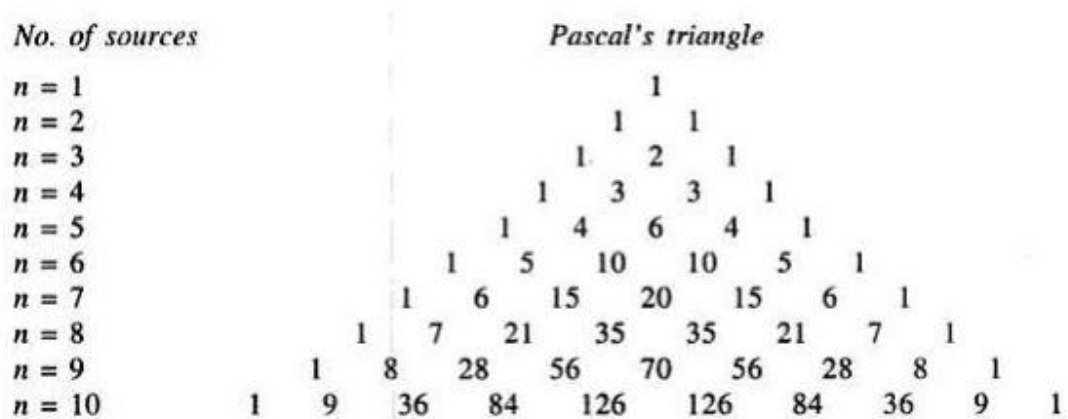
**Figure (2.3):** Pascal's Triangle.

In binomial arrays, the element spacing is ≤ wavelength/2, the HPBW of the array becomes as follows [35]:

$$\text{HPBW} = \frac{1.06}{\sqrt{N-1}} = \frac{1.06}{\sqrt{\frac{2L}{\lambda}}} = \frac{0.75}{\sqrt{L\lambda}} \quad \text{(Radians)} \qquad (2.16)$$

Where, L= (N-1) λ/2

and directivity is formulated as the following equation [35]:

16

$$D_0 = 1.77\sqrt{N} = 1.77\sqrt{1 + 2L\lambda} \tag{2.17}$$

When an identical array of 2-points sources is superimposed one on top of the other, three effective sources with an amplitude ratio of 1:2:1 are emerged. Moreover, when such elements are stacked in a similar way, an array of 4-sources with current amplitudes in the ratio 1:3:3:1 is formed. By replacing n = 3 and 4 in the above expression, the far-field pattern emerges, as shown in Figures 2.4(a) and (b) [35].



(a)



(b)
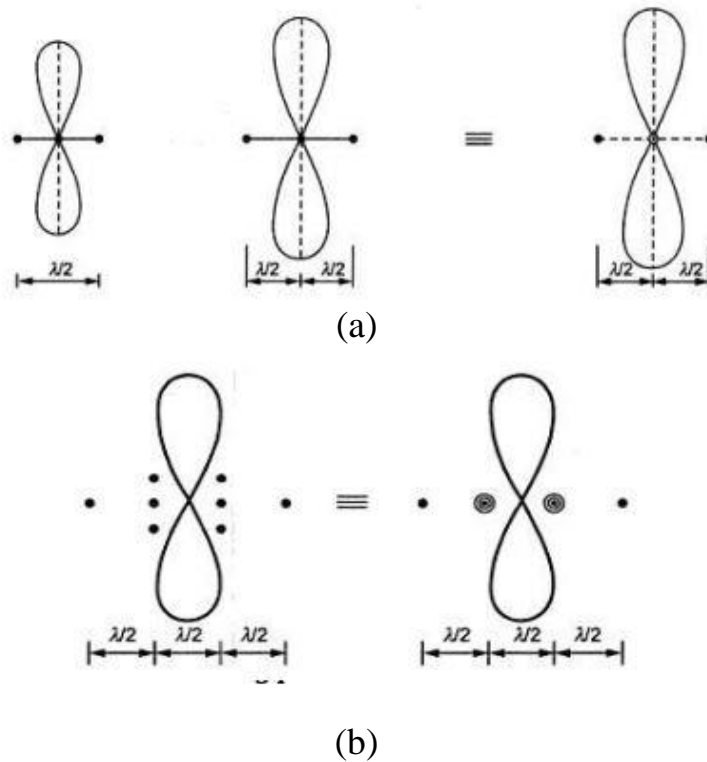
**Figure (2.4):** Radiation pattern of binomial array of (a) 2-element array with amplitude ratio 1:2:1 (b) 3-element array with amplitude ratio 1:3:3:1.

Moreover, binomial arrays provide single-beam radiation at the cost of directivity reduction; given the same length of an array, the directivity is smaller than that of uniform arrays. In other words, secondary lobes appear in a uniform array type, but principal lobes are narrower than in a binomial array type. The main drawbacks of the binomial arrays can be summarized as follows:

- The directivity of the array is reduced.

- Larger current amplitude ratios are required when the length of the array is increased.

### 2.3.4 Array Factor

Consider having an array which is symmetrically positioned isotropic elements (P) along the z-axis. Its factor is calculated taking into considerations that the elements are excited with nonuniform amplitudes and the same current phase ($\theta=0^\circ$ for simplicity).

### 2.3.5 Dolph-Chebyshev Steps of Design

The steps followed in the procedure of Dolph-Chebyshev Design can be as the following [35]:

**Step_1:** Select AF for P elements.

$$(AF)_p = \sum_{n=1}^{M} a_n \cos[(2n-1)u] \qquad p = 2M \ (even)$$

(2.18)

$$(AF)_p = \sum_{n=1}^{M} a_n \cos[2(n-1)u] \qquad p = 2M+1 \ (odd)$$

**Step_2:** In the array, replace each cos(mu) term with its expansion in terms of powers of *cos(u)*.

**Step_3:** Calculate $x_o$ for the needed main lobe to side lobe ratio *(R_o)*:

$$R_0 = T_{P-1}(x_0) = \cosh[(P-1)\cosh^{-1}x_0]$$

$$x_0 = \cosh\left[\frac{\cosh^{-1}R_0}{P-1}\right] \qquad (2.19)$$

Where, P is an integer equal to one less than the number of array elements.

**Step_4:** Substitute $cos(u) = x/x_o$ into the array factor of **Step 2**.

**Step_5:** Equate the array factor of **Step 4** to $T_{P-1}(x)$ and determine the array coefficients.

## 2.4 Beamforming

The radiation patterns from each individual element combine constructively with the neighboring elements aiming at generating an effective pattern of radiation. This pattern transmits energy in the desired direction in phased antenna arrays. At the same time, the antenna array is designed and the signals are forwarded in undesired directions that interfere with each other in a destructive way, causing nulls and side lobes. The overall antenna array system is designed and developed for the purpose of maximizing the radiated energy in the main lobe, whilst limiting the energy in the side lobes to a level that is acceptable and reasonable. The direction of the main lobe, or beam, is controlled by manipulating the radio signals applied to each of the individual antenna elements in the array. Each antenna is fed with the same transmitted signal but the phase and amplitude of the signal fed to each element are adjusted, steering the beam in the desired direction (see Figure 2.5) [36].
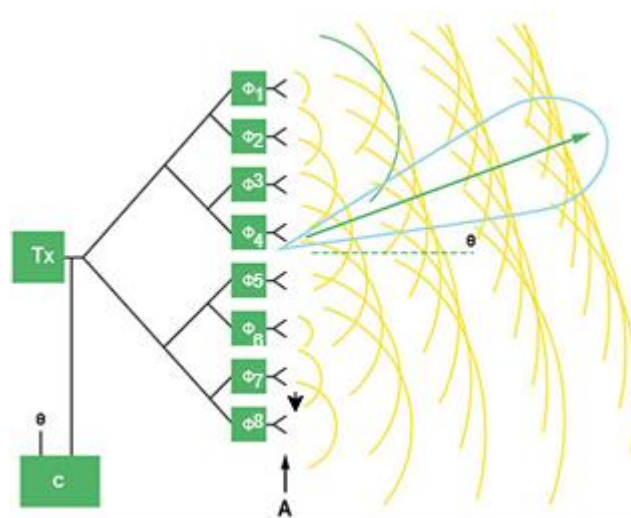


**Figure (2.5):** Phased Array Antenna Systems Enable Beamforming and Steering [36].

Because the amplitude and phase of signals are electronically controlled, correction processes can be vastly performed in nanoseconds, allowing for quick beam steering.

Input signal phase can be changed on all radiating elements for the purpose of generating beam steering. Using phase shifting, the process of targeting the signal can be done at a particular receiver. Using radiation elements, the antenna is able to direct a single beam to a particular direction. In order to support many different users, different frequency beams can be guided in different directions. Moreover, the base station can dynamically find the direction of a signal as the endpoint moves, and hence, it provides an ability to track users. When the beam cannot track a user, the endpoint will be switched to another beam (see Figure (2.6) [37].
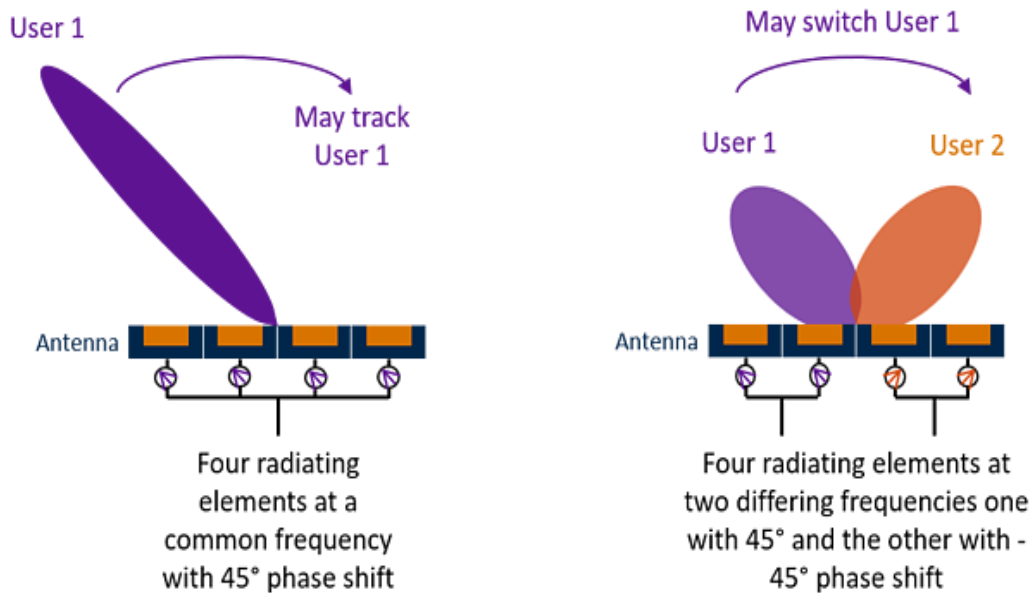


**Figure (2.6):** Beam Steering and Beam Switching [37].

## 2.5 Microphone Array Beamforming

The transmitting and receiving responses are tightly coupled. As known, this feature in acoustics is complicated, their arrays have loudspeaker elements for transmitting purposes and microphone elements for receiving purposes. The recently developed microphone arrays in the literature have become more popular in a variety of our life's devices that have a feature of voice control. Moreover, seeking the physical directions of the sources of sound is related to the physical array configuration. Also, the classic beamforming applications needs the directional responses of the embedded elements across the desired spectrum. Two or more spaced devices (antennas, microphones) with similar responses and orientations are generally classified as an array (important for antennas that are polarized, or any elements with directionality). This allows calculating the directional array response by multiplying an array factor with a response of a single element. A stand-alone (single) element can be omnidirectional, the element pattern is rarely omnidirectional after it is incorporated in an array structure due to mutual interaction, and the wave scattering of the platform supporting the array. The precise numerical modeling for calculating embedded patterns is possible. Although microphone mutual coupling appears to be minimal, compared to antennas, this is not the case with microphone arrays. The platform has vibrational coupling, which influences the embedded patterns. Mutual coupling may become crucial for compact arrays.

The responses of the element's embedded microphone are different from the antenna elements in antenna arrays. The reason behind this is that the differences in physics of acoustics and electromagnetics, and bandwidths.

The magnitude of the directional responses is also influenced by the array platform's propagation shadowing and wave scattering. The spherical modes of the array elements are limited to lowest, which is due to that the

array elements can be electrically small. Also, the array platform can be electrically large, therefore, the associated embedded element patterns become complicated compared to the isolated element types as a result of having higher-order spherical modes. Moreover, the geometric analytic model cannot be relied upon to precisely anticipate the directional response a microphones' array. This is also true when it comes to antennas, for example, electrically compact elements deployed on an electrically complex printed circuit board platform require simulation to accurately predict the patterns [37].

## 2.6 Tracking Systems

The previous section describes the basic concepts of the beamforming technique. Now. According to the literature, the characteristics of the target are important and can be summarized as follows:

- Range of the target
- Velocity
- Azimuth angle
- Elevation angle

Depending on what sort of tracking is employed, we can have tracking in range, Doppler, Azimuth, or Elevation, or all combined.

Just a narrow beam of the antenna may not be sufficient for the accurate tracking of the target considering the aforementioned characteristics. Auxiliary methods of tracking for the precise location of the target have to be used. There are three techniques for angle tracking.

- Lobe Switching/Sequential Lobing/Sequential Switching.
- Conical Scanning/Switching.
- Monopulse Tracking/Simultaneous Lobing.

Now, considering each of the aforementioned methods in detail:

## 2.6.1 Lobe Switching/Sequential Lobbing/Sequential Switching:

Lobe switching or sequential switching are other terms for sequential lobbing. Their accuracy in performing tracking tasks is restricted by the pencil beam width and noise generated by electronic/mechanical switching mechanisms. It is, however, incredibly simple to put into practice. In consecutive lobbing, the pencil beam should be symmetrical. Tracking process can be performed by switching the pencil beam in a continuous way between two pre-determined symmetrical positions around the antenna's Line of Sight (LOS) axis, which is the reason for the term sequential lobbing. When a switching happens between two positions, the system measures the level of the returned signal. Then, using the difference between the two levels, the angular error signal is calculated.

When a target of interest is tracked on the tracking axis, the difference in voltage will be zero, which is the error signal (see Figure 2.7 (a) and (b)) [38]. However, a nonzero error signal is produced if the target is off the tracking axis. The sign of the difference of the voltage defines the next direction. It should be mentioned that the goal of such a case is making the voltage difference is equal to zero. Two more switching locations in the orthogonal coordinate are necessary to acquire the angular error in that coordinate. Thus, a cluster of four antennas or five antennas can be used to track in two coordinates. The middle antenna is utilized in transmitting, while the other four are used to receive.
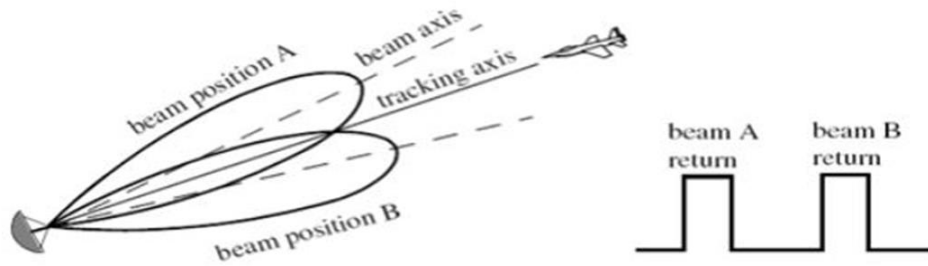
**(a)** Target is located on the track axis.
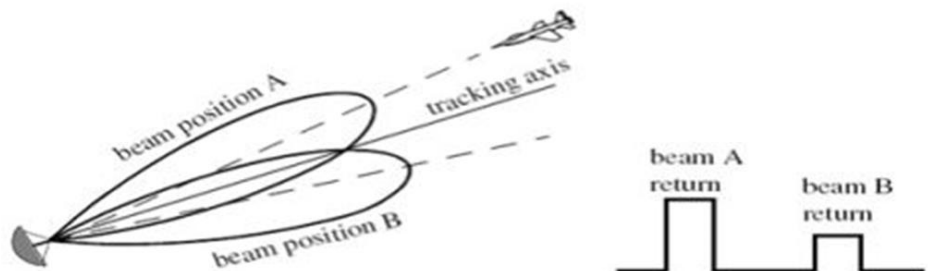


**(b)** Target is off-track axis.

**Figure (2.7):** Sequential Lobbing Technique [38].

Here, the antenna beam direction is switched between two positions, and hence the name lobe switching (see also Figure 2.8) [39].
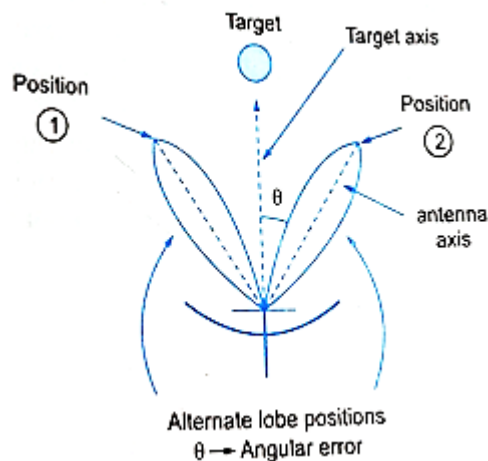


**Figure (2.8):** Illustrates Tracking Objects [39].

At the switching rate, the echo signals from the target will fluctuate, otherwise the target is positioned approximately in the middle of the two directions. When once the latter condition is achieved, the strength of echo signals will be the same for both the antenna position, but the angular

tracking error is to be determined. This tracking error is applied to the servomechanism unit which attempts to position the antenna beam on the target. When the angular error is equal to zero, the target is positioned along the reference direction. Thus, sequential lobbing is used for tracking a target accurately in only one plane (see the flowchart provided in Figure 2.9) [40].
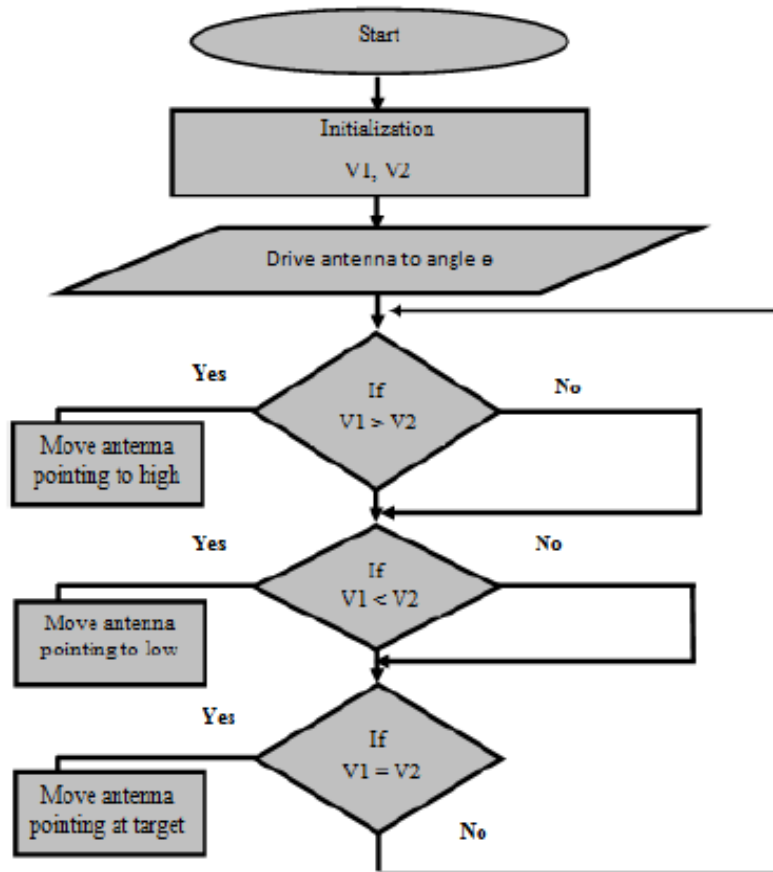


**Figure (2.9):** Flowchart of sequential lobbing technique [40].

### 2.6.2 Conical Switching

It is a Logical Extension of lobe switching in which beam from the parabolic antenna, mounted slightly off-center, is rotated about the axis of the parabola as shown in Figure (2.10) [41].
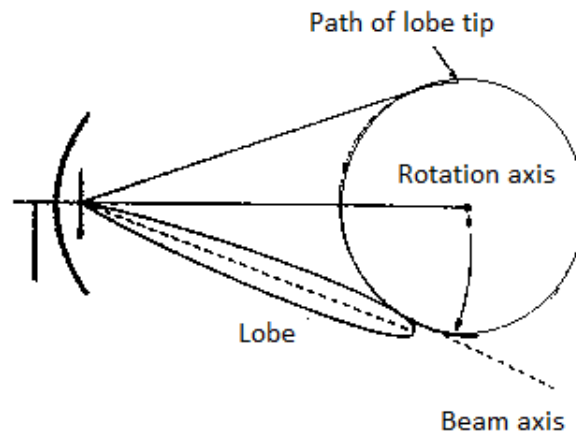


**Figure (2.10):** Conical switching [41].

Since the revolution of solid is a cone as the tip of the pencil radiation pattern moves in a circle, it gets the name Conical Scan. In this technique, when a target is present within the radiation, the target's echo signal will be amplitude modulated at a frequency equal to the beam's rotation frequency. The echo signal's conical scan modulation can be utilized in servo control system, which positions the antenna on target in azimuth and elevation. The conical scan modulation then reaches zero, and the target is precisely tracked. Moreover, the disadvantages can be summarized as follows:

- The motion of the antenna is considered complex in Conical Scanning and Lobe Switching, where an additional servo mechanism is required.
- To locate a target, many returned pulses are needed.
- The conical scan is highly susceptible to electronic countermeasures. This is due to that the scan rate is detectable in a rapid way in the radar signal, and can be contaminated to compound the track servo mechanisms.

26

## 2.6.3 Mono-pulse Tracking

A perfect system is one that could obtain all of the information obtained by conical scanning based on a single pulse only. Mono-pulse tracking is the name for such a system. Angle tracking in modern RADARs is usually performed using this technique. Four feeds and one parabolic reflector are used in an amplitude comparison mono-pulse system. These are four horn antennas that are displaced about the central focus of the reflector as demonstrated in Figure 2.11 [42].
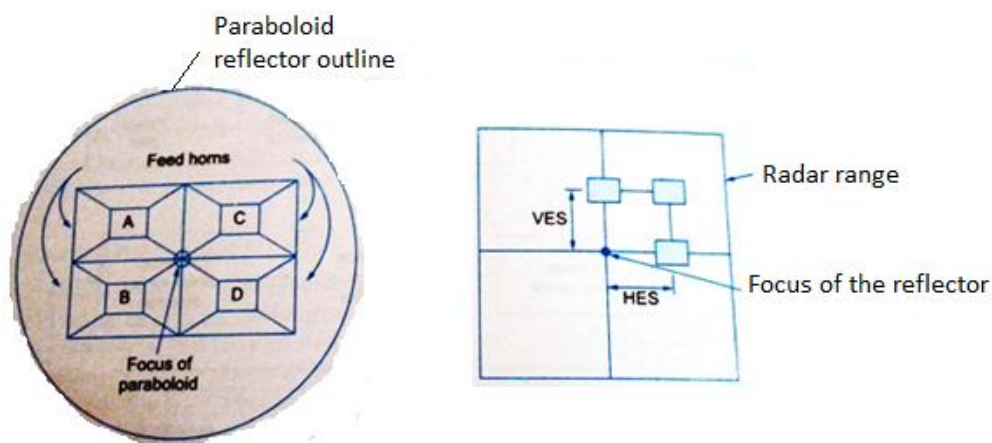


**Figure (2.11):** Monopulse tracking [42].

The transmitter, simultaneously, feeds the horns. For this reason, the sum signal is transmitted. The echo is received by a receiver duplexer using a hybrid ring to provide signals. In fact, no difference is recorded in the case of the target is precisely in the axial direction. However, whenever the target is acquired to lie inside these four-beams, any deviation of the target from the reflector's axial direction will be indicated by the vertical difference signal, a horizontal difference signal, or both, as illustrated in the figure above.

# Chapter Three

# Design of Microphone Array Beamforming

## 3.1 Overview

In this chapter, the proposed microphones array architecture will be explained. Different scenarios that achieve beamscanning coverage angles from (30 to 150) degrees will also be explained by assigning the coefficient of the array element for each case.

## 3.2 Microphones Array Architecture

In this work, 57 elements were used and distributed according to Figure (3.1).
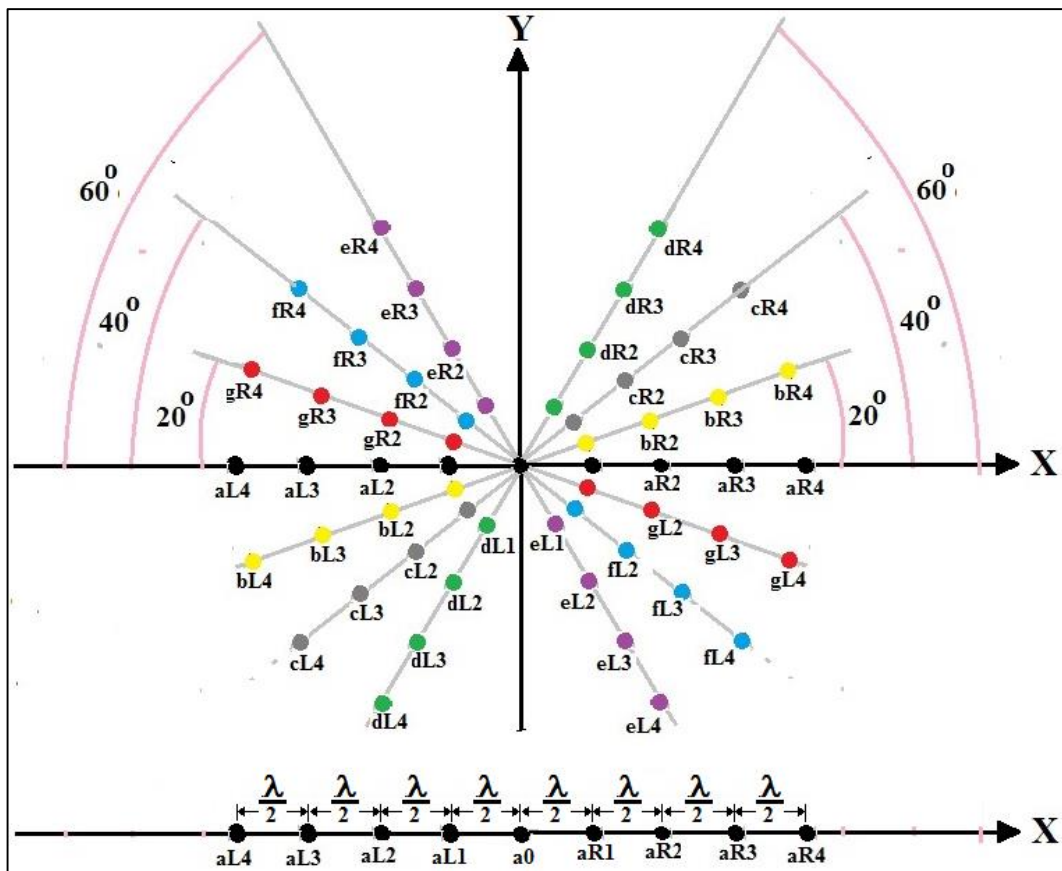


**Figure (3.1):** The Proposed Architecture of the Microphones Array.

Figure (3.1) shows seven groups of linear microphone arrays (a, b, c, d, e, f, and g). Each of them consists of nine elements distributed on a straight line and used to construct the proposed microphone array. These seven linear array groups are arranged in the *X-Y* plane in the following angles (*0, 20, 40, 60, 120, 140, 160*). A uniform distance of (*λ/2*) has been assigned to separate between the nine elements (microphones) in each group of arrays. Also, it can be noted clearly that the element (*a0*) is a common element in all seven groups. This array provides coverage angles from *30* degree to *150* degree in the *X-Y* plane.

## 3.3 Microphone Array Beamforming Implementation

It is well-known that many types of element weightings can be used to get the suitable beamform generated due to antennas array, phase weighting, amplitude weighting, and the combination of amplitude and phase weighting.

In the phase weighting technique, all elements of the array are fed with the same amplitude of RF signals, the control of beam form can be achieved by varying the phase in the different array elements. On the other hand, in the amplitude weighting technique, there is no change in the phase of the RF signal in the array elements but the control of the beam form can be done by varying the amplitude of this signal in the different elements of the array. On the other hand, the amplitude-phase weighting technique depends on varying both the amplitude and the phase of the RF signal in the different elements of the array. In this work the amplitude weighting technique has been used in the microphone array to attain the required beam form in the specific direction. The acoustic tracking system requires a given radiation pattern with suppressed Side Lobe Level (SLL), minimum Half-Power Beamwidth

(HPBW). The binomial distribution is the best type of the amplitude weighting that must be used to evaluate the element coefficient that should be multiplied by the array elements input signal.

For nine elements array the binomial distribution coefficient is assigned as shown in Figure (3.2) [35]:

$$aL4 = aR4 = 1 \qquad\qquad aL3 = aR3 = 8$$

$$aL2 = aR2 = 28 \qquad\qquad aL1 = aR1 = 56$$

$$a0 = 70$$
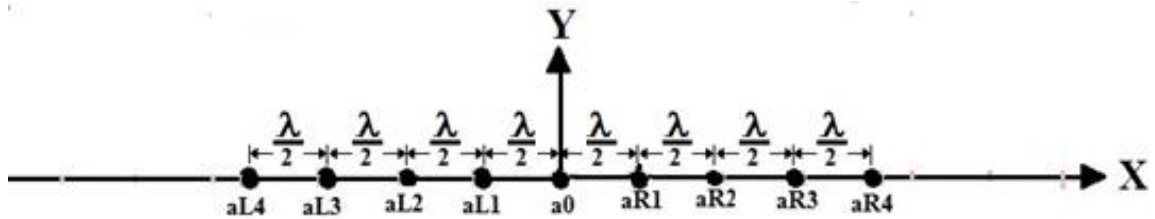


**Figure (3.2):** Nine-Elements Array Uniform Distances.

The design of the antenna array was conducted at 1500 Hz operation frequency, 342 m/s speed of sound and the wavelength (λ) is 2.28 cm. The array factor pattern using MATLAB code that was built for this purpose depending on the coefficient array element above is shown in Figure (3.3).
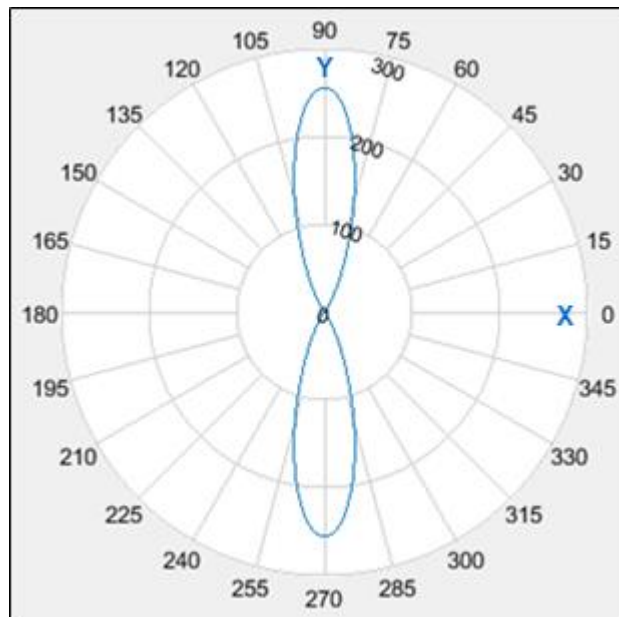
**Figure (3.3):** The Array Factor Pattern for 9 Elements Linear Array on the x-Axis.

Based on Figure (3.3), the following details can be extracted:

- Half power beamwidth using eq. (2.16) = 21.21º
- Main lobe direction = 90º
- Back lobe direction = -90º
- Main lobe level = 256 calculated from (70+56×2+28×2+4×2+1×2)
- Side lobe level = 0
- First null direction = 180º

## 3.4 Microphone Array Beamscanning Implementation

In order to achieve the wide-angle scan range (from *30* to *150* degree), many scenarios should be used, each scenario consists of nine elements. In some scenarios, the system can get a scan for one angle while other scenarios can give many angles by changing the amplitude weighting coefficients for the different elements of the array within the specific scenario. The scenarios that configure from the element in one group cannot give scan more than one angle, but the scenarios that consist of more than one group of arrays can produce many scans angle by changing the amplitude weighting coefficient for the different elements.

Thus, the implementation of the amplitude weighting microphone array beamscanning system can be divided into two major types:

- Single angle beamscanning scenarios.
- Multi angles beamscanning scenarios.

### 3.4.1 Single Angle Beamscanning Scenarios

All the scenarios that use nine elements from the same array group (the elements lie in the straight line) give only one scan angle, these scenarios give beams in the directions (*110, 130, 150, 30, 50, and 70*) degrees. These

scenarios and the amplitude weighting coefficients are shown in Figures (3.4) to (3.9). In addition to the first one that is illustrated in Figures (3.2) and (3.3), which produce the beam direction in $90^o$ degree.
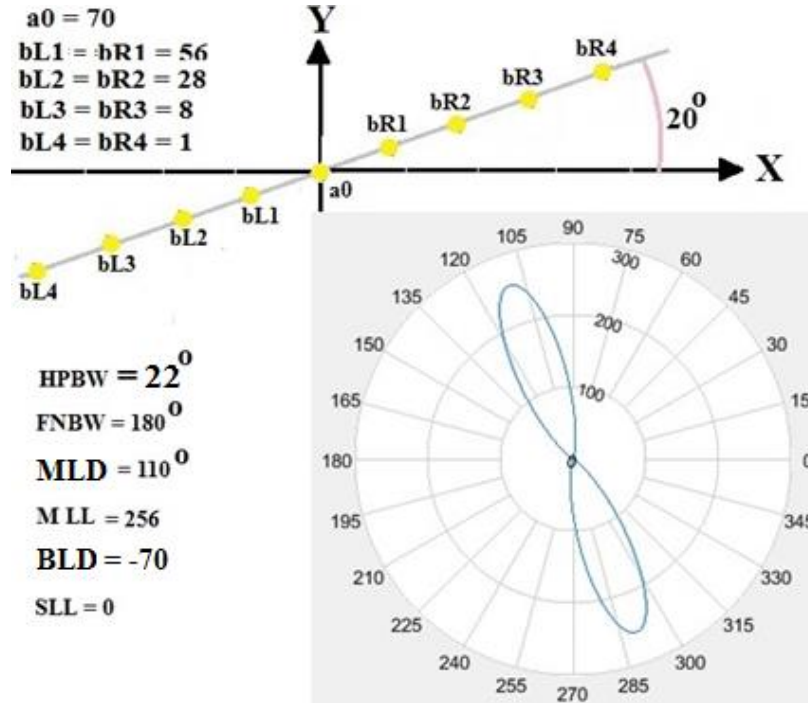


**Figure (3.4):** Array Factor Pattern for Group B Elements.
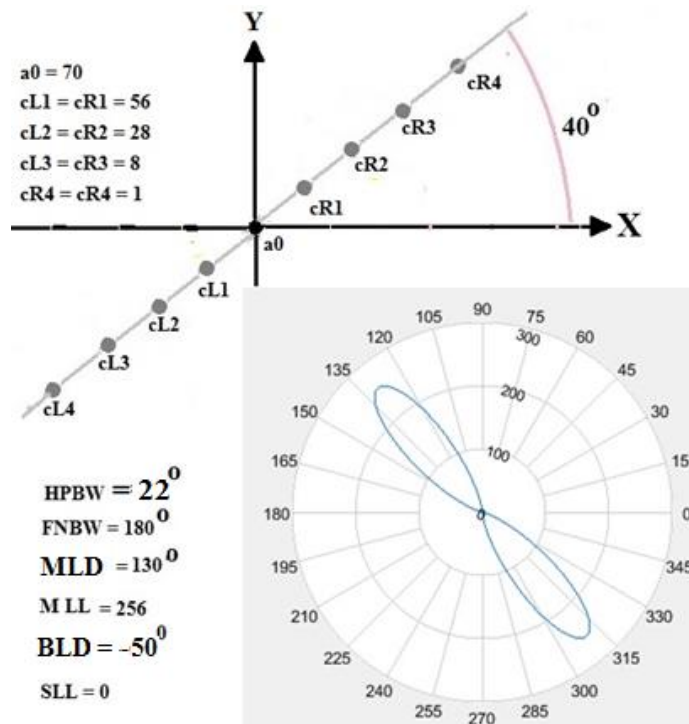


**Figure (3.5):** Array Factor Pattern for Group C Elements.
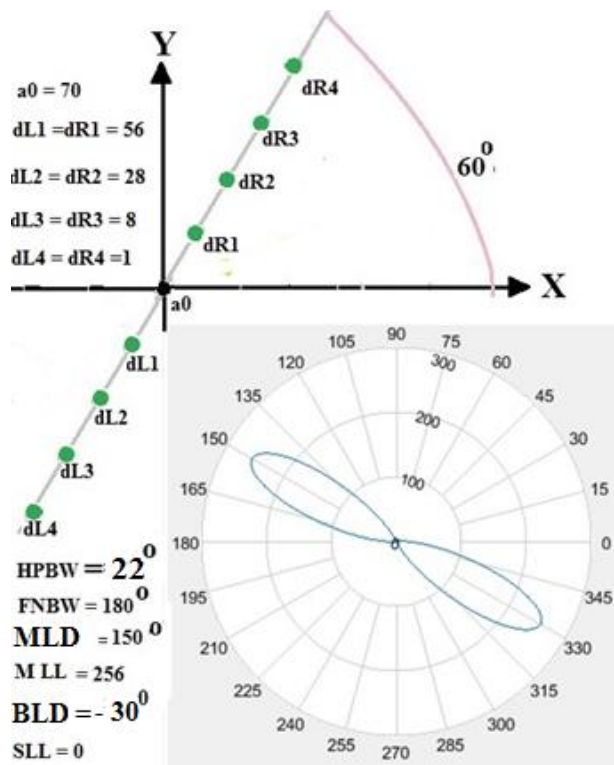
**Figure (3.6):** Array Factor Pattern for Group D Elements.
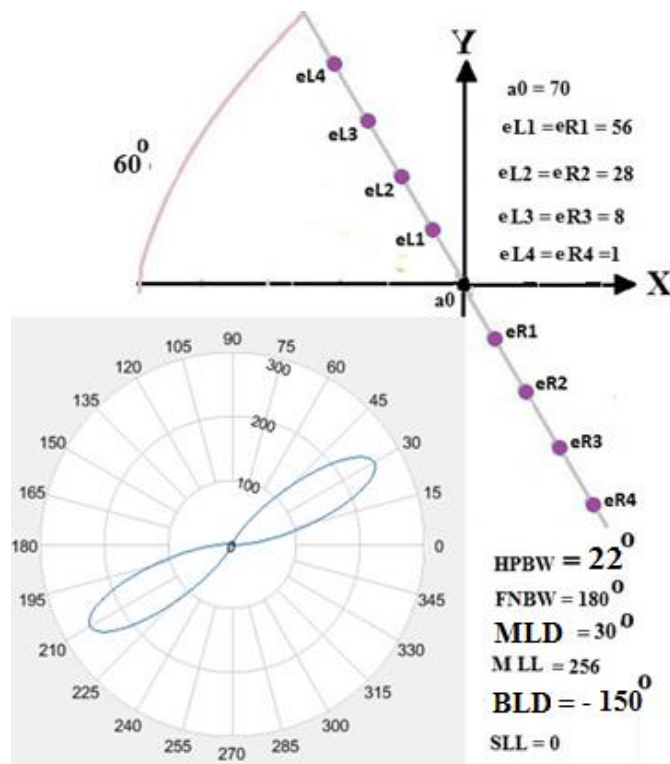


**Figure (3.7):** Array Factor Pattern for Group E Elements.
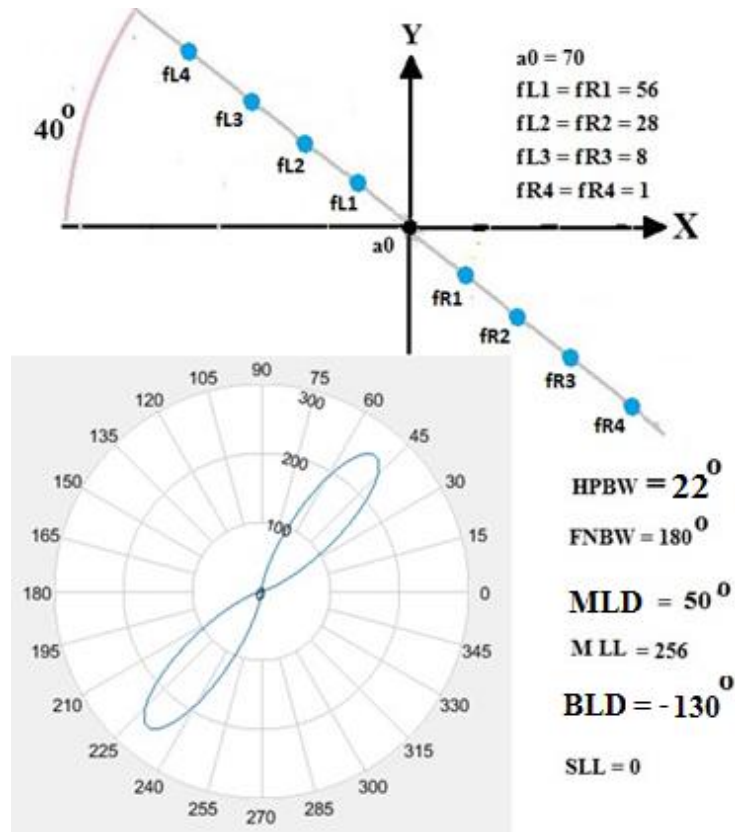
**Figure (3.8):** Array Factor Pattern for Group F Elements.
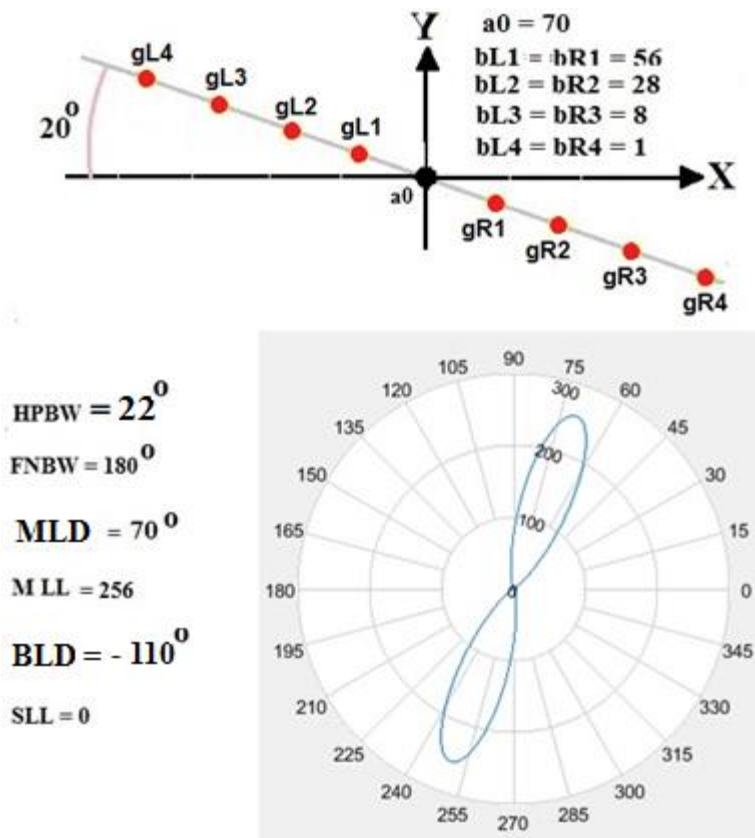


**Figure (3.9):** Array Factor Pattern for Group G Elements.

### 3.4.2  Multi Angles Beamscanning Scenarios

In order to realize the beamscaning for all the angles within the desired coverage angles, six scenarios have been implemented. Each of them uses nine elements from different groups one of them is the *a0* element which lies in the center of the array, four right elements from a specific group of arrays and four left elements from other groups of arrays. By changing the amplitude weighting coefficients of the elements of each scenario, nine scan angles can be achieved within each scenario with the two degrees interval from each other. These scenarios can be classified according to scan angle range of them as follows:

1. Scan region angles (from 32 to 48 degrees).
2. Scan region angles (from 52 to 68 degrees).
3. Scan region angles (from 72 to 88 degrees).
4. Scan region angles (from 92 to 108 degrees).
5. Scan region angles (from 112 to 128 degrees).
6. Scan region angles (from 132 to 148 degrees).

Each of the above scenarios is described in detail in the following sections.

### 3.4.2.1    Scan Region Angles (from 32 to 48 degrees)

In this case, the nine elements array consists of four left elements from the group (e) and four right elements from the group (f) in addition to the element (a0). By changing the amplitude coefficients of these array elements, achieved beam pattern directed toward the angles (*32, 34, 36, 38, 40 42, 44 46, and 48*) degree. The array configuration for this case and the scan zone angles are demonstrated in Figure (3.10), while the elements amplitude coefficients that are assigned to produce the specific angles within this scan region angles are stated in Table (3.1) and the array factor pattern for these subcases are depicted in Figure (3.11).

**Figure (3.10):** Array Elements Configuration to Achieve the Scan Angles (32 to 42) Degree.

**Table (3.1):** Amplitude Weighting Coefficients for Nine Array Elements that are used to Achieve the Scan Angles (32 to 48) degree.

| Case | eL4 | eL3 | eL2 | eL1 | a0 | fR1 | fR2 | fR3 | fR4 | Beam Direction |
|------|-----|-----|-----|-----|-----|-----|-----|-----|-----|----------------|
| A | 2.2 | 18.4 | 56.4 | 100.8 | 70 | 8.6 | 3.6 | 1.2 | 0.1 | 32 |
| B | 1.9 | 17.4 | 55.4 | 99.0 | 70 | 14.8 | 8.8 | 2.8 | 0.3 | 34 |
| C | 1.6 | 12.8 | 44.8 | 86.6 | 70 | 22.4 | 11.2 | 3.2 | 0.4 | 36 |
| D | 1.4 | 11.2 | 39.2 | 78.4 | 70 | 33.6 | 16.8 | 4.8 | 0.6 | 38 |
| E | 1 | 8 | 28 | 56 | 70 | 56 | 28 | 8 | 1 | 40 |
| F | 0.6 | 4.8 | 16.8 | 33.6 | 70 | 78.4 | 39.2 | 11.2 | 1.4 | 42 |
| G | 0.4 | 3.8 | 11.2 | 21.4 | 70 | 87.6 | 44.8 | 12.8 | 1.6 | 44 |
| H | 0.3 | 2.6 | 7.6 | 17.2 | 70 | 102.4 | 52.4 | 15.4 | 2.0 | 46 |
| I | 0.1 | 1.2 | 3.6 | 8.6 | 70 | 100.8 | 56.4 | 18.4 | 2.2 | 48 |
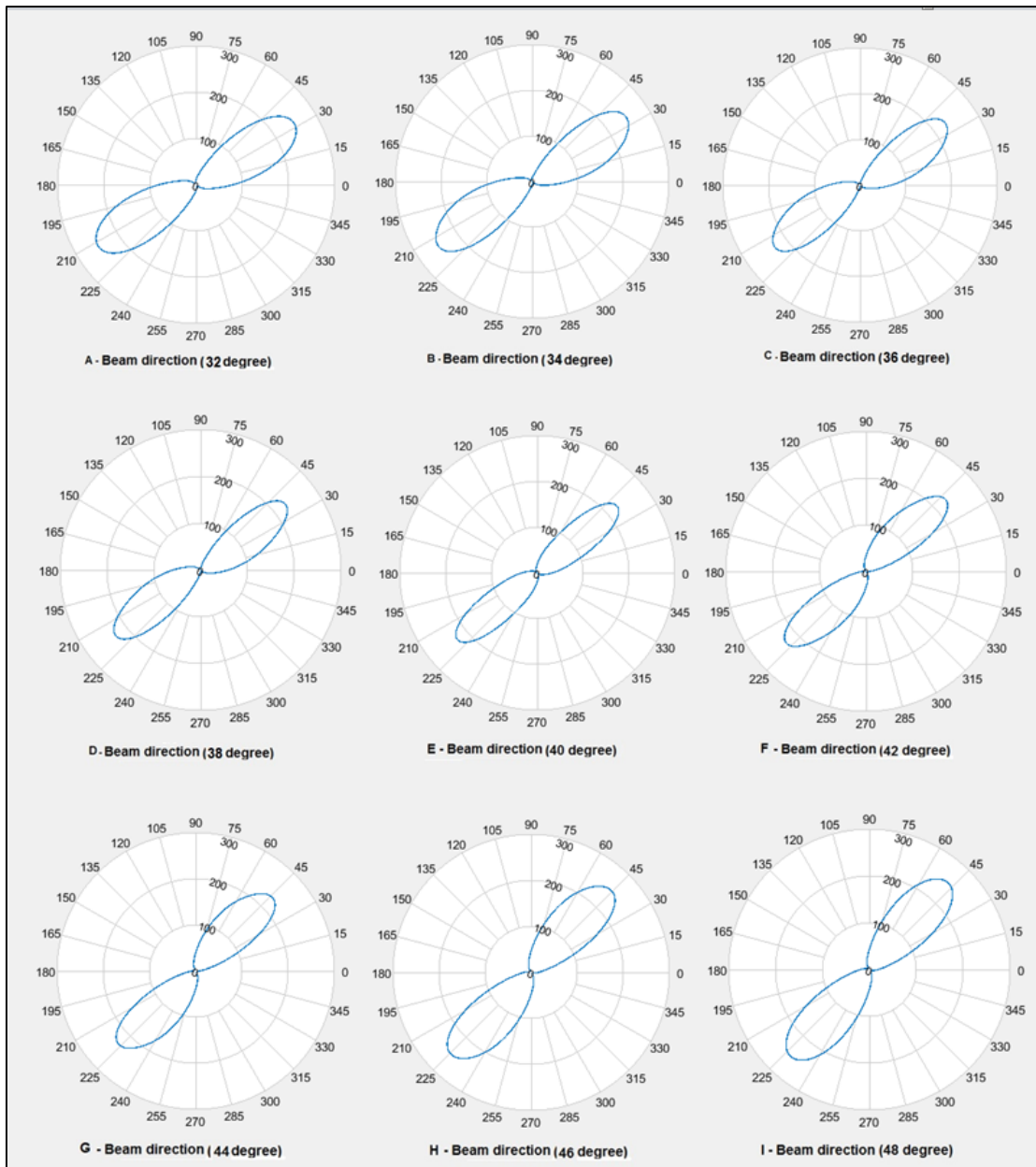
**Figure (3.11):** Array Factor Pattern for Scanning Region Angles (32 to 48) Degree.

Based on Figure (3.11), it can be observed that all the desired scan angles have been achieved. However, there is no exact similarity between the HPBW and the maximum main lobe level and other properties between the beam pattern for the different angle scan cases. This unsimilarity of these parameters are illustrated by the values in Table (3.2).

37

**Table (3.2):** Array Factor Parameters for all Scan Angle Cases within (32-48) Angles.

| Case | Main lobe direction | HPBW | Main lobe level | Back lobe direction | Back lobe level |
|------|---------------------|------|-----------------|---------------------|-----------------|
| A | 32 | 34 | 250 | 212 | 250 |
| B | 34 | 33 | 250 | 214 | 250 |
| C | 36 | 32 | 230 | 216 | 230 |
| D | 38 | 29 | 230 | 218 | 230 |
| E | 40 | 26 | 227 | 220 | 227 |
| F | 42 | 29 | 230 | 222 | 230 |
| G | 44 | 32 | 230 | 224 | 230 |
| H | 46 | 33 | 250 | 226 | 250 |
| I | 48 | 34 | 250 | 228 | 250 |

### 3.4.2.2 Scan Region Angles (from 52 to 68 degree)

In this case, the nine elements array consists of four left elements from the group (f) and four right elements from the group (g) in addition to the element ($a_0$). By changing the amplitude coefficients of these array elements, achieved beam pattern will be directed toward the angles (*52, 54, 56, 58, 60 62, 64 66, and 68)* degree. The array configuration for this case and the scan zone angles are demonstrated in Figure (3.12), while the elements amplitude coefficients that are assigned to produce the specific angles within this scan region angles are stated in Table (3.3), and the array factor pattern for these subcases are depicted in Figure (3.13).
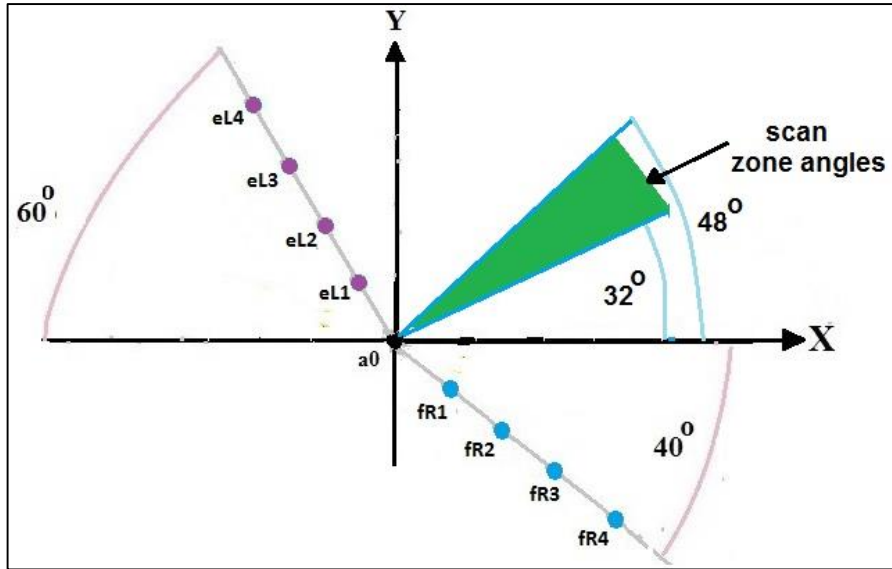
**Figure (3.12):** Array Elements Configuration to Achieve the Scan Angles (52 to 68) Degree.

**Table (3.3):** Amplitude Weighting Coefficients for Nine Array Elements that used to Achieve the Scan Angles (52 to 68) degree.

| Case | fL4 | fL3 | fL2 | fL1 | a0 | gR1 | gR2 | gR3 | gR4 | Beam direction |
|------|-----|-----|-----|-----|----|-----|-----|-----|-----|----------------|
| A | 2.2 | 18.4 | 56.4 | 100.8 | 70 | 8.6 | 3.6 | 1.2 | 0.1 | 52 |
| B | 1.9 | 17.4 | 55.4 | 99.0 | 70 | 14.8 | 8.8 | 2.8 | 0.3 | 54 |
| C | 1.6 | 12.8 | 44.8 | 86.6 | 70 | 22.4 | 11.2 | 3.2 | 0.4 | 56 |
| D | 1.4 | 11.2 | 39.2 | 78.4 | 70 | 33.6 | 16.8 | 4.8 | 0.6 | 58 |
| E | 1 | 8 | 28 | 56 | 70 | 56 | 28 | 8 | 1 | 60 |
| F | 0.6 | 4.8 | 16.8 | 33.6 | 70 | 78.4 | 39.2 | 11.2 | 1.4 | 62 |
| G | 0.4 | 3.8 | 11.2 | 21.4 | 70 | 87.6 | 44.8 | 12.8 | 1.6 | 64 |
| H | 0.3 | 2.6 | 7.6 | 17.2 | 70 | 102.4 | 52.4 | 15.4 | 2.0 | 66 |
| I | 0.1 | 1.2 | 3.6 | 8.6 | 70 | 100.8 | 56.4 | 18.4 | 2.2 | 68 |
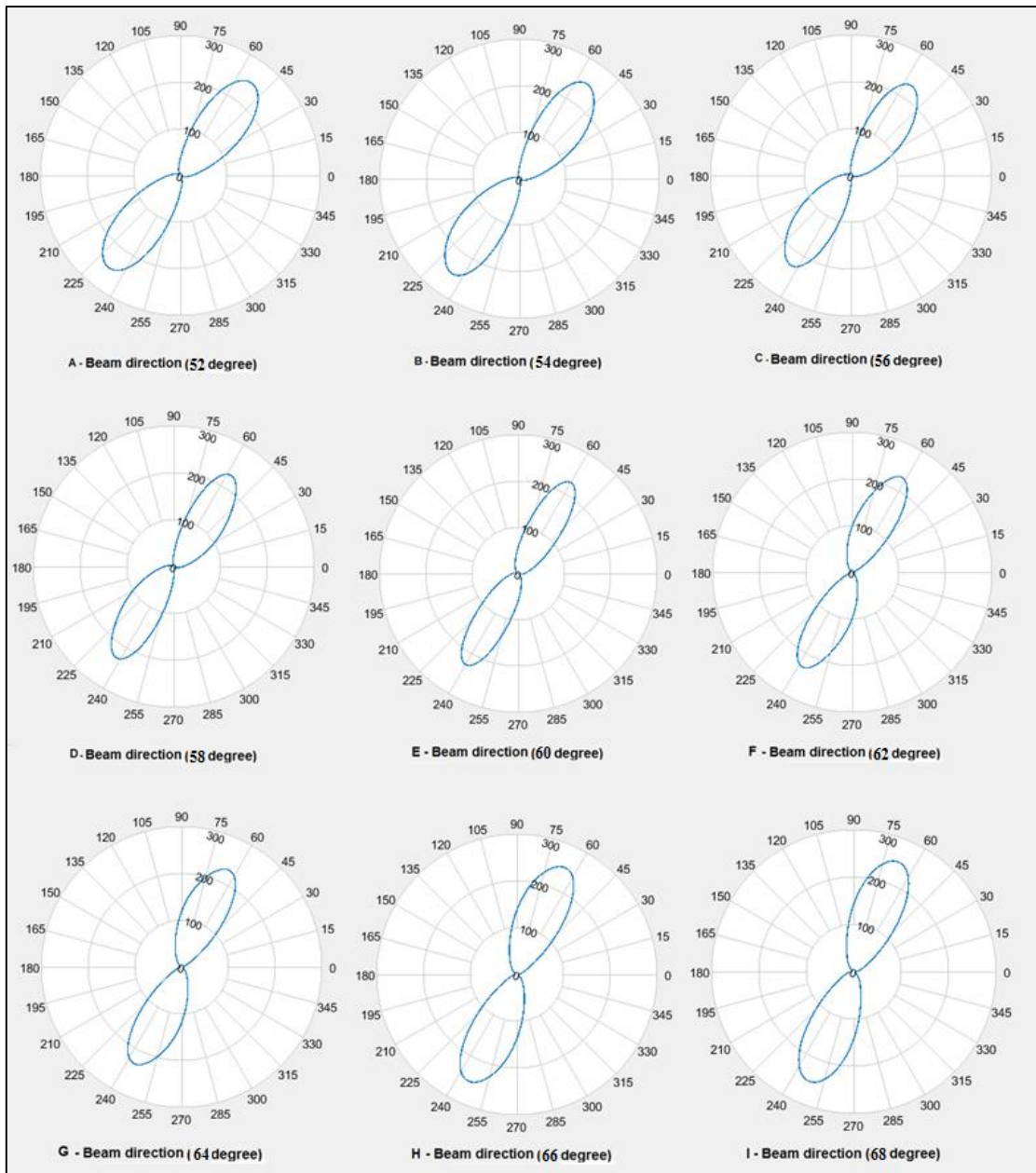
**Figure (3.13):** Array Factor Pattern for Scanning Region Angles (52 to 68) Degree.

According to Figure (3.13), we can see that all the desired scan angles have been achieved, but there is no similarity between the HPBW and the maximum main lobe level and other properties between the beam pattern for the different angles scan cases. This unsimilarity of these parameters can be illustrated in Table (3.4).

**Table (3.4):** Array factor parameters for all scan angle case within (52-68) angles.

| Case | Main lobe direction | HPBW | Main lobe level | Back lobe direction | Back lobe level |
|------|------|------|------|------|------|
| A | 52 | 34 | 250 | -128 | 250 |
| B | 54 | 33 | 250 | -126 | 250 |
| C | 56 | 32 | 230 | -124 | 230 |
| D | 58 | 29 | 230 | -122 | 230 |
| E | 60 | 26 | 227 | -120 | 227 |
| F | 62 | 29 | 230 | -118 | 230 |
| G | 64 | 32 | 230 | -116 | 230 |
| H | 66 | 33 | 250 | -114 | 250 |
| I | 68 | 34 | 250 | -112 | 250 |

### 3.4.2.3  Scan Region Angles (from 72 to 88 degree)

In this case, the nine elements array consist of four left elements from the group (g) and four right elements from the group (a) in addition to the element (a0). By changing the amplitude coefficients of this array elements, achieved beam pattern will be directed toward the angles (*72, 74, 76, 78, 80 82, 84 86, and 88*) degree.

The array configuration for this case and the scan zone angles are shown in Figure (3.14), while the elements amplitude coefficients that are assigned to produce the specific angles within this scan region angles are

stated in Table (3.5), and the array factor pattern for these subcases are presented in Figure (3.15).
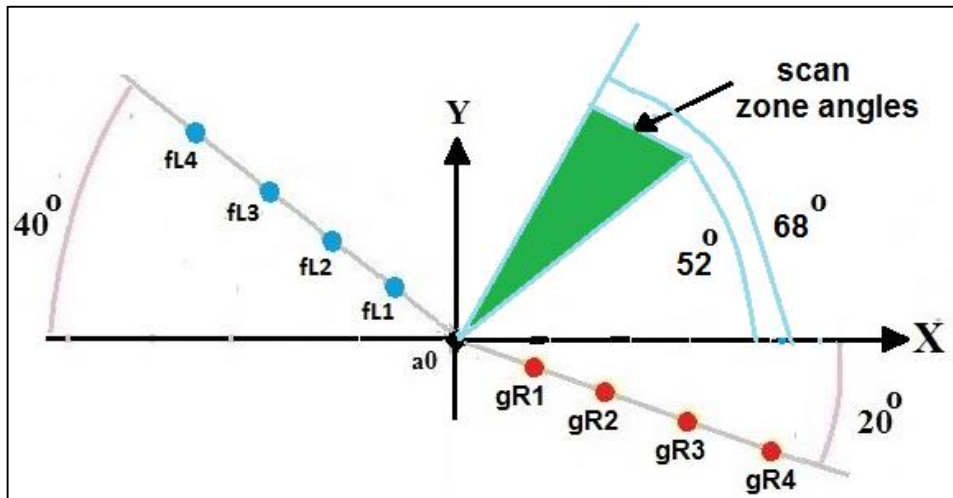


**Figure (3.14):** Array Elements Configuration to Achieve the Scan Angles (72 to 88) Degree.

**Table (3.5):** Amplitude Weighting Coefficients for Nine Array Elements that used to Achieve the Scan Angles (72 to 88) degree.

| Case | gL4 | gL3 | gL2 | gL1 | a0 | aR1 | aR2 | aR3 | aR4 | Beam direction |
|------|-----|-----|-----|-----|----|-----|-----|-----|-----|----------------|
| A | 2.2 | 18.4 | 56.4 | 100.8 | 70 | 8.6 | 3.6 | 1.2 | 0.1 | 72 |
| B | 1.9 | 17.4 | 55.4 | 99.0 | 70 | 14.8 | 8.8 | 2.8 | 0.3 | 74 |
| C | 1.6 | 12.8 | 44.8 | 86.6 | 70 | 22.4 | 11.2 | 3.2 | 0.4 | 76 |
| D | 1.4 | 11.2 | 39.2 | 78.4 | 70 | 33.6 | 16.8 | 4.8 | 0.6 | 78 |
| E | 1 | 8 | 28 | 56 | 70 | 56 | 28 | 8 | 1 | 80 |
| F | 0.6 | 4.8 | 16.8 | 33.6 | 70 | 78.4 | 39.2 | 11.2 | 1.4 | 82 |
| G | 0.4 | 3.8 | 11.2 | 21.4 | 70 | 87.6 | 44.8 | 12.8 | 1.6 | 84 |
| H | 0.3 | 2.6 | 7.6 | 17.2 | 70 | 102.4 | 52.4 | 15.4 | 2.0 | 86 |
| I | 0.1 | 1.2 | 3.6 | 8.6 | 70 | 100.8 | 56.4 | 18.4 | 2.2 | 88 |
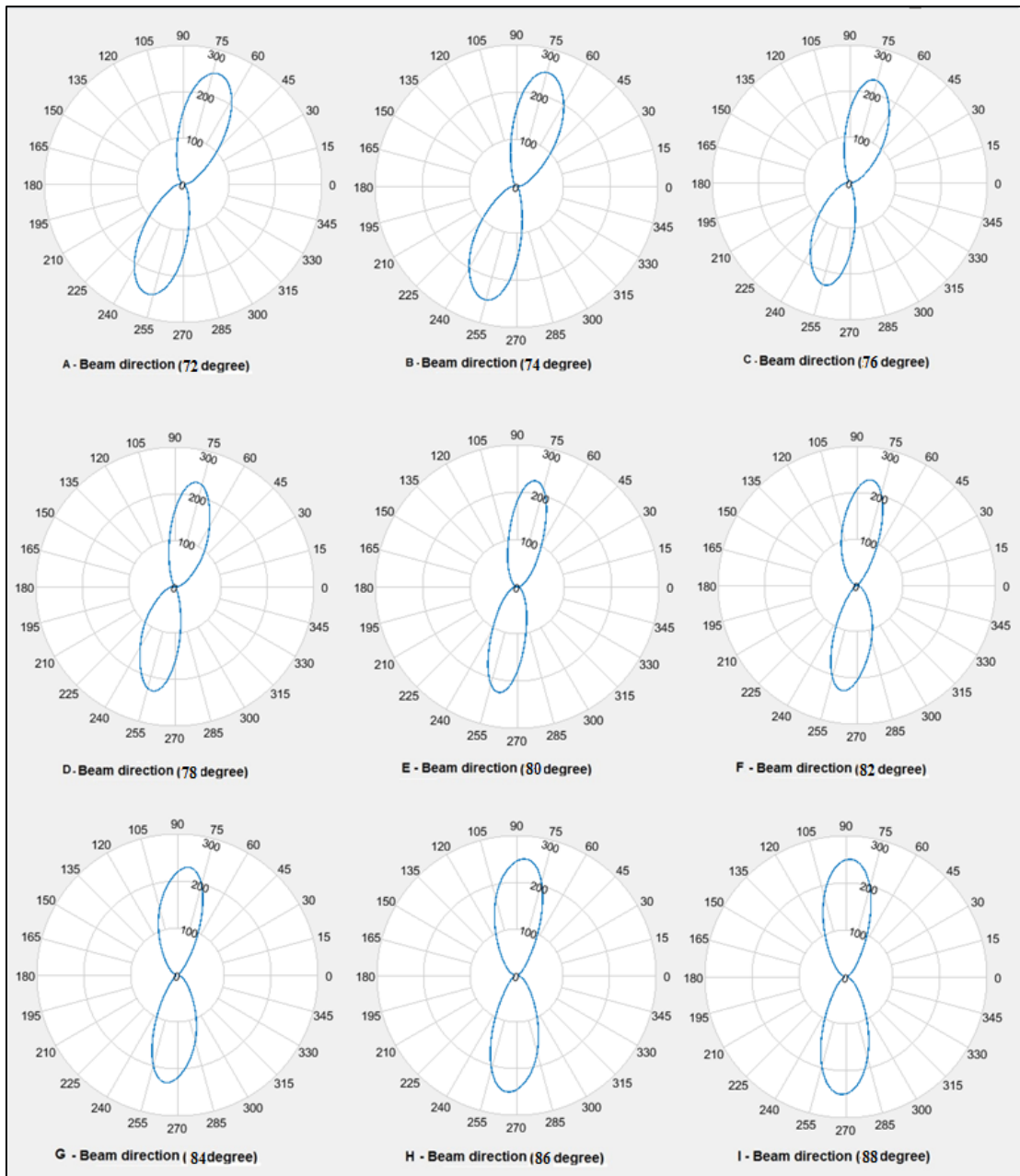
**Figure (3.15):** Array Factor Pattern for Scanning Region angles (37 to 88) Degree.

Based on Figure (3.15), it can be noticed that all desired scan angles have been achieved, but there is no similarity between the HPBW and the maximum main lobe level and other properties between the beam pattern for the different angle scan cases. This unsimilarity of these parameters can be illustrated in Table (3.6).

**Table (3.6):** Array Factor Parameters for all Scan Angle Cases within (72-88) Angles.

| Case | Main lobe direction | HPBW | Main lobe level | Back lobe direction | Back lobe level |
|------|------|------|------|------|------|
| A | 72 | 34 | 250 | -108 | 250 |
| B | 74 | 33 | 250 | -106 | 250 |
| C | 76 | 32 | 230 | -104 | 230 |
| D | 78 | 29 | 230 | -102 | 230 |
| E | 80 | 26 | 227 | -100 | 227 |
| F | 82 | 29 | 230 | -98 | 230 |
| G | 84 | 32 | 230 | -96 | 230 |
| H | 86 | 33 | 250 | -94 | 250 |
| I | 88 | 34 | 250 | -92 | 250 |

### 3.4.2.4 Scan Region Angles (from 92 to 108 degree)

In this case, the nine elements array consists of four left elements from the group (a) and four right elements from the group (b) in addition to the element (a0). By changing the amplitude coefficients of these array elements, the achieved beam pattern will be directed toward the angles (*92, 94, 96, 98, 100, 102, 104, 106, and 108*) degree. The array configuration for this case and the scan zone angles are shown in Figure (3.16), while the elements amplitude coefficients that are assigned to produce the specific angles within this scan region angles are stated in Table (3.6) and the array factor pattern for these subcases are demonstrated in Figure (3.17).
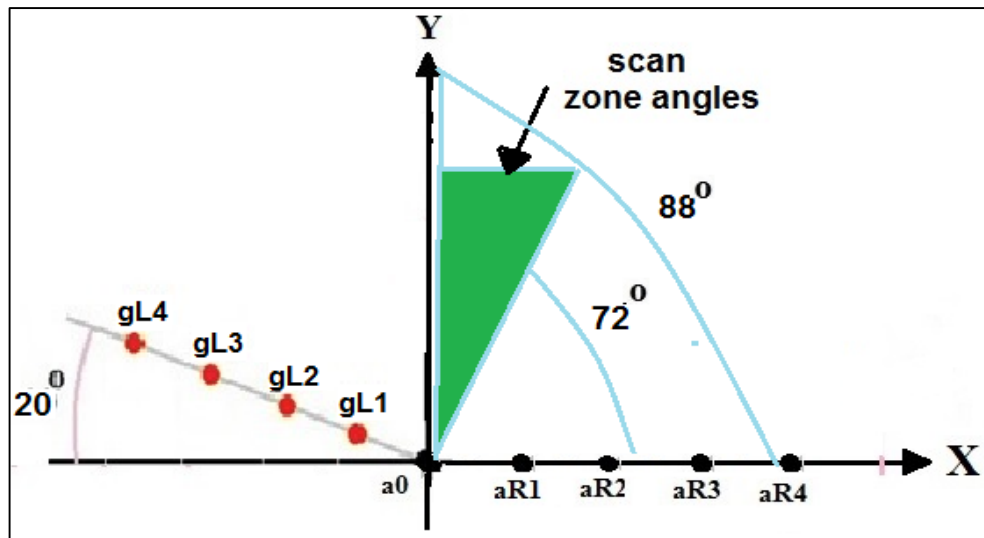
**Figure (3.16):** Array Elements Configuration to Achieve the Scan Angles (92 to 108) Degree.

**Table (3.7):** Amplitude Weighting Coefficients for Nine Array Elements that used to Achieve the Scan Angles (92 to 108) degree.

| Case | aL4 | aL3 | aL2 | aL1 | a0 | bR1 | bR2 | bR3 | bR4 | Beam direction |
|------|-----|-----|-----|-----|----|-----|-----|-----|-----|----------------|
| A | 2.2 | 18.4 | 56.4 | 100.8 | 70 | 8.6 | 3.6 | 1.2 | 0.1 | 92 |
| B | 1.9 | 17.4 | 55.4 | 99.0 | 70 | 14.8 | 8.8 | 2.8 | 0.3 | 94 |
| C | 1.6 | 12.8 | 44.8 | 86.6 | 70 | 22.4 | 11.2 | 3.2 | 0.4 | 96 |
| D | 1.4 | 11.2 | 39.2 | 78.4 | 70 | 33.6 | 16.8 | 4.8 | 0.6 | 98 |
| E | 1 | 8 | 28 | 56 | 70 | 56 | 28 | 8 | 1 | 100 |
| F | 0.6 | 4.8 | 16.8 | 33.6 | 70 | 78.4 | 39.2 | 11.2 | 1.4 | 102 |
| G | 0.4 | 3.8 | 11.2 | 21.4 | 70 | 87.6 | 44.8 | 12.8 | 1.6 | 104 |
| H | 0.3 | 2.6 | 7.6 | 17.2 | 70 | 102.4 | 52.4 | 15.4 | 2.0 | 106 |
| I | 0.1 | 1.2 | 3.6 | 8.6 | 70 | 100.8 | 56.4 | 18.4 | 2.2 | 108 |
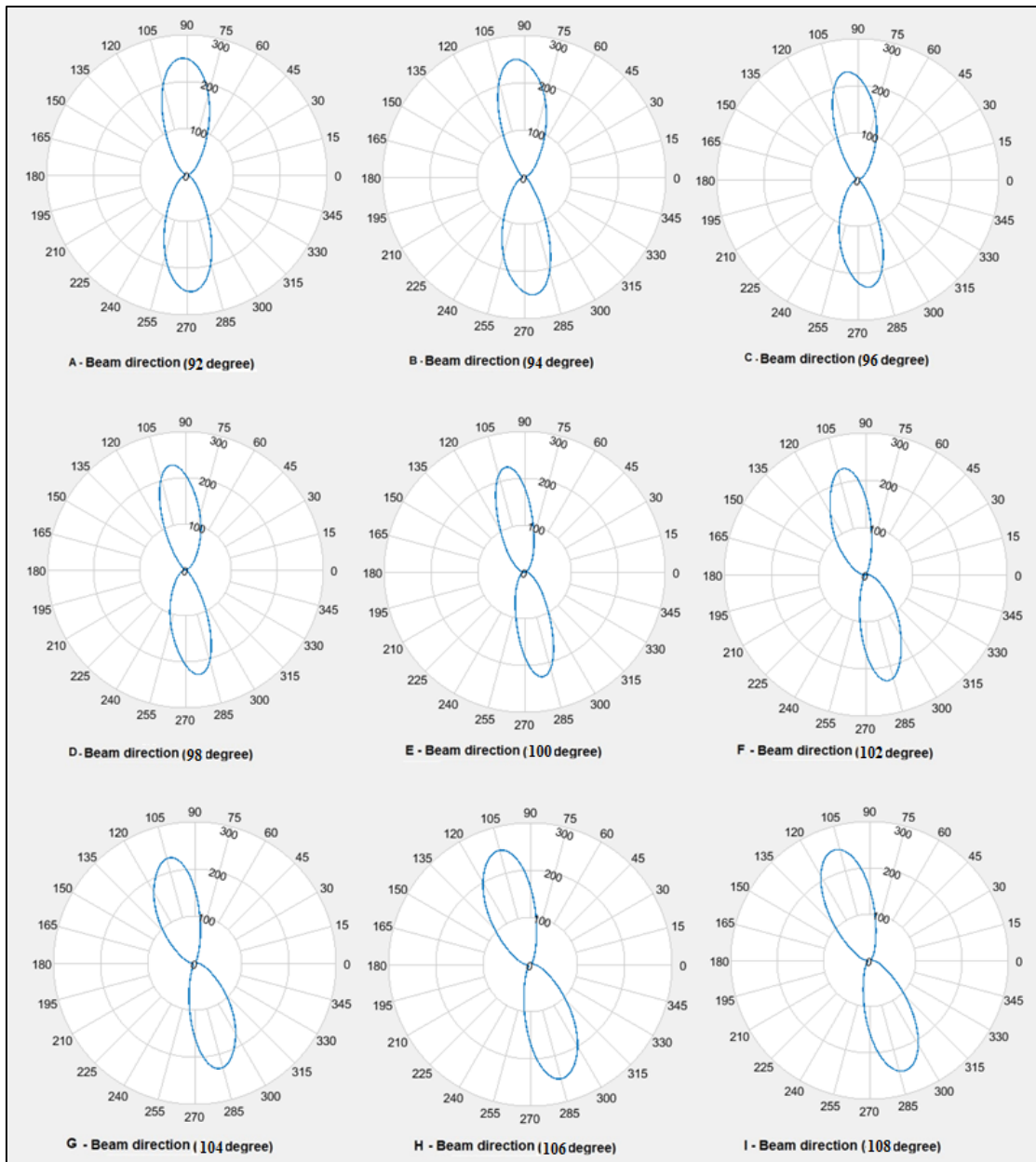
**Figure (3.17):** Array Factor Pattern for Scanning Region Angles (92 to 108) Degree.

According to Figure (3.17) shown above, all the desired scan angles have been achieved, but there is no similarity between the HPBW and the maximum main lobe level and other properties between the beam pattern for the different angle scan cases. This unsimilarity of these parameters can be illustrated in Table (3.8).

**Table (3.8):** Array Factor Parameters for all Scan Angle Cases within (92-108) Angles.

| Case | Main lobe direction | HPBW | Main lobe level | Back lobe direction | Back lobe level |
|------|------|------|------|------|------|
| A | 92 | 34 | 250 | -88 | 250 |
| B | 94 | 33 | 250 | -86 | 250 |
| C | 96 | 32 | 230 | -84 | 230 |
| D | 98 | 29 | 230 | -82 | 230 |
| E | 100 | 26 | 227 | -80 | 227 |
| F | 102 | 29 | 230 | -78 | 230 |
| G | 104 | 32 | 230 | -76 | 230 |
| H | 106 | 33 | 250 | -74 | 250 |
| I | 108 | 34 | 250 | -72 | 250 |

### 3.4.2.5   Scan Region Angles (from 112 to 128 degree).

In this scenario, the nine elements array consist of four left elements from the group (b) and four right elements from group (c) in addition to the element (*a0*). By changing the amplitude coefficients of these array elements, the achieved beam pattern will be directed toward the angles (*112, 114, 116, 118, 120, 122, 124, 126, and 128*) degree. The array configuration for this case and the scan zone angles are shown in Figure (3.18), while the elements amplitude coefficients that are assigned to produce the specific angles within this scan region angles are stated in Table (3.9) and the array factor pattern for these subcases are demonstrated in Figure (3.19).
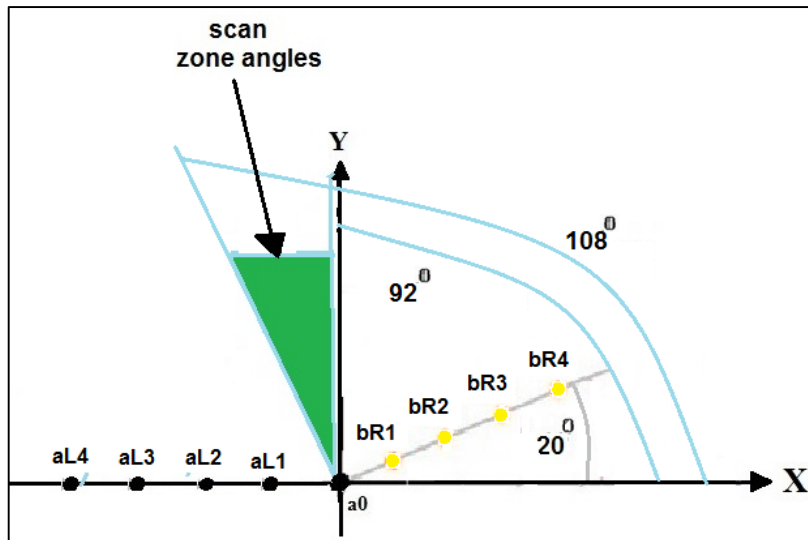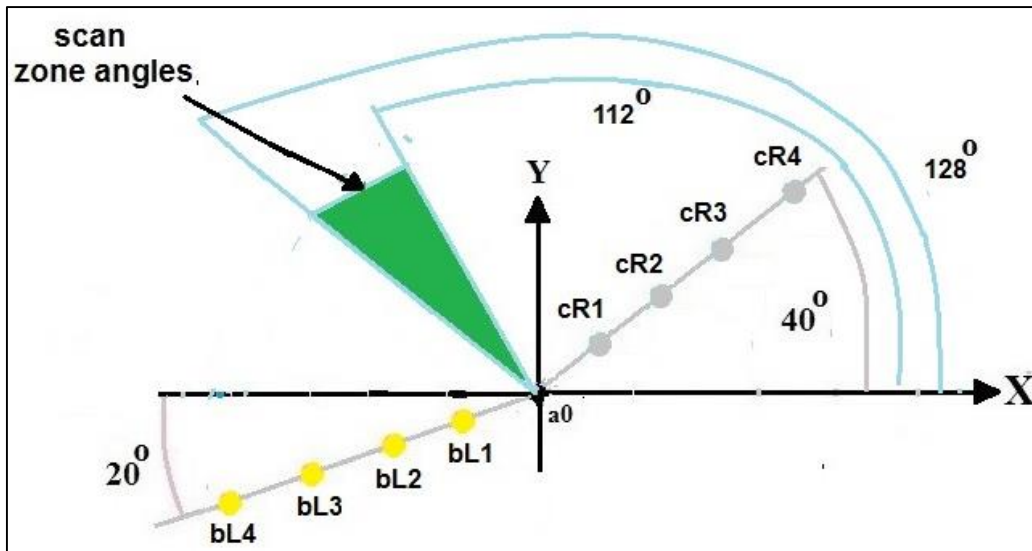
**Figure (3.18):** Array Elements Configuration to Achieve the Scan Angles (112 to 128) Degree.

**Table (3.9):** Amplitude Weighting Coefficients for Nine Array Elements that used to Achieve the Scan Angles (112 to 128) degree.

| Case | bL4 | bL3 | bL2 | bL1 | a0 | cR1 | cR2 | cR3 | cR4 | Beam direction |
|------|-----|-----|-----|-----|----|-----|-----|-----|-----|----------------|
| A | 2.2 | 18.4 | 56.4 | 100.8 | 70 | 8.6 | 3.6 | 1.2 | 0.1 | 112 |
| B | 1.9 | 17.4 | 55.4 | 99.0 | 70 | 14.8 | 8.8 | 2.8 | 0.3 | 114 |
| C | 1.6 | 12.8 | 44.8 | 86.6 | 70 | 22.4 | 11.2 | 3.2 | 0.4 | 116 |
| D | 1.4 | 11.2 | 39.2 | 78.4 | 70 | 33.6 | 16.8 | 4.8 | 0.6 | 118 |
| E | 1 | 8 | 28 | 56 | 70 | 56 | 28 | 8 | 1 | 120 |
| F | 0.6 | 4.8 | 16.8 | 33.6 | 70 | 78.4 | 39.2 | 11.2 | 1.4 | 122 |
| G | 0.4 | 3.8 | 11.2 | 21.4 | 70 | 87.6 | 44.8 | 12.8 | 1.6 | 124 |
| H | 0.3 | 2.6 | 7.6 | 17.2 | 70 | 102.4 | 52.4 | 15.4 | 2.0 | 126 |
| I | 0.1 | 1.2 | 3.6 | 8.6 | 70 | 100.8 | 56.4 | 18.4 | 2.2 | 128 |

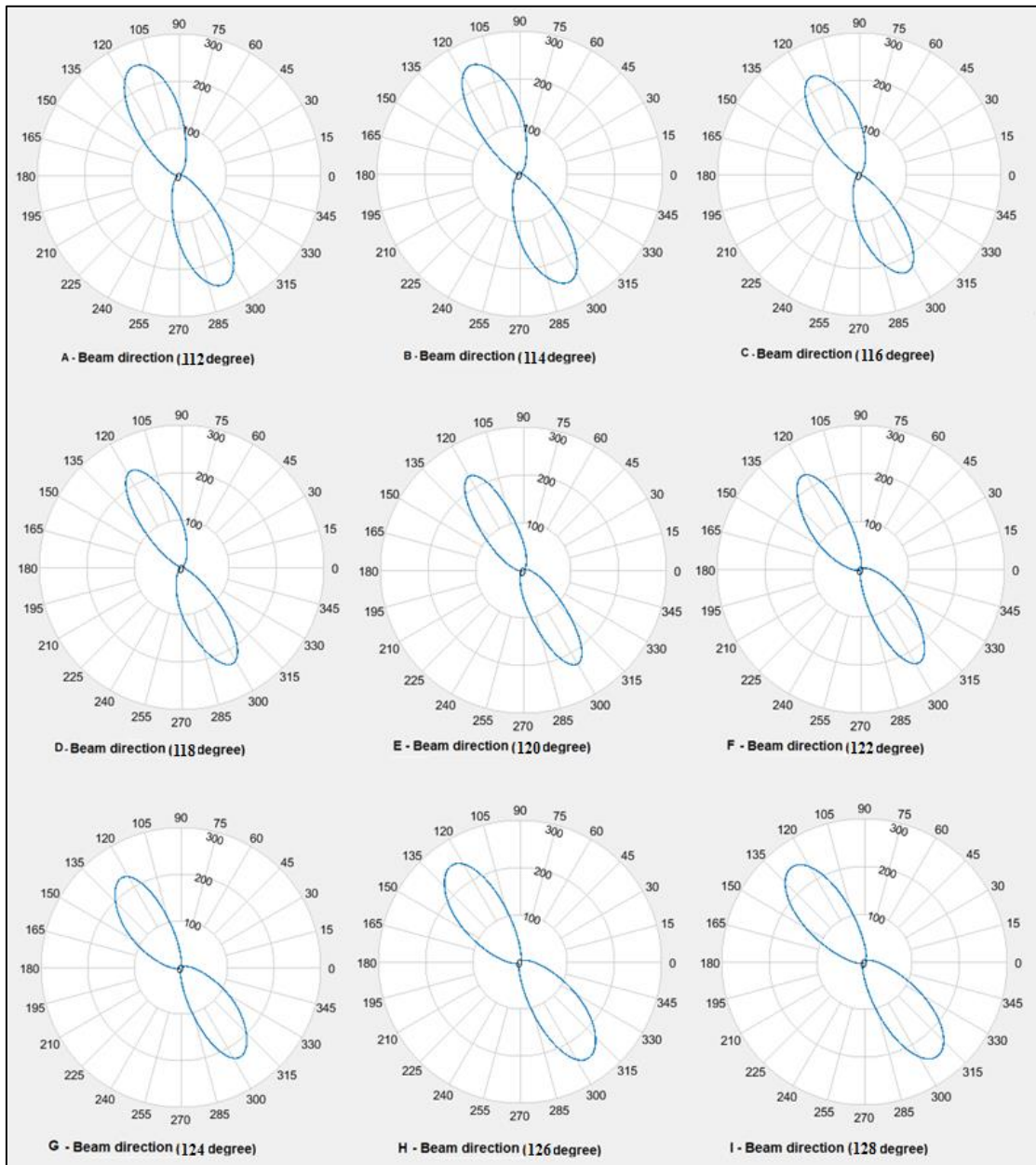**Figure (3.19):** Array Factor Pattern for Scanning Region Angles (112 to 128) Degree.

Based on Figure (3.19) shown above, all desired scan angles have been achieved, but there is no similarity between the HPBW and the maximum main lobe level and other properties between the beam pattern for the different angle scan cases. This unsimilarity of these parameters can be illustrated in Table (3.10).

49

**Table (3.10):** Array factor parameters for all scan angle cases within (112-128) angles.

| Case | Main lobe direction | HPBW | Main lobe level | Back lobe direction | Back lobe level |
|------|------|------|------|------|------|
| A | 112 | 34 | 250 | -68 | 250 |
| B | 114 | 33 | 250 | -66 | 250 |
| C | 116 | 32 | 230 | -64 | 230 |
| D | 118 | 29 | 230 | -62 | 230 |
| E | 120 | 26 | 227 | -60 | 227 |
| F | 122 | 29 | 230 | -58 | 230 |
| G | 124 | 32 | 230 | -56 | 230 |
| H | 126 | 33 | 250 | -54 | 250 |
| I | 128 | 34 | 250 | -52 | 250 |

### 3.4.2.6 Scan Region Angles (from 132 to 148 degree)

In this scenario, the nine elements array consist of four left elements from the group (c) and four right elements from group (d) in addition to the element (*a0*). By changing the amplitude coefficients of these array elements, the achieved beam pattern will be directed toward the angles (*132, 134, 136, 138, 140, 142, 144, 146, and 148*) degree. The array configuration for this case and the scan zone angles are depicted in Figure (3.20), while the elements amplitude coefficients that are assigned to produce the specific angles within this scan region angles are stated in Table (3.11) and the array factor pattern for these subcases are demonstrated in Figure (3.21).
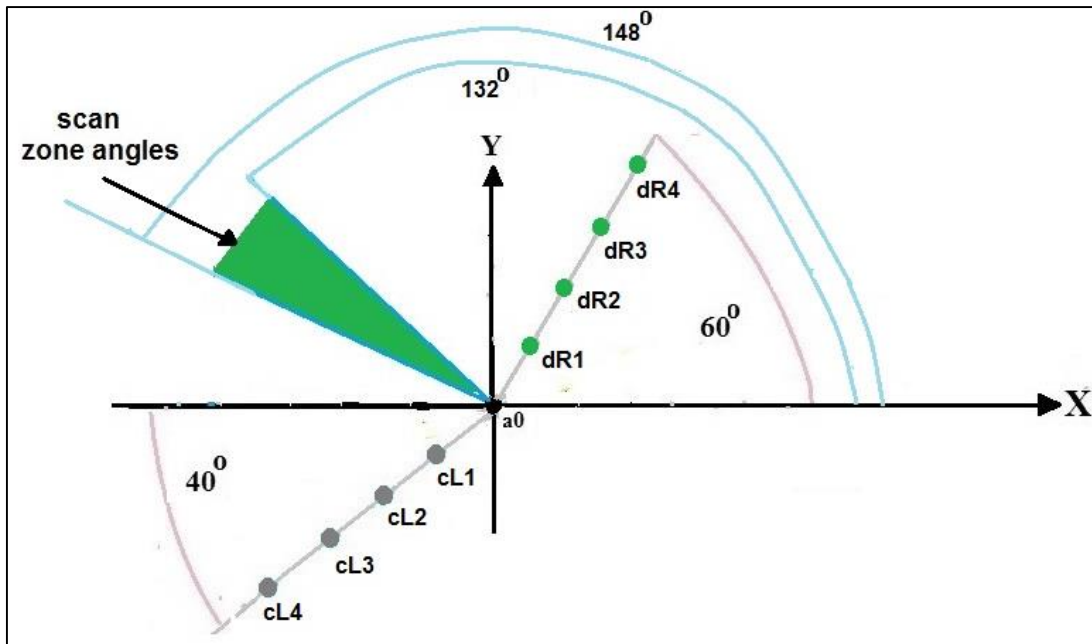
**Figure (3.20):** Array Elements Configuration to Achieve the Scan Angles (132 to 148) Degree.

**Table (3.11):** Amplitude Weighting Coefficients for Nine Array Elements that used to Achieve the Scan Angles (132 to 148) degree.

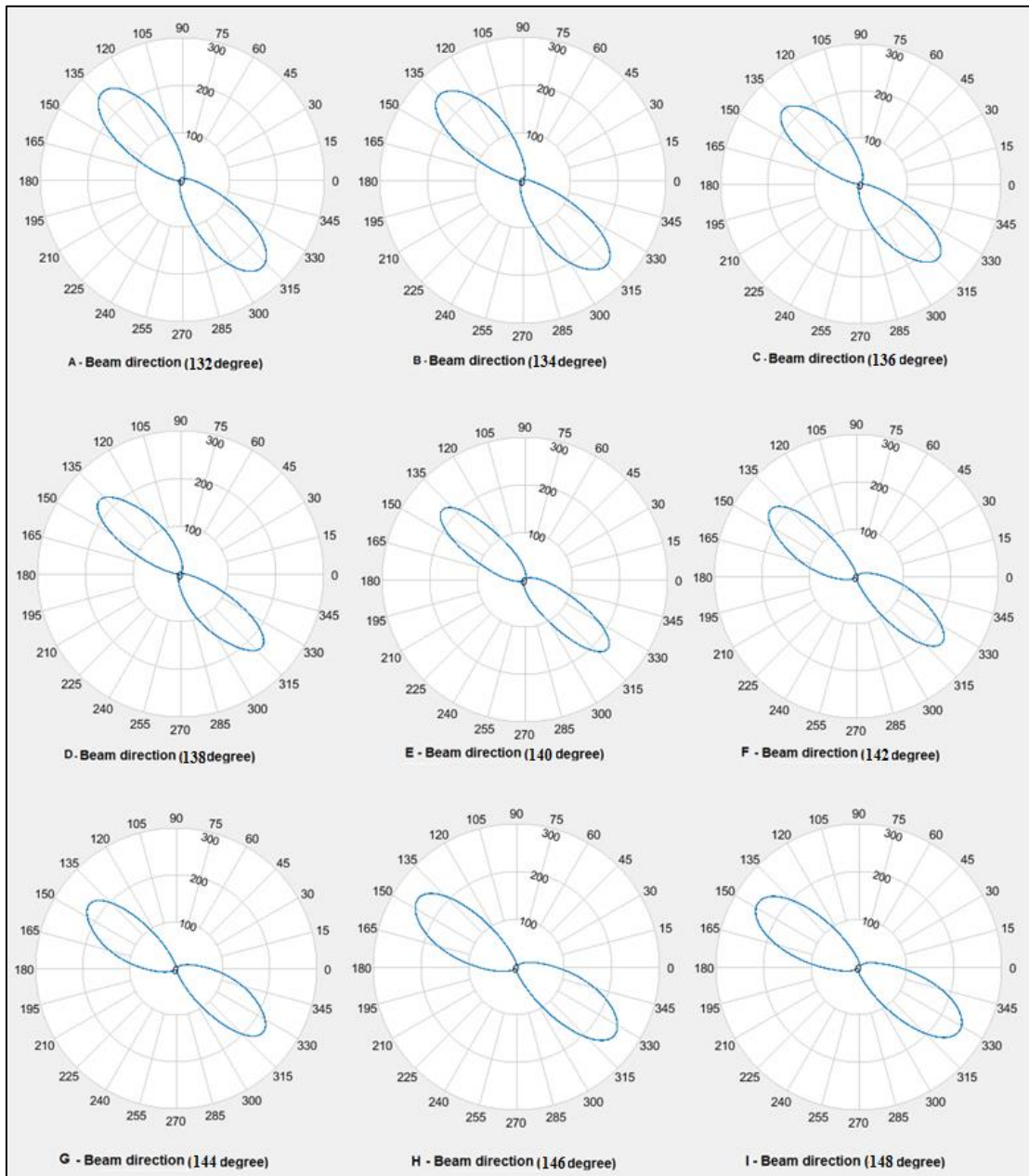| Case | cL4 | cL3 | cL2 | cL1 | a0 | dR1 | dR2 | dR3 | dR4 | Beam direction |
|------|-----|-----|-----|-----|----|-----|-----|-----|-----|----------------|
| A | 2.2 | 18.4 | 56.4 | 100.8 | 70 | 8.6 | 3.6 | 1.2 | 0.1 | 132 |
| B | 1.9 | 17.4 | 55.4 | 99.0 | 70 | 14.8 | 8.8 | 2.8 | 0.3 | 134 |
| C | 1.6 | 12.8 | 44.8 | 86.6 | 70 | 22.4 | 11.2 | 3.2 | 0.4 | 136 |
| D | 1.4 | 11.2 | 39.2 | 78.4 | 70 | 33.6 | 16.8 | 4.8 | 0.6 | 138 |
| E | 1 | 8 | 28 | 56 | 70 | 56 | 28 | 8 | 1 | 140 |
| F | 0.6 | 4.8 | 16.8 | 33.6 | 70 | 78.4 | 39.2 | 11.2 | 1.4 | 142 |
| G | 0.4 | 3.8 | 11.2 | 21.4 | 70 | 87.6 | 44.8 | 12.8 | 1.6 | 144 |
| H | 0.3 | 2.6 | 7.6 | 17.2 | 70 | 102.4 | 52.4 | 15.4 | 2.0 | 146 |
| I | 0.1 | 1.2 | 3.6 | 8.6 | 70 | 100.8 | 56.4 | 18.4 | 2.2 | 148 |

**Figure (3.21):** Array Factor Pattern for Scanning Region Angles (132 to 148) Degree.

According to Figure (3.21), all the desired scan angles have been achieved but there is no similarity between the HPBW and the maximum main lobe level and other properties between the beam pattern for the different angle scan cases. this non-similarity of these parameters can be illustrated in Table (3.12).

**Table (3.12)**: Array Factor Parameters for all Scan Angle Cases within (132-148) Angles.

| Case | Main lobe direction | HPBW | Main lobe level | Back lobe direction | Back lobe level |
|------|------|------|------|------|------|
| A | 132 | 34 | 250 | -48 | 250 |
| B | 134 | 33 | 250 | -46 | 250 |
| C | 136 | 32 | 230 | -44 | 230 |
| D | 138 | 29 | 230 | -42 | 230 |
| E | 140 | 26 | 227 | -40 | 227 |
| F | 142 | 29 | 230 | -38 | 230 |
| G | 144 | 32 | 230 | -36 | 230 |
| H | 146 | 33 | 250 | -34 | 250 |
| I | 148 | 34 | 250 | -32 | 250 |

## 3.5 Results Analysis

According to the results presented in the previous sections of this chapter Figures (3.3) to (3.9), Figures (3.11), (3.13), (3.15), (3.17), (3.19), and Figure (3-21) as well as the results presented in Tables (3.2), (3.4), (3.6), (3.8), (3.10) and (3.12), the following can be observed:

1) The proposed model of the microphone array system achieved a beam scanning of angles between *30* and *150* degrees, with a resolution of two degrees for each step, based on the amplitude weighting technique.

2) Using an array of nine elements in the different scenarios achieves half-power beamwidth between (*22* to *34*) degrees as demonstrated in Figure (3.22).

3) The maximum amplitude for the main beam for the different cases is within the range (*255* to *227*) units as depicted in Figure (3.23).

4) In all cases, the sidelobe level is *zero* or so small that can be proximated to *zero*.

Furthermore, Figures (3.22) and (3.23) demonstrated that the beam patterns in different angles do not have the same specifications in HPBW and the maximum amplitude in the scan angle direction. However, it can be observed that there is a similarity in the HPBW and the maximum amplitude within the beam pattern in the following groups of angels:

A. All the beam patterns in the angles (*30, 50, 70, 90, 110, 130, and 150* degrees) have the same HPBW of *22* degrees and the same maximum amplitude of *256* in the desired direction of the beam.

B. The HPBW of *34* degrees and maximum amplitude of *250* can be obtained from the following beam pattern group that directed in the angles (*32, 48, 52, 68, 72, 88, 92, 108, 112, 128, 132, and 148* degrees).

C. The following group angles produce HPBW of 33 degrees and the maximum amplitude of 250: (*34, 46, 54, 66, 74, 86, 94, 106, 114, 126, 134, and 146* degrees).

D. The beam patterns in the angles (*36, 44, 56, 64, 76, 84, 96, 104, 116, 124, 136, and 144* degrees) have the same HPBW of *32* degrees and the same maximum amplitude of *230* in the desired direction of the beam.

E. The HPBW of 29 degrees and maximum amplitude of 230 can be obtained from the following beam pattern group that is directed in the angles: (*38, 42, 58, 62, 78, 82, 98, 102, 118, 122, 138, and 142* degrees).

F. The following group angles produce HPBW of 27 degrees and the maximum amplitude of 227: (*40, 60, 80, 100, 120, and 140,* degrees).
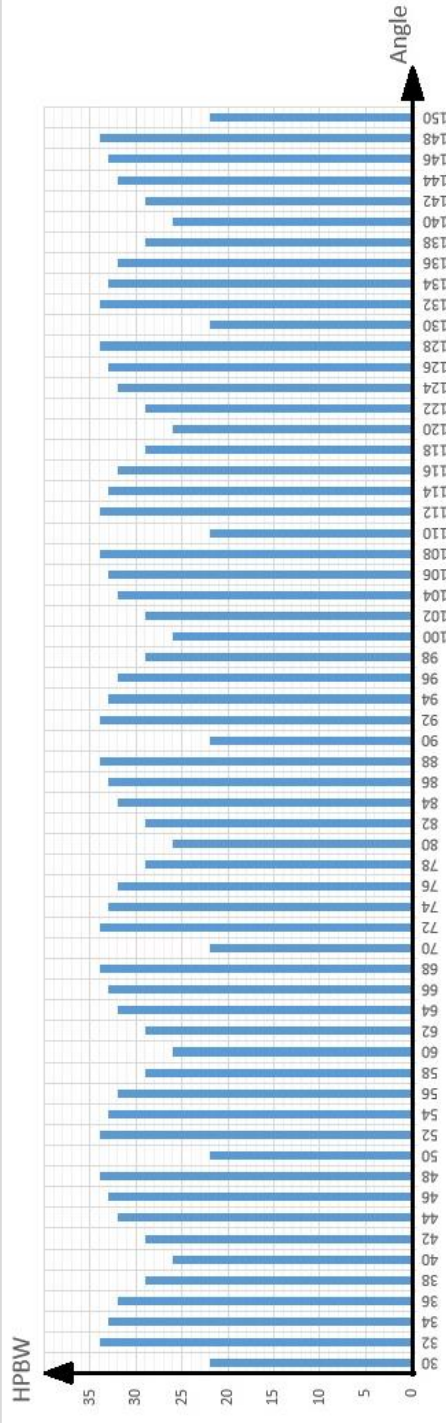
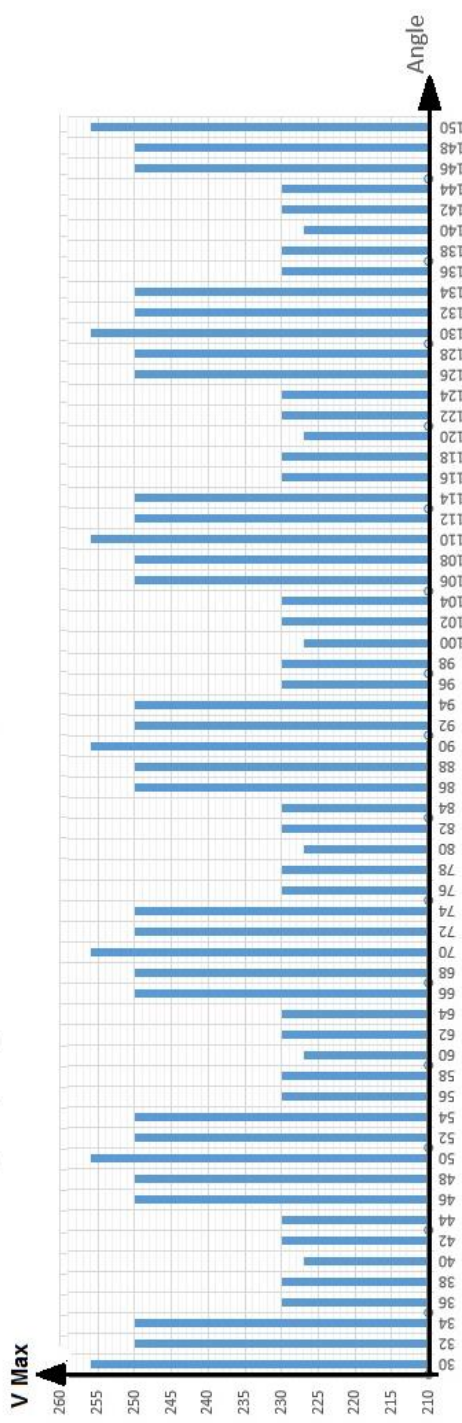**Figure (3-22)** HPBW for nine elements array vers main lobe direction



Figure (3-23) Maximum amplitude for nine elements array vers main lobe direction

55

## 3.6 Comparison to Other Works

**Table (3.13):** Compare the Proposed Design with Other Works

| Reference | Weighting Type | Number of array element | Scanning Range |
|---|---|---|---|
| [15] | Amplitude | 3 | $\pm 20°$ |
| [16] | Amplitude | 7 | $\pm 13°$ |
| [27] | Amplitude | 2 | $\pm 30°$ |
| Proposed design | Amplitude | 57 | Scan from 30°- 150° with scan angle 20° |

# CHAPTER FOUR

# Design of Acoustic Tracking System

## 4.1 Overview

In this chapter, the acoustic tracking system using the proposed microphone array beam scanning system in chapter three is explained. The results of this system will analyzed and discussed.

## 4.2 Introduction to the Proposed Acoustic Tracking System Design

As illustrated in Chapter Two section (2-6), there are three types of tracking techniques; Lobe switching, Conical scanning, and Monopules tracking. In all of these technologies either one beam pattern is used as in conical scanning, or by using two or more than two identical beams patterns. However the proposed beam scanning system in Chapter Three does not achieve identical beams patterns in all cases or scan angles.

But the good spot point of the beam scanning system results is the similarity in the HPBW and the maximum amplitude between the scanning angles within each of the six groups listed in Chapter Three Section 3.4, benefiting from this phenomenon. The design of Lobe switching tracking system can be assign the difference between the center of the two lobs as (beam pattern) by 20 degrees. In this way the identical between the two beam patterns will be achieved in all cases within the tracking range angles from 30 to 150 degrees.

## 4.3 The Proposed Acoustic Tracking System Based on Lobe Switching Technique

The basic strategy of the lobe switching tracking technique depends on the directed antenna beam being rapidly switched between two positions around the estimated location of the target.

The levels of the echo signals that reflected from the target will fluctuate according to the deviation from the center of the beam pattern in the switching rate of the lobes. If the two lobes are identical, the difference between the two levels that came from the two switching lobes can represent the deviation from the center of the zone covered by these two lobes. If the difference of these two levels approaches zero the location of the target will be in the center of this zone otherwise the sign of the difference (minus or plus) refers to the deviation from the zone center either left or right, while the absolute value between the two returned echo signals indicate to the deviation in degrees from the coverage zone center.

When the difference of levels between the two echoes signals goes up to a specific threshold value, then the present two lobes must be replaced by two new lobes either to the left or right according to the sign of the difference between the echo signals.

The lobe switching tracking system tries to make the value for the difference of the two echoes signals which approaches to zero that represents the perfect case of the tracking process. Then, one can abstract the lobe switching tracking system by the following steps and the flowchart shown in Figure (4.1).

1. Getting the initial location of the target from external sources or the target localization technique.

2. Generating the two suitable lobes by using the beam scanning system illustrated in Chapter Three, with tack in the care that the difference of the center of these two lobes must be equal to 20 degrees, and these lobes lie at the same angle from the estimated target location

3. Starting to operate one of them and switch off the other sequentially and exchange the operated lobe by the other and repeat this process in the same time interval.

4. Extracting the echo values from each step which represents the value of the echo signal from the lobe that operated at this moment.

5. Getting the difference between the two echoes that came from two different lobes by subtracting one of them from the other.

6. Comparing the subtraction result by the threshold value and go to the following cases:

   a. If the absolute value of the subtracting result is equal to or below the threshold value: no operation must be taken and the target is in the center or the scan zone of these two lobes.

   b. If the absolute value of the subtracting result is greater or equal to the threshold value we must take into consideration the sign of this result: if the sign is negative the present switching two lobes must be exchanged with two new lobes with a shift of the center of each of them by two degrees toward the subtracted echo lobe. Otherwise, the shift by two degrees must be subtracted from its echo of the lobe.

7. If no echo came from the two lobes we must go to step (1) and get to the initial location of the target and continue to the former steps (2,3,4,5, 6, …).
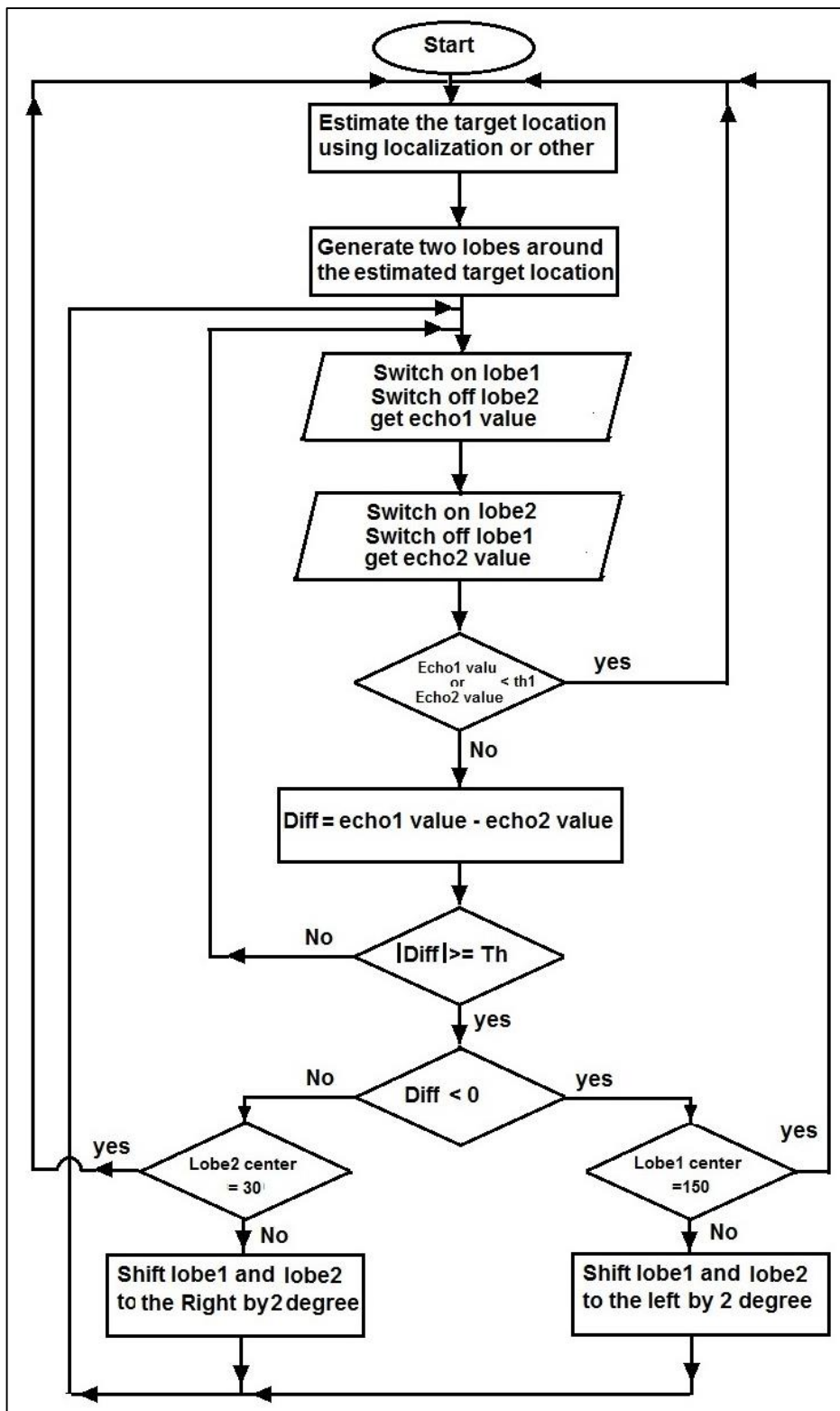
8. Repeating the past steps (1,2,3,4,5,6, ….).

**Figure (4.1):** Flowchart of the Proposed Acoustic Lobe Switching Tracking System.

60

## 4.4 The Proposed Acoustic Tracking System Results

Depending on the eight steps and the flowchart illustrated in the past paragraph a MATLAB program (listed in appendix A) has been written to implement the proposed acoustic tracking system based on the microphone array beamforming system using the lobe switching technique. The program was tested within the six zones which were illustrated in Chapter Three. The target trajectory has been suggested in a way that can test this tracking system in all directions of the target within the zone. In each zone the system tested for target movement from the center of the lobe1 to the center of the lob2. Figure (4.2) shows the beam pattern for lobe1 that is directed toward 30 degrees, lobe2 that is directed toward 50 degrees, the echo1 values, the echo 2 values, and the difference between echo1 values and echo2 values.
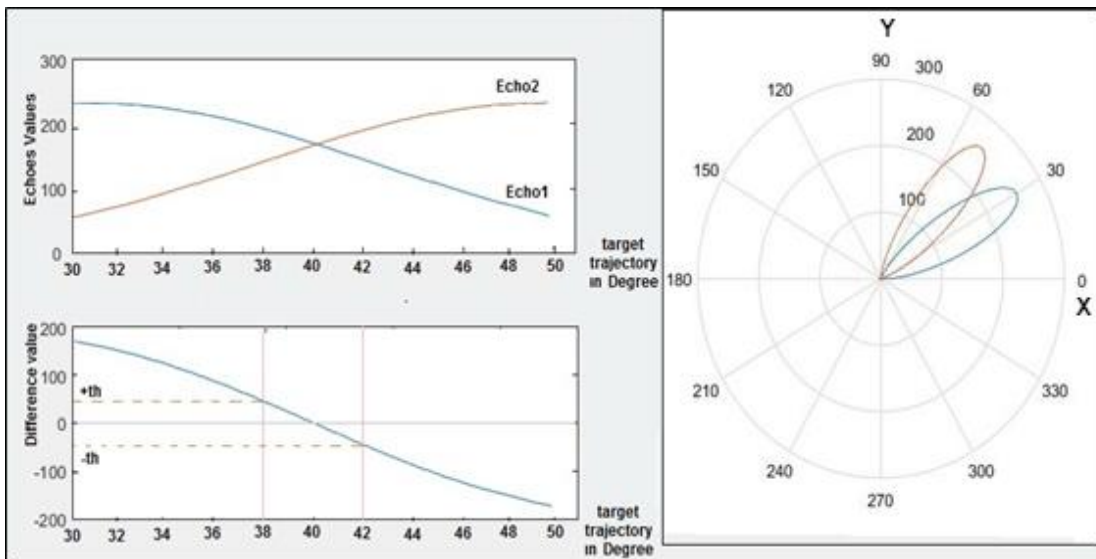


**Figure (4.2):** Echo1 and Echo2 Values, Difference Values, Lobe1(30), Lob2(50) Pattern.

Because of the similarity between the lobes that the centers of them directed toward (30, 50, 70, 90, 110, 130, 150), the echoes values and the different values that appeared in Figure (4-2) can be seen for the tracking cases in which lobe1 and lobe2 where directed toward ((50,70), (70,90), (90,110), (110,130), (130,150)) degrees.

61

Also, the similarity between the lobes patterns that the centers of them directed toward (32, 52, 72, 92, 112, 132) degrees, the tracking case in which the centers of lobes are (32,52) degrees shown in Figure (4.3), gives the same shape of the echoes values, and the different values the tracking case in which the centers of lobes are (52,72), (72,92),(92,112), and (112,132) degrees.
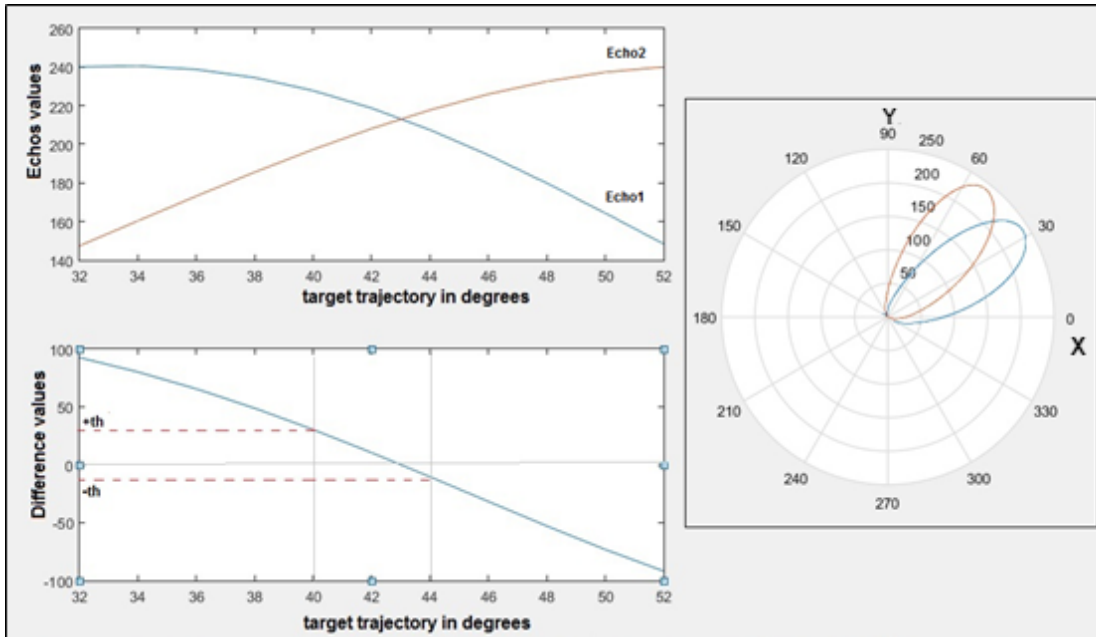


**Figure (4.3):** Echo1 and Echo2 Values, Difference Values, And Lobe1(32), Lob2(52) Pattern.

In the same way, the similarity of the specification for different lobes that is stated in paragraphs (3.4) in Chapter Three, we can assume:

1- Figure (4.4) shows echoes values, and the difference values in the tracking case in which the centers of lobes are (34,54) which can be considered that they are a sample of the tracking cases that the center of lobes are in (54,74), (74,94), (94,114), and (114,134) degrees.

2- Figure (4.5) shows echoes values, and the difference values in the tracking case in which the centers of lobes are (36,56) which can be considered that they are a sample of the tracking cases that the center of lobes is in (56,76), (76,96), (96,116), and (116,136) degrees.

3- Figure (4.6) shows echoes values, and the difference values in the tracking case in which the centers of lobes are (38,58) which can be considered that they are a sample of the tracking cases that the center of lobes is in (58,78), (78,98), (98,118), and (118,138) degrees.

4- Figure (4.7) shows echoes values, and the difference values in the tracking case in which the centers of lobes are (40,60) which can be considered that they are a sample of the tracking cases that the center of lobes is in (60,80), (80,100), (100,120), and (120,140) degrees.

5- Figure (4.8) shows echoes values, and the difference values in the tracking case in which the centers of lobes are (42,62) which can be considered that they are a sample of the tracking cases that the center of lobes is in (62,82), (82,102), (102,122), and (122,142) degrees.

6- Figure (4.9) shows echoes values, and the difference values in the tracking case in which the centers of lobes are (44,64) which can be considered that they are a sample of the tracking cases that the center of lobes is in (64,84), (84,104), (104,124), and (124,144) degrees.

7- Figure (4.10) shows echoes values, and the difference values in the tracking case in which the centers of lobes are (46,66) which can be considered that they are a sample of the tracking cases that the center of lobes is in (66,86), (86,106), (106,126), and (126,146) degrees.

8- Figure (4.11) shows echoes values, and the difference values in the tracking case in which the centers of lobes are (48,68) which can be considered that they are a sample of the tracking cases that the center of lobes is in (68,88), (88,108), (108,128), and (128,148) degrees.
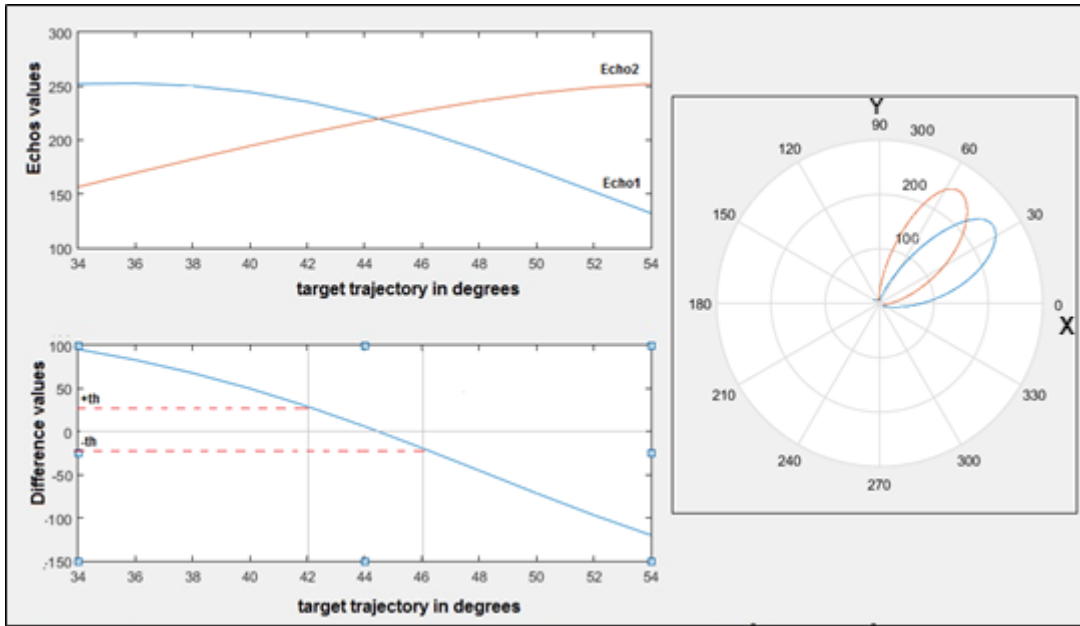
**Figure (4.4):** Echo1 and Echo2 Values, Difference Values, Lobe1(34), Lob2(54) Pattern.
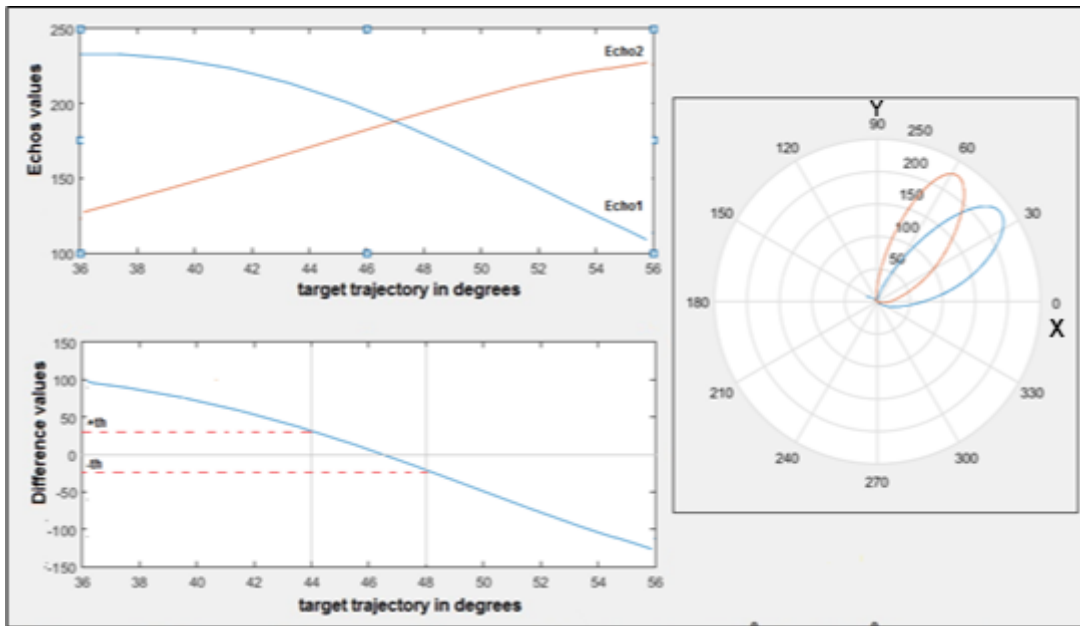


**Figure (4.5):** Echo1 and Echo2 Values, Difference Values, Lobe1(36), Lob2(56) Pattern.
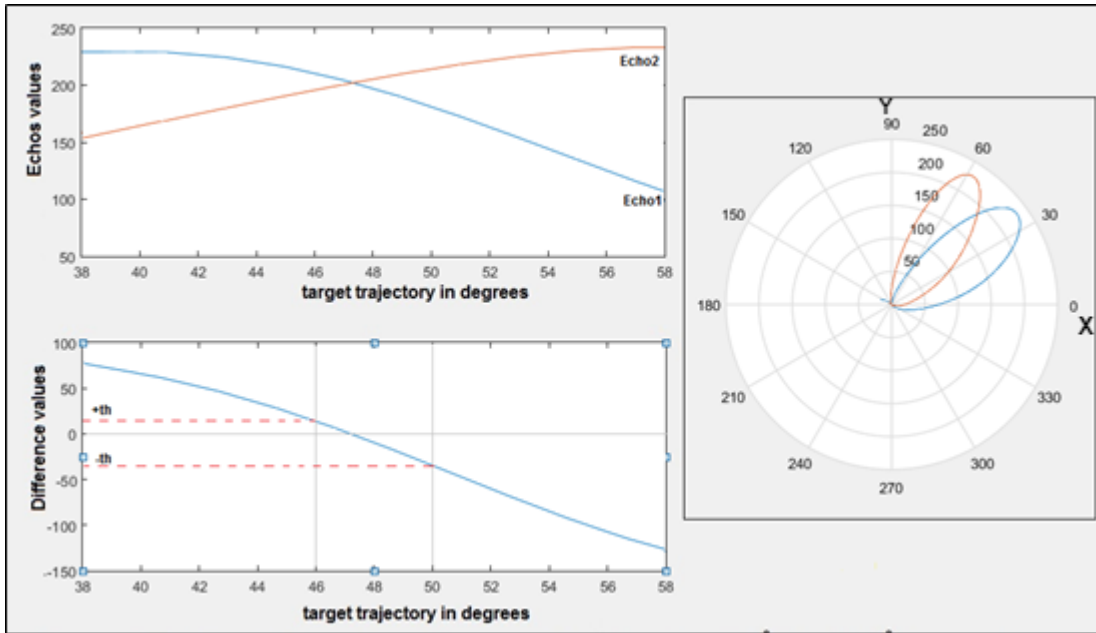
**Figure (4.6):** Echo1 and Echo2 Values, Difference Values, Lobe1(38), Lob2(58) Pattern.
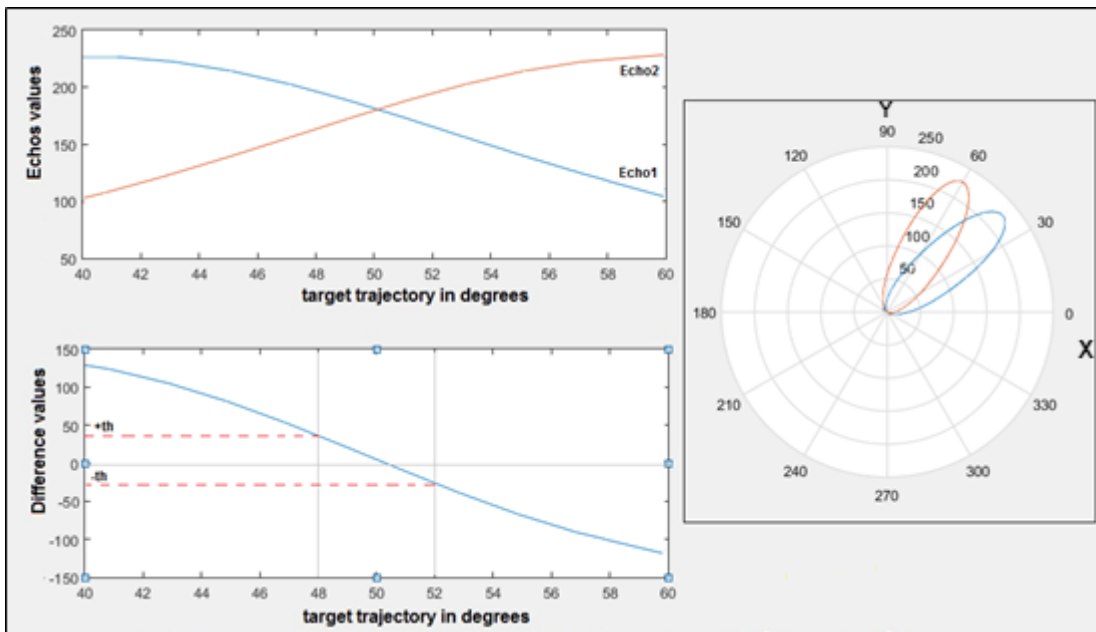


**Figure (4.7):** Echo1 and Echo2 Values, Difference Values, Lobe1(40), Lob2(60) Pattern.
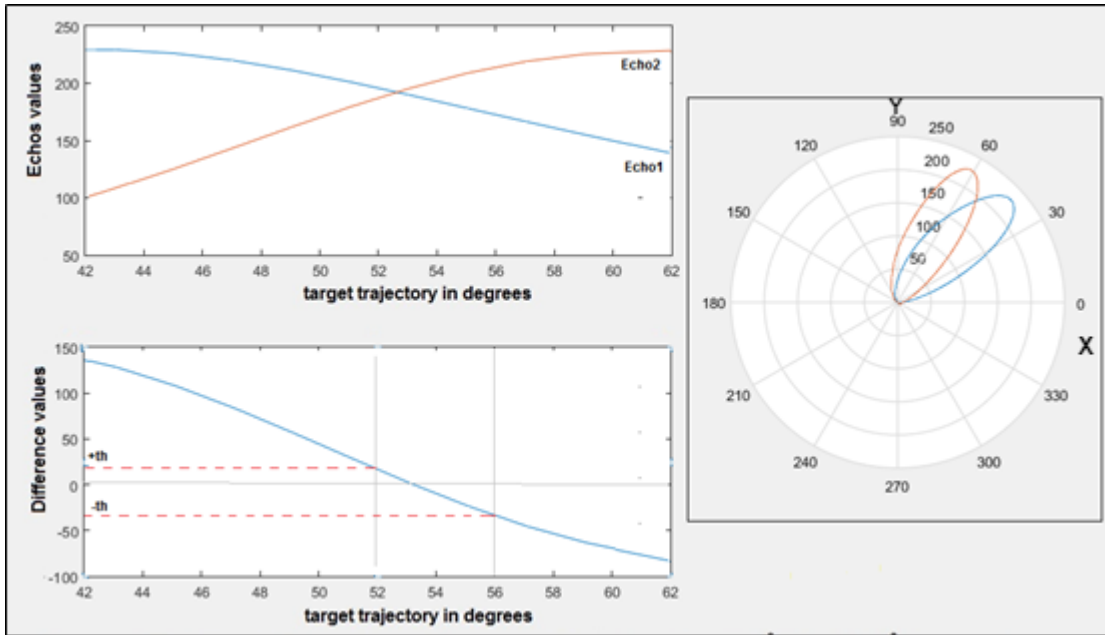
**Figure (4.8):** Echo1 and Echo2 Values, Difference Values, Lobe1(42), Lob2(62) Pattern.
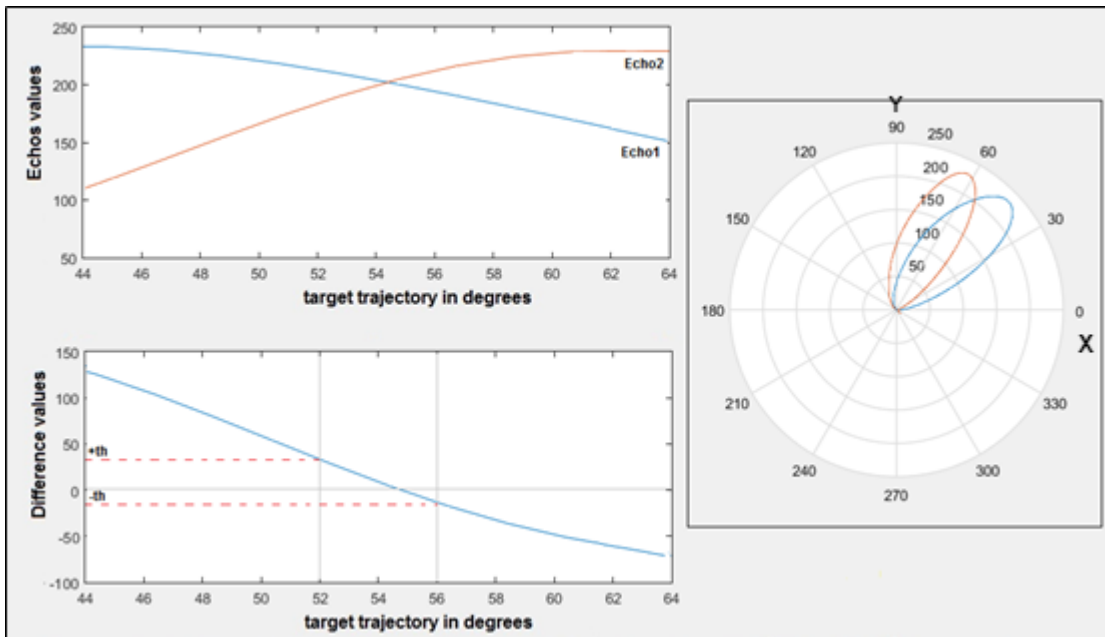


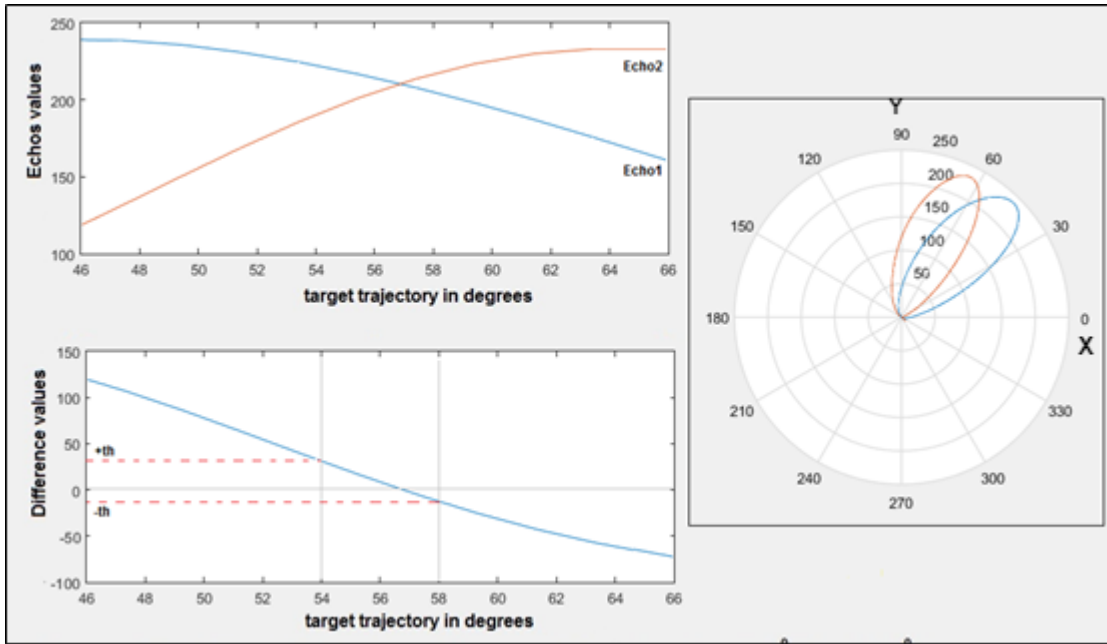**Figure (4.9):** Echo1 and Echo2 Values, Difference Values, Lobe1(44), Lob2(64) Pattern.

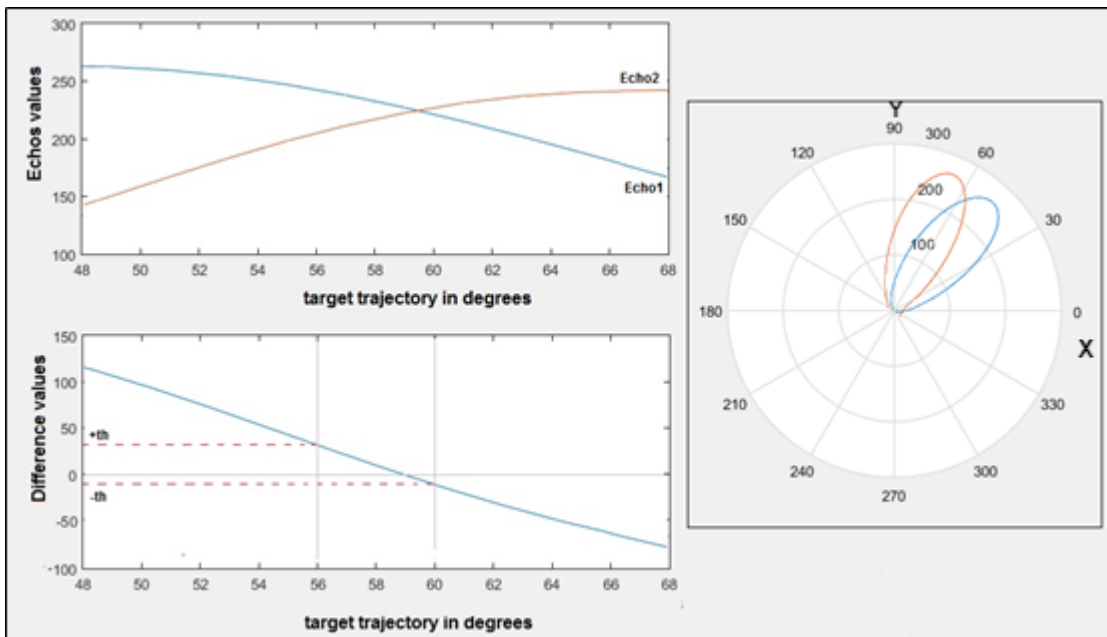**Figure (4.10):** Echo1 and Echo2 Values, Difference Values, Lobe1(46), Lob2(66) Pattern.



**Figure (4.11):** Echo1 and Echo2 Values, Difference Values, Lobe1(48), Lob2(68) Pattern.

## 4.5 Results Analysis

From the results illustrated in Figures (4.2) to (4.11), it can be observed that despite the similarity of the HPBW and the maximum values in the center of the lobes that participate in the lobe switching tracking process in each case, there was an error rate in calculating the location of the target within the tracking zone, where in the zero difference values (lobe1 echo-lobe2 echo) do not lie in the center of the tracking zone in this case. This is occurs because each of the two lobes used does not have a similarity in both sides around the center of this lobe. These error rates (the deviation of zero differences values from the tracking center) according to the tracking cases are shown in Figure (4.12). To decrease the effects of these errors, two threshold values must be assigned for each tracking case which represents the values of the two echoes difference. One of them is at the right side from the center of the tracking zone by 2 degrees (+th) and the other at the left side from the tracking zone center (-th). Table (4.1) listed the suggested threshold values for the ten tracking cases illustrated above.
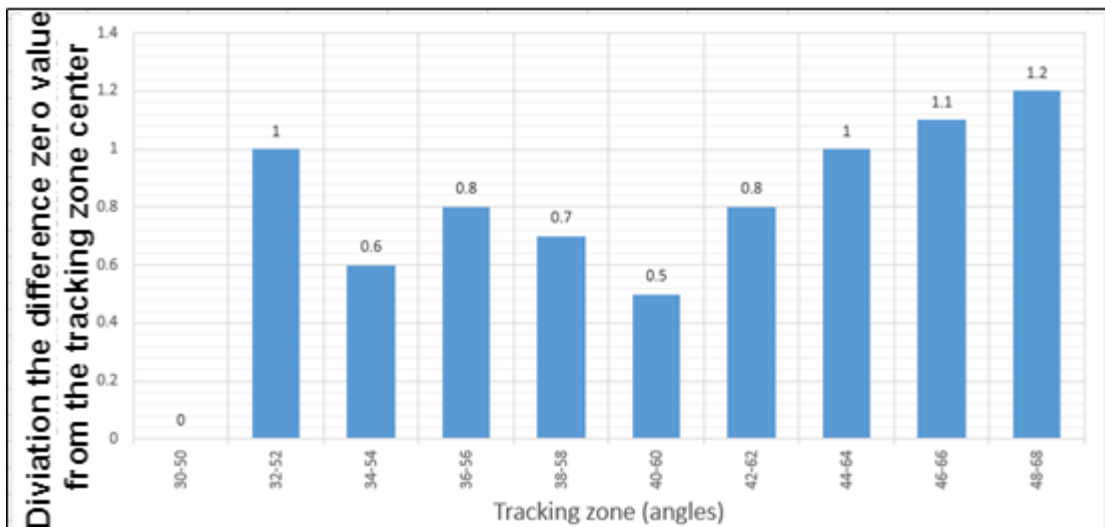


**Figure (4.12):** The Derivation of Zero Differences Values from the Tracking Zones Center.

**Table (4.1):** The Suggested Threshold Values for the Different Tracking Zones.

| Cases | Tracking zone | +Ve values | -Ve values |
|-------|---------------|------------|------------|
| 1 | (30 - 50) | 50 | -50 |
| 2 | (32 – 52) | 75 | -25 |
| 3 | (34 – 54) | 60 | -40 |
| 4 | (36 – 56) | 55 | -45 |
| 5 | (38 – 58) | 25 | -75 |
| 6 | (40 – 60) | 65 | -35 |
| 7 | (42 – 62) | 30 | -70 |
| 8 | (44 – 64) | 70 | -30 |
| 9 | (46 – 66) | 75 | -25 |
| 10 | (48 – 68) | 80 | -20 |

# Chapter Five

# Conclusion and Future Work Suggestions

## 5.1 - Conclusions

From this work, the following can be concluded:

1.  Using the amplitude weighting technique, the proposed microphone array construction shown in Figure (3.1) was successful in beam scanning through the zone from 30 degrees to 150 degrees with a two-degree resolution.

2.  The amplitude weighting technique for the linear array can only achieve beam scanning if one side of the array has deviated from the other side's distribution line direction.

3.  The amplitude weighting causes the beam pattern to be distorted.

4.  The binomial distribution for the array coefficients reduces or cancels the side lobes of the array pattern.

5.  The proposed acoustic tracking system can be used for applications that do not require high tracking angle resolution.

6.  Because there is no symmetry between the two sides of the lobes around the center of the lobe, the acoustic tracking system based on the microphone array using amplitude weighting produces inaccurate results.

**5.2 - Suggestions for Future Works**

1 - Increasing the resolution tracking system by increasing the number of elements of the array in the work which leads to a decrease in the HPBW for the scanning lobes.

2   - Trying to get identical specifications for all scanning lobes by using intelligent or adaptive algorithms for the calculation of the array coefficients.

3 - Trying to get a symmetrical beam pattern around the center of the lobe for the scanning lobes.

4 - Increasing the tracking zone from (30-150) degrees to or more than (0-180) degrees by increasing the array group to this proposed tracking system.

5 - Studying and developing the proposed tracking system to be suitable for tracking speech signals or wideband acoustic signals.

6 - Implementing the proposed tracking system using DSP or FPGA kits or other tools.

7 – Trying to use Dolph-Chebyshev array for amplitude excitation.

# References

[1] Li, H. J., & Kiang, Y. W. Radar and inverse scattering. *The Electrical Engineering Handbook*, pp.671-690. 2005

[2] Heupel, M. R., Semmens, J. M., & Hobday, A. J. "Automated acoustic tracking of aquatic animals: scales, design and deployment of listening station arrays." *Marine and Freshwater Research*, vol. 57, no.1, pp.1-13, 2006.

[3] Benesty, J., Chen, J., & Huang, Y. *Microphone array signal processing* (Vol. 1). Springer Science & Business Media, 2008. .

[4] Lei, L., Lie, J. P., Gershman, A. B., & See, C. M. S. "Robust adaptive beamforming in partly calibrated sparse sensor arrays." *IEEE Transactions on Signal Processing*, vol. 58, no.3, pp. 1661-1667, 2009.

[5] Uchendu, I., & Kelly, J. R. "Survey of beam steering techniques available for millimeter wave applications." *Progress In Electromagnetics Research B*, vol. 68, pp.35-54, 2016.

[6] Nayeri, P., Yang, F., & Elsherbeni, A. Z. "Beam-Scanning Reflectarray Antennas: A technical overview and state of the art." *IEEE Antennas and Propagation Magazine*, vol. 57, no.4, pp.32-47, 2015.

[7] Spalt, T. B. *Background noise reduction in wind tunnels using adaptive noise cancellation and cepstral echo removal techniques for microphone array applications* (Doctoral dissertation, Virginia Tech), 2010.

[8] Billingsley, J., & Kinns, R. "The acoustic telescope." *Journal of Sound and Vibration*, vol. 48, no.4, pp.485-510, 1976.

[9] Brooks, T. F., Marcolini, M. A., & Pope, D. S. "Main rotor broadband noise study in the DNW." *Journal of the American Helicopter Society*, vol.34, no. 2, pp.3-12, 1989.

[10] Gramann, R. A., & Mocio, J. W. "Aeroacoustic measurements in wind tunnels using adaptive beamforming methods." *The Journal of the Acoustical Society of America*, vol. 97, no.6, pp.3694-3701, 1995.

[11] Dam, H. Q., Nordholm, S., Grbic, N., & Dam, H. H. "Speech enhancement employing adaptive beamformer with recursively updated soft constraints." In *Proc. IWAENC* (pp. 307-310), Sep. 2003.

[12] Hou, Z., & Jia, Y. "A new adaptive blocking matrix with exact FIR structure for robust generalized sidelobe canceller." In *International Workshop on Acoustic Echo and Noise Control* (pp. 239-242), 2003.

[13] Abad Gareta, A. *A multi-microphone approach to speech processing in a smart-room environment*. Universitat Politècnica de Catalunya, 2007.

[14] Moir, T. J., & Qi, T. Automotive 3-microphone noise canceller in a frequently moving noise source environment. 2007.

[15] Sayidmarie, K. H., & Jasem, B. M. "Performance of array beam scanning by variation of amplitude excitation." In *4th Int. Multi-Conference on Systems, Signals & Devices*, Vol. 3, pp. 19-22, March 2007.

[16] Sayidmarie, K. H., & Jasem, B. J. "Amplitude-only beam scanning in linear antenna arrays." In *2010 7th International Multi-Conference on Systems, Signals and Devices*, pp. 1-6, June 2010.

[17] Krüger, A., Warsitz, E., Häb-Umbach, R., & durch Eigenwertzerlegung, S. Blinde akustische Strahlformung für Anwendungen im KFZ. *34. Deutsche Jahrestagung für Akustik*. 2008.

[18] Souden, M., Benesty, J., & Affes, S. "A study of the LCMV and MVDR noise reduction filters. *IEEE Transactions on Signal Processing*, vol. 58, no. 9, pp. 4925-4935, 2010.

[19] Comminiello, D., Scarpiniti, M., Parisi, R., Cirillo, A., Falcone, M., & Uncini, "A. Multi-stage collaborative microphone array beamforming in presence of nonstationary interfering signals." In *Machine Listening in Multisource Environments*, 2011.

[20] Suleiman, A., Mahmod, M., & Hamdon, O. W. "Real-Time TMS3206713 DSP-Based Adaptive Noise Cancellation for Speech Signal Processing." In *4th Mosharaka International Conference on Communications, Computers and Applications (MIC-CCA 2011)* (Vol. 4, No. 1). Mosharaka for Research and Studies. 2011.

[21] Sayidmarie, K. H., & Saghurchy, M. N. "Array beam scanning by variation of elements amplitude-only excitations." In *2011 4th IEEE*

*International Symposium on Microwave, Antenna, Propagation and EMC Technologies for Wireless Communications*, pp. 749-753, Nov. 2011.

[22] Mohammed, J. R. and Sayidmarie, K. H. "A new technique for obtaining wide-angular nulling in the sum and difference patterns of monopulse antenna." *IEEE Antennas and Wireless Propagation Letters*, vol. 11, pp.1245-1248, 2012.

[23] Omar W.H. "DSP Based Adaptive Noise Cancellation For Speech Signal Processing." *IEEE*, 2012.

[24] Tronc, J., Angeletti, P., Song, N., Haardt, M., Arendt, J., & Gallinaro, G. "Overview and comparison of on-ground and on-board beamforming techniques in mobile satellite service applications." *International Journal of Satellite Communications and Networking*, vol. 32, no.4, pp. 291-308, 2013.

[25] Bodhe, S. K., Hogade, B. G., & Nandgaonkar, S. D. "Beamforming Techniques for Smart Antenna using Rectangular." *International Journal of Electrical and Computer Engineering*, vol. 4, no. 2, p. 257, 2014.

[26] Younis, M., Lopez-Dekker, P., Krieger, G., & Moreira, A. "Digital beamforming signal-to-noise ratio gain in multi-channel SAR." In *Proceedings of the IEEE International Geoscience and Remote Sensing Symposium (IGARSS)*, 2015.

[27] Sayidmarie, K. H., & Shakeeb, A. R. "Array Beam Scanning and Switching by Variation of Amplitude-Only Excitations." *International Journal of Electromagnetics and Applications*, vol. 7, no. 2, pp. 25-30, 2017.

[28] Shakeeb, A. R., & Sayidmarie, K. H. "A cellular base station antenna configuration for variable coverage. *International Journal of Electrical and Computer Engineering (IJECE)*, vol. 9, no. 3, pp. 1887-1893, 2019.

[29] Huang, G., Chen, J., & Benesty, J. "On the design of differential beamformers with arbitrary planar microphone array geometry." *The Journal of the Acoustical Society of America*, vol. 144, no. 1, EL66-EL70. 2018.

[30] Grondin, F., & Michaud, F. "Lightweight and optimized sound source localization and tracking methods for open and closed microphone array configurations." *Robotics and Autonomous Systems*, vol. 113, pp. 63-80, 2019.

[31] Merino-Martínez, et al. "Assessment of the accuracy of microphone array methods for aeroacoustic measurements." *Journal of Sound and Vibration*, vol. 470, p. 115176. 2020.

[32] Khatami, I., & Abdollahzadeh Jamalabadi, M. Y. "Optimal design of microphone array in a planar circular configuration by genetic algorithm enhanced beamforming." *Journal of Thermal Analysis and Calorimetry*, vol. 145, no. 4, pp.1817-1825, 2021.

[33] Rumsey, Francis, and Tim McCormick. *Sound and recording: an introduction*. Routledge, 2012.

[34] Raichel, Daniel R. *The science and applications of acoustics*. Springer Science & Business Media, 2006.

[35] Balanis C. A., *Antenna Theory Analysis and Design*, 4th ed. Hoboken, New Jersey: John Wiley & Sons, Inc., 2016.

[36] Vook, Frederick W., Amitava Ghosh, and Timothy A. Thomas. "MIMO and beamforming solutions for 5G technology." *2014 IEEE MTT-S International Microwave Symposium (IMS2014)*. IEEE, 2014.

[37] Al-Tarifi, Monjed A., Mohammad S. Sharawi, and Atif Shamim. "Massive MIMO antenna system for 5G base stations with directive ports

and switched beamsteering capabilities." *IET Microwaves, Antennas & Propagation* vol. 12, no.10, pp.1709-1718, 2018.

[38] Haykin, S., Zia, A., Arasaratnam, I., & Xue, Y. "Cognitive tracking radar." In *2010 IEEE Radar Conference*, pp. 1467-1470, May2010 .

[39] Jensen, Christian S., and Stardas Pakalnis. "TRAX-Real-World Tracking of Moving Objects." *VLDB*. Vol. 7. 2007.

[40] Hussein, Mahmoud Yahia, and Abdelrasoul Jabar Alzubaidi. "Target Tracking Radar." *Target* 4.05, 2014.

[41] Aboul-Seoud, Ahmed K., et al. "A conformal conical phased array antenna for modern radars." *2014 IEEE Aerospace Conference*, 2014.

[42] Sherman, Samuel M., and Daivd K. Barton. *Monopulse principles and techniques*. Artech House, 2011.

# Appendix-A

## Matlab Code

```matlab
clc;
close all;
clear all;

lambda=342/1500; % velocity/operation frequency
k=(2*pi)/lambda;
thetadeg=0:1:360;
thetarad=deg2rad(thetadeg);
d=lambda/2;
theta0=90;
dthla=-0; dthra=0;
dthlb=-20; dthrb=+20;
dthlc=-40; dthrc=40;
dthld=-60; dthrd=60;
dthle=60; dthre=-60;
dthlf=40; dthrf=-40;
dthlg=20; dthrg=-20;
dthlrada=deg2rad(dthla);
dthrrada=deg2rad(dthra);
dthlradb=deg2rad(dthlb);
dthrradb=deg2rad(dthrb);
dthlradc=deg2rad(dthlc);
dthrradc=deg2rad(dthrc);
dthlradd=deg2rad(dthld);
dthrradd=deg2rad(dthrd);
dthlrade=deg2rad(dthle);
dthrrade=deg2rad(dthre);
dthlradf=deg2rad(dthlf);
dthrradf=deg2rad(dthrf);
dthlradg=deg2rad(dthlg);
dthrradg=deg2rad(dthrg);
theta0rad=deg2rad(theta0);
beta=-k*d*cos(theta0rad);


A(:,:,30)=[0,0,0,0,70,0,0,0,0;0,0,0,0,0,0,0,0,0;0,0,0,0,0,0,0,0,0;0,0,
0,0,0,0,0,0,0;1,8,28,56,0,56,28,8,1;0,0,0,0,0,0,0,0,0;0,0,0,0,0,0,0,0,
0];
A(:,:,50)=[0,0,0,0,70,0,0,0,0;0,0,0,0,0,0,0,0,0;0,0,0,0,0,0,0,0,0;0,0,
0,0,0,0,0,0,0;0,0,0,0,0,0,0,0,0;1,8,28,56,0,56,28,8,1;0,0,0,0,0,0,0,0,
0];
A(:,:,70)=[0,0,0,0,70,0,0,0,0;0,0,0,0,0,0,0,0,0;0,0,0,0,0,0,0,0,0;0,0,
0,0,0,0,0,0,0;0,0,0,0,0,0,0,0,0;0,0,0,0,0,0,0,0,0;1,8,28,56,0,56,28,8,
1];
A(:,:,90)=[1,8,28,56,70,56,28,8,1;0,0,0,0,0,0,0,0,0;0,0,0,0,0,0,0,0,0;
0,0,0,0,0,0,0,0,0;0,0,0,0,0,0,0,0,0;0,0,0,0,0,0,0,0,0;0,0,0,0,0,0,0,0,
0];
A(:,:,110)=[0,0,0,0,70,0,0,0,0;1,8,28,56,0,56,28,8,1;0,0,0,0,0,0,0,0,0
;0,0,0,0,0,0,0,0,0;0,0,0,0,0,0,0,0,0;0,0,0,0,0,0,0,0,0;0,0,0,0,0,0,0,0
,0];
A(:,:,130)=[0,0,0,0,70,0,0,0,0;0,0,0,0,0,0,0,0,0;1,8,28,56,0,56,28,8,1
;0,0,0,0,0,0,0,0,0;0,0,0,0,0,0,0,0,0;0,0,0,0,0,0,0,0,0;0,0,0,0,0,0,0,0
,0];
A(:,:,150)=[0,0,0,0,70,0,0,0,0;0,0,0,0,0,0,0,0,0;0,0,0,0,0,0,0,0,0;1,8
,28,56,0,56,28,8,1;0,0,0,0,0,0,0,0,0;0,0,0,0,0,0,0,0,0;0,0,0,0,0,0,0,0
,0];
```

A

A(:,:,32)=[0,0,0,0,70,0,0,0,0;0,0,0,0,0,0,0,0,0;0,0,0,0,0,0,0,0,0;0,0,
0,0,0,0,0,0,0;1.8,14.4,50.4,100.8,0,0,0,0,0;0,0,0,0,0,9.6,3.6,1.2,0.1;
0,0,0,0,0,0,0,0,0];
A(:,:,34)=[0,0,0,0,70,0,0,0,0;0,0,0,0,0,0,0,0,0;0,0,0,0,0,0,0,0,0;0,0,
0,0,0,0,0,0,0;2.16,16.6,58.4,98,0,0,0,0,0;0,0,0,0,0,15.8,9.2,2.0,0.3;0
,0,0,0,0,0,0,0,0];
A(:,:,36)=[0,0,0,0,70,0,0,0,0;0,0,0,0,0,0,0,0,0;0,0,0,0,0,0,0,0,0;0,0,
0,0,0,0,0,0,0;1.6,12.8,44.8,89.6,0,0,0,0,0;0,0,0,0,0,22.4,11.2,3.2,0.4
;0,0,0,0,0,0,0,0,0];
A(:,:,38)=[0,0,0,0,70,0,0,0,0;0,0,0,0,0,0,0,0,0;0,0,0,0,0,0,0,0,0;0,0,
0,0,0,0,0,0,0;1.4,11.2,39.2,78.4,0,0,0,0,0;0,0,0,0,0,33.6,16.8,4.8,0.6
;0,0,0,0,0,0,0,0,0];
A(:,:,40)=[0,0,0,0,70,0,0,0,0;0,0,0,0,0,0,0,0,0;0,0,0,0,0,0,0,0,0;0,0,
0,0,0,0,0,0,0;1,8,28,56,0,0,0,0,0;0,0,0,0,0,56,28,8,1;0,0,0,0,0,0,0,0,
0];
A(:,:,42)=[0,0,0,0,70,0,0,0,0;0,0,0,0,0,0,0,0,0;0,0,0,0,0,0,0,0,0;0,0,
0,0,0,0,0,0,0;0.6,4.8,16.8,33.6,0,0,0,0,0;0,0,0,0,0,78.4,39.2,11.2,1.4
;0,0,0,0,0,0,0,0,0];
A(:,:,44)=[0,0,0,0,70,0,0,0,0;0,0,0,0,0,0,0,0,0;0,0,0,0,0,0,0,0,0;0,0,
0,0,0,0,0,0,0;0.4,3.2,11.2,22.4,0,0,0,0,0;0,0,0,0,0,89.6,44.8,12.8,1.6
;0,0,0,0,0,0,0,0,0];
A(:,:,46)=[0,0,0,0,70,0,0,0,0;0,0,0,0,0,0,0,0,0;0,0,0,0,0,0,0,0,0;0,0,
0,0,0,0,0,0,0;0.3,2.6,7.6,15.2,0,0,0,0,0;0,0,0,0,0,96.8,49.4,14.4,1.8;
0,0,0,0,0,0,0,0,0];
A(:,:,48)=[0,0,0,0,70,0,0,0,0;0,0,0,0,0,0,0,0,0;0,0,0,0,0,0,0,0,0;0,0,
0,0,0,0,0,0,0;0.1,1.0,4.2,9.2,0,0,0,0,0;0,0,0,0,0,110.8,58.4,18.4,2.4;
0,0,0,0,0,0,0,0,0];


A(:,:,52)=[0,0,0,0,70,0,0,0,0;0,0,0,0,0,0,0,0,0;0,0,0,0,0,0,0,0,0;0,0,
0,0,0,0,0,0,0;0,0,0,0,0,0,0,0,0;1.8,14.4,50.4,100.8,0,0,0,0,0;0,0,0,0,
0,9.6,3.6,1.2,0.1];
A(:,:,54)=[0,0,0,0,70,0,0,0,0;0,0,0,0,0,0,0,0,0;0,0,0,0,0,0,0,0,0;0,0,
0,0,0,0,0,0,0;0,0,0,0,0,0,0,0,0;2.16,16.6,58.4,98,0,0,0,0,0;0,0,0,0,0,
15.8,9.2,2.0,0.3];
A(:,:,56)=[0,0,0,0,70,0,0,0,0;0,0,0,0,0,0,0,0,0;0,0,0,0,0,0,0,0,0;0,0,
0,0,0,0,0,0,0;0,0,0,0,0,0,0,0,0;1.4,11.2,39.2,78.4,0,0,0,0,0;0,0,0,0,0
,33.6,16.8,4.8,0.6];
A(:,:,58)=[0,0,0,0,70,0,0,0,0;0,0,0,0,0,0,0,0,0;0,0,0,0,0,0,0,0,0;0,0,
0,0,0,0,0,0,0;0,0,0,0,0,0,0,0,0;1.6,12.8,44.8,89.6,0,0,0,0,0;0,0,0,0,0
,22.4,11.2,3.2,0.4];
A(:,:,60)=[0,0,0,0,70,0,0,0,0;0,0,0,0,0,0,0,0,0;0,0,0,0,0,0,0,0,0;0,0,
0,0,0,0,0,0,0;0,0,0,0,0,0,0,0,0;1,8,28,56,0,0,0,0,0;0,0,0,0,0,56,28,8,
1];
A(:,:,62)=[0,0,0,0,70,0,0,0,0;0,0,0,0,0,0,0,0,0;0,0,0,0,0,0,0,0,0;0,0,
0,0,0,0,0,0,0;0,0,0,0,0,0,0,0,0;0.8,6.4,22.4,44.8,0,0,0,0,0;0,0,0,0,0,
67.2,33.6,9.6,1.2];
A(:,:,64)=[0,0,0,0,70,0,0,0,0;0,0,0,0,0,0,0,0,0;0,0,0,0,0,0,0,0,0;0,0,
0,0,0,0,0,0,0;0,0,0,0,0,0,0,0,0;0.6,4.8,16.8,33.6,0,0,0,0,0;0,0,0,0,0,
78.4,39.2,11.2,1.4];
A(:,:,66)=[0,0,0,0,70,0,0,0,0;0,0,0,0,0,0,0,0,0;0,0,0,0,0,0,0,0,0;0,0,
0,0,0,0,0,0,0;0,0,0,0,0,0,0,0,0;0.4,3.2,11.2,22.4,0,0,0,0,0;0,0,0,0,0,
89.6,44.8,12.8,1.6];
A(:,:,68)=[0,0,0,0,90,0,0,0,0;0,0,0,0,0,0,0,0,0;0,0,0,0,0,0,0,0,0;0,0,
0,0,0,0,0,0,0;0,0,0,0,0,0,0,0,0;0.2,1.6,5.6,11.2,0,0,0,0,0;0,0,0,0,0,1
00.8,50.4,14.4,1.8];

B

A(:,:,72)=[0,0,0,0,70,11.2,5.6,1.6,0.2;0,0,0,0,0,0,0,0,0;0,0,0,0,0,0,0
,0,0;0,0,0,0,0,0,0,0,0;0,0,0,0,0,0,0,0,0;0,0,0,0,0,0,0,0,0;1.8,14.4,50
.4,100,0,0,0,0,0];
A(:,:,74)=[0,0,0,0,70,22.4,11.2,3.2,0.4;0,0,0,0,0,0,0,0,0;0,0,0,0,0,0,
0,0,0;0,0,0,0,0,0,0,0,0;0,0,0,0,0,0,0,0,0;0,0,0,0,0,0,0,0,0;1.6,12.8,4
4.8,89.6,0,0,0,0,0];
A(:,:,76)=[0,0,0,0,70,33.6,16.8,4.8,0.6;0,0,0,0,0,0,0,0,0;0,0,0,0,0,0,
0,0,0;0,0,0,0,0,0,0,0,0;0,0,0,0,0,0,0,0,0;0,0,0,0,0,0,0,0,0;1.4,11.2,3
9.2,78.4,0,0,0,0,0];
A(:,:,78)=[0,0,0,0,70,44.8,22.4,6.4,0.8;0,0,0,0,0,0,0,0,0;0,0,0,0,0,0,
0,0,0;0,0,0,0,0,0,0,0,0;0,0,0,0,0,0,0,0,0;0,0,0,0,0,0,0,0,0;1.2,9.6,33
.6,67.2,0,0,0,0,0];
A(:,:,80)=[0,0,0,0,70,56,28,8,1;0,0,0,0,0,0,0,0,0;0,0,0,0,0,0,0,0,0;0,
0,0,0,0,0,0,0,0;0,0,0,0,0,0,0,0,0;0,0,0,0,0,0,0,0,0;1,8,28,56,0,0,0,0,
0];
A(:,:,82)=[0,0,0,0,70,67.2,33.6,9.6,1.2;0,0,0,0,0,0,0,0,0;0,0,0,0,0,0,
0,0,0;0,0,0,0,0,0,0,0,0;0,0,0,0,0,0,0,0,0;0,0,0,0,0,0,0,0,0;0.8,6.4,22
.4,44.8,0,0,0,0,0];
A(:,:,84)=[0,0,0,0,70,78.4,39.2,11.2,1.4;0,0,0,0,0,0,0,0,0;0,0,0,0,0,0
,0,0,0;0,0,0,0,0,0,0,0,0;0,0,0,0,0,0,0,0,0;0,0,0,0,0,0,0,0,0;0.6,4.8,1
6.8,33.6,0,0,0,0,0];
A(:,:,86)=[0,0,0,0,70,89.6,44.8,12.8,1.6;0,0,0,0,0,0,0,0,0;0,0,0,0,0,0
,0,0,0;0,0,0,0,0,0,0,0,0;0,0,0,0,0,0,0,0,0;0,0,0,0,0,0,0,0,0;0.4,3.2,1
1.2,22.4,0,0,0,0,0];
A(:,:,88)=[0,0,0,0,70,100.8,50.4,14.4,1.8;0,0,0,0,0,0,0,0,0;0,0,0,0,0,
0,0,0,0;0,0,0,0,0,0,0,0,0;0,0,0,0,0,0,0,0,0;0,0,0,0,0,0,0,0,0;0.2,1.6,
5.6,11.2,0,0,0,0,0];

A(:,:,92)=[1.8,14.4,50.4,100.8,70,0,0,0,0;0,0,0,0,0,11.2,5.6,1.6,0.2;0
,0,0,0,0,0,0,0,0;0,0,0,0,0,0,0,0,0;0,0,0,0,0,0,0,0,0;0,0,0,0,0,0,0,0,0
;0,0,0,0,0,0,0,0,0];
A(:,:,94)=[1.6,12.8,45.4,89.6,70,0,0,0,0;0,0,0,0,0,22.4,11.2,3.2,0.4;0
,0,0,0,0,0,0,0,0;0,0,0,0,0,0,0,0,0;0,0,0,0,0,0,0,0,0;0,0,0,0,0,0,0,0,0
;0,0,0,0,0,0,0,0,0];
A(:,:,96)=[1.4,11.2,39.2,78.4,70,0,0,0,0;0,0,0,0,0,33.6,16.8,4.8,0.6;0
,0,0,0,0,0,0,0,0;0,0,0,0,0,0,0,0,0;0,0,0,0,0,0,0,0,0;0,0,0,0,0,0,0,0,0
;0,0,0,0,0,0,0,0,0];
A(:,:,98)=[1.2,9.6,33.6,67.2,70,0,0,0,0;0,0,0,0,0,44.8,22.4,6.4,0.8;0,
0,0,0,0,0,0,0,0;0,0,0,0,0,0,0,0,0;0,0,0,0,0,0,0,0,0;0,0,0,0,0,0,0,0,0;
0,0,0,0,0,0,0,0,0];
A(:,:,100)=[1,8,28,56,70,0,0,0,0;0,0,0,0,0,56,28,8,1;0,0,0,0,0,0,0,0,0
;0,0,0,0,0,0,0,0,0;0,0,0,0,0,0,0,0,0;0,0,0,0,0,0,0,0,0;0,0,0,0,0,0,0,0
,0];
A(:,:,102)=[0.8,6.4,22.8,44.8,70,0,0,0,0;0,0,0,0,0,67.2,33.6,9.6,1.2;0
,0,0,0,0,0,0,0,0;0,0,0,0,0,0,0,0,0;0,0,0,0,0,0,0,0,0;0,0,0,0,0,0,0,0,0
;0,0,0,0,0,0,0,0,0];
A(:,:,104)=[0.6,4.8,16.8,33.6,70,0,0,0,0;0,0,0,0,0,78.4,39.2,11.2,1.4;
0,0,0,0,0,0,0,0,0;0,0,0,0,0,0,0,0,0;0,0,0,0,0,0,0,0,0;0,0,0,0,0,0,0,0,
0;0,0,0,0,0,0,0,0,0];
A(:,:,106)=[0.4,3.2,11.2,22.4,70,0,0,0,0;0,0,0,0,0,89.6,44.8,12.8,1.6;
0,0,0,0,0,0,0,0,0;0,0,0,0,0,0,0,0,0;0,0,0,0,0,0,0,0,0;0,0,0,0,0,0,0,0,
0;0,0,0,0,0,0,0,0,0];
A(:,:,108)=[0.2,1.6,5.6,11.2,70,0,0,0,0;0,0,0,0,0,100.8,50.4,14.4,1.8;
0,0,0,0,0,0,0,0,0;0,0,0,0,0,0,0,0,0;0,0,0,0,0,0,0,0,0;0,0,0,0,0,0,0,0,
0;0,0,0,0,0,0,0,0,0];

A(:,:,112)=[0,0,0,0,70,0,0,0,0;1.8,14.4,50.4,100.8,0,0,0,0,0;0,0,0,0,0
,11.2,5.6,1.6,0.2;0,0,0,0,0,0,0,0,0;0,0,0,0,0,0,0,0,0;0,0,0,0,0,0,0,0,
0;0,0,0,0,0,0,0,0,0];

C

```
A(:,:,114)=[0,0,0,0,70,0,0,0,0;1.6,12.8,45.4,89.6,0,0,0,0,0;0,0,0,0,0,
22.4,11.2,3.2,0.4;0,0,0,0,0,0,0,0,0;0,0,0,0,0,0,0,0,0;0,0,0,0,0,0,0,0,
0;0,0,0,0,0,0,0,0,0];
A(:,:,116)=[0,0,0,0,70,0,0,0,0;1.4,11.2,39.2,78.4,0,0,0,0,0;0,0,0,0,0,
33.6,16.8,4.8,0.6;0,0,0,0,0,0,0,0,0;0,0,0,0,0,0,0,0,0;0,0,0,0,0,0,0,0,
0;0,0,0,0,0,0,0,0,0];
A(:,:,118)=[0,0,0,0,70,0,0,0,0;1.2,9.6,33.6,67.2,0,0,0,0,0;0,0,0,0,0,4
4.8,22.4,6.4,0.8;0,0,0,0,0,0,0,0,0;0,0,0,0,0,0,0,0,0;0,0,0,0,0,0,0,0,0
;0,0,0,0,0,0,0,0,0];
A(:,:,120)=[0,0,0,0,70,0,0,0,0;1,8,28,56,0,0,0,0,0;0,0,0,0,0,56,28,8,1
;0,0,0,0,0,0,0,0,0;0,0,0,0,0,0,0,0,0;0,0,0,0,0,0,0,0,0;0,0,0,0,0,0,0,0
,0];
A(:,:,122)=[0,0,0,0,70,0,0,0,0;0.8,6.4,22.8,44.8,0,0,0,0,0;0,0,0,0,0,6
7.2,33.6,9.6,1.2;0,0,0,0,0,0,0,0,0;0,0,0,0,0,0,0,0,0;0,0,0,0,0,0,0,0,0
;0,0,0,0,0,0,0,0,0];
A(:,:,124)=[0,0,0,0,70,0,0,0,0;0.6,4.8,16.8,33.6,0,0,0,0,0;0,0,0,0,0,7
8.4,39.2,11.2,1.4;0,0,0,0,0,0,0,0,0;0,0,0,0,0,0,0,0,0;0,0,0,0,0,0,0,0,
0;0,0,0,0,0,0,0,0,0];
A(:,:,126)=[0,0,0,0,70,0,0,0,0;0.4,3.2,11.2,22.4,0,0,0,0,0;0,0,0,0,0,8
9.6,44.8,12.8,1.6;0,0,0,0,0,0,0,0,0;0,0,0,0,0,0,0,0,0;0,0,0,0,0,0,0,0,
0;0,0,0,0,0,0,0,0,0];
A(:,:,128)=[0,0,0,0,70,0,0,0,0;0.2,1.6,5.6,11.2,0,0,0,0,0;0,0,0,0,0,10
0.8,50.4,14.4,1.8;0,0,0,0,0,0,0,0,0;0,0,0,0,0,0,0,0,0;0,0,0,0,0,0,0,0,
0;0,0,0,0,0,0,0,0,0];

A(:,:,132)=[0,0,0,0,70,0,0,0,0;0,0,0,0,0,0,0,0,0;1.8,14.4,50.4,100.8,0
,0,0,0,0;0,0,0,0,0,11.2,5.6,1.6,0.2;0,0,0,0,0,0,0,0,0;0,0,0,0,0,0,0,0,
0;0,0,0,0,0,0,0,0,0];
A(:,:,134)=[0,0,0,0,70,0,0,0,0;0,0,0,0,0,0,0,0,0;1.6,12.8,44.8,89.6,0,
0,0,0,0;0,0,0,0,0,22.4,11.2,3.2,0.4;0,0,0,0,0,0,0,0,0;0,0,0,0,0,0,0,0,
0;0,0,0,0,0,0,0,0,0];
A(:,:,136)=[0,0,0,0,70,0,0,0,0;0,0,0,0,0,0,0,0,0;1.4,11.2,39.2,78.4,0,
0,0,0,0;0,0,0,0,0,33.6,16.8,4.8,0.6;0,0,0,0,0,0,0,0,0;0,0,0,0,0,0,0,0,
0;0,0,0,0,0,0,0,0,0];
A(:,:,138)=[0,0,0,0,70,0,0,0,0;0,0,0,0,0,0,0,0,0;1.2,9.6,33.6,67.2,0,0
,0,0,0;0,0,0,0,0,44.8,22.8,6.4,0.8;0,0,0,0,0,0,0,0,0;0,0,0,0,0,0,0,0,0
;0,0,0,0,0,0,0,0,0];
A(:,:,140)=[0,0,0,0,70,0,0,0,0;0,0,0,0,0,0,0,0,0;0,0,0,0,0,56,28,8,1;1
,8,28,56,0,0,0,0,0;0,0,0,0,0,0,0,0,0;0,0,0,0,0,0,0,0,0;0,0,0,0,0,0,0,0
,0];
A(:,:,142)=[0,0,0,0,70,0,0,0,0;0,0,0,0,0,0,0,0,0;0.8,6.4,22.4,44.8,0,0
,0,0,0;0,0,0,0,0,67.2,33.6,9.6,1.2;0,0,0,0,0,0,0,0,0;0,0,0,0,0,0,0,0,0
;0,0,0,0,0,0,0,0,0];
A(:,:,144)=[0,0,0,0,70,0,0,0,0;0,0,0,0,0,0,0,0,0;0.6,4.8,16.8,33.6,0,0
,0,0,0;0,0,0,0,0,78.4,39.2,11.2,1.4;0,0,0,0,0,0,0,0,0;0,0,0,0,0,0,0,0,
0;0,0,0,0,0,0,0,0,0];
A(:,:,146)=[0,0,0,0,70,0,0,0,0;0,0,0,0,0,0,0,0,0;0.4,3.2,11.2,22.4,0,0
,0,0,0;0,0,0,0,0,89.6,44.8,12.8,1.6;0,0,0,0,0,0,0,0,0;0,0,0,0,0,0,0,0,
0;0,0,0,0,0,0,0,0,0];
A(:,:,148)=[0,0,0,0,70,0,0,0,0;0,0,0,0,0,0,0,0,0;0.2,1.6,5.6,11.2,0,0,
0,0,0;0,0,0,0,0,100.8,50.4,14.4,1.8;0,0,0,0,0,0,0,0,0;0,0,0,0,0,0,0,0,
0;0,0,0,0,0,0,0,0,0];

x=48;

al4=A(1,1,x); al3=A(1,2,x); al2=A(1,3,x); al1=A(1,4,x); a0=A(1,5,x);
ar1=A(1,6,x); ar2=A(1,7,x); ar3=A(1,8,x); ar4=A(1,9,x);
bl4=A(2,1,x); bl3=A(2,2,x); bl2=A(2,3,x); bl1=A(2,4,x); b0=A(2,5,x);
br1=A(2,6,x); br2=A(2,7,x); br3=A(2,8,x); br4=A(2,9,x);
cl4=A(3,1,x); cl3=A(3,2,x); cl2=A(3,3,x); cl1=A(3,4,x); c0=A(3,5,x);
cr1=A(3,6,x); cr2=A(3,7,x); cr3=A(3,8,x); cr4=A(3,9,x);
```

D

```
dl4=A(4,1,x); dl3=A(4,2,x); dl2=A(4,3,x); dl1=A(4,4,x); d0=A(4,5,x);
dr1=A(4,6,x); dr2=A(4,7,x); dr3=A(4,8,x); dr4=A(4,9,x);
el4=A(5,1,x); el3=A(5,2,x); el2=A(5,3,x); el1=A(5,4,x); e0=A(5,5,x);
er1=A(5,6,x); er2=A(5,7,x); er3=A(5,8,x); er4=A(5,9,x);
fl4=A(6,1,x); fl3=A(6,2,x); fl2=A(6,3,x); fl1=A(6,4,x); f0=A(6,5,x);
fr1=A(6,6,x); fr2=A(6,7,x); fr3=A(6,8,x); fr4=A(6,9,x);
gl4=A(7,1,x); gl3=A(7,2,x); gl2=A(7,3,x); gl1=A(7,4,x); g0=A(7,5,x);
gr1=A(7,6,x); gr2=A(7,7,x); gr3=A(7,8,x); gr4=A(7,9,x);


AFA=al4*exp(1i*(k*4*d*cos((thetarad+dthlrada))+beta))
+al3*exp(1i*(k*3*d*cos((thetarad+dthlrada))+beta))+
al2*exp(1i*(k*2*d*cos((thetarad+dthlrada))+beta))+
al1*exp(1i*(k*d*cos((thetarad+dthlrada))+beta))+a0+ ar1*exp(-
1i*(k*d*cos((thetarad-dthrrada))-beta)) +ar2*exp(-
1i*(k*2*d*cos((thetarad-dthrrada))-beta)) +ar3*exp(-
1i*(k*3*d*cos((thetarad-dthrrada))-beta)) +ar4*exp(-
1i*(k*4*d*cos((thetarad-dthrrada))-beta));
AFB=bl4*exp(1i*(k*4*d*cos((thetarad+dthlradb))+beta))
+bl3*exp(1i*(k*3*d*cos((thetarad+dthlradb))+beta))+
bl2*exp(1i*(k*2*d*cos((thetarad+dthlradb))+beta))+
bl1*exp(1i*(k*d*cos((thetarad+dthlradb))+beta))+b0+ br1*exp(-
1i*(k*d*cos((thetarad-dthrradb))-beta)) +br2*exp(-
1i*(k*2*d*cos((thetarad-dthrradb))-beta)) +br3*exp(-
1i*(k*3*d*cos((thetarad-dthrradb))-beta)) +br4*exp(-
1i*(k*4*d*cos((thetarad-dthrradb))-beta));
AFC=cl4*exp(1i*(k*4*d*cos((thetarad+dthlradc))+beta))
+cl3*exp(1i*(k*3*d*cos((thetarad+dthlradc))+beta))+
cl2*exp(1i*(k*2*d*cos((thetarad+dthlradc))+beta))+
cl1*exp(1i*(k*d*cos((thetarad+dthlradc))+beta))+c0+ cr1*exp(-
1i*(k*d*cos((thetarad-dthrradc))-beta)) +cr2*exp(-
1i*(k*2*d*cos((thetarad-dthrradc))-beta)) +cr3*exp(-
1i*(k*3*d*cos((thetarad-dthrradc))-beta)) +cr4*exp(-
1i*(k*4*d*cos((thetarad-dthrradc))-beta));
AFd=dl4*exp(1i*(k*4*d*cos((thetarad+dthlradd))+beta))
+dl3*exp(1i*(k*3*d*cos((thetarad+dthlradd))+beta))+
dl2*exp(1i*(k*2*d*cos((thetarad+dthlradd))+beta))+
dl1*exp(1i*(k*d*cos((thetarad+dthlradd))+beta))+d0+ dr1*exp(-
1i*(k*d*cos((thetarad-dthrradd))-beta)) +dr2*exp(-
1i*(k*2*d*cos((thetarad-dthrradd))-beta)) +dr3*exp(-
1i*(k*3*d*cos((thetarad-dthrradd))-beta)) +dr4*exp(-
1i*(k*4*d*cos((thetarad-dthrradd))-beta));


AFe=el4*exp(1i*(k*4*d*cos((thetarad+dthlrade))+beta))
+el3*exp(1i*(k*3*d*cos((thetarad+dthlrade))+beta))+
el2*exp(1i*(k*2*d*cos((thetarad+dthlrade))+beta))+
el1*exp(1i*(k*d*cos((thetarad+dthlrade))+beta))+e0+ er1*exp(-
1i*(k*d*cos((thetarad-dthrrade))-beta)) +er2*exp(-
1i*(k*2*d*cos((thetarad-dthrrade))-beta)) +er3*exp(-
1i*(k*3*d*cos((thetarad-dthrrade))-beta)) +er4*exp(-
1i*(k*4*d*cos((thetarad-dthrrade))-beta));
AFf=fl4*exp(1i*(k*4*d*cos((thetarad+dthlradf))+beta))
+fl3*exp(1i*(k*3*d*cos((thetarad+dthlradf))+beta))+
fl2*exp(1i*(k*2*d*cos((thetarad+dthlradf))+beta))+
fl1*exp(1i*(k*d*cos((thetarad+dthlradf))+beta))+f0+ fr1*exp(-
1i*(k*d*cos((thetarad-dthrradf))-beta)) +fr2*exp(-
1i*(k*2*d*cos((thetarad-dthrradf))-beta)) +fr3*exp(-
1i*(k*3*d*cos((thetarad-dthrradf))-beta)) +fr4*exp(-
1i*(k*4*d*cos((thetarad-dthrradf))-beta));
AFg=gl4*exp(1i*(k*4*d*cos((thetarad+dthlradg))+beta))
+gl3*exp(1i*(k*3*d*cos((thetarad+dthlradg))+beta))+
gl2*exp(1i*(k*2*d*cos((thetarad+dthlradg))+beta))+
```

```
gl1*exp(1i*(k*d*cos((thetarad+dthlradg))+beta))+g0+ gr1*exp(-
1i*(k*d*cos((thetarad-dthrradg))-beta)) +gr2*exp(-
1i*(k*2*d*cos((thetarad-dthrradg))-beta)) +gr3*exp(-
1i*(k*3*d*cos((thetarad-dthrradg))-beta)) +gr4*exp(-
1i*(k*4*d*cos((thetarad-dthrradg))-beta));


AF=AFA+AFB+AFC+AFd+AFe+AFf+AFg;



x=68;

al4=A(1,1,x); al3=A(1,2,x); al2=A(1,3,x); al1=A(1,4,x); a0=A(1,5,x);
ar1=A(1,6,x); ar2=A(1,7,x); ar3=A(1,8,x); ar4=A(1,9,x);
bl4=A(2,1,x); bl3=A(2,2,x); bl2=A(2,3,x); bl1=A(2,4,x); b0=A(2,5,x);
br1=A(2,6,x); br2=A(2,7,x); br3=A(2,8,x); br4=A(2,9,x);
cl4=A(3,1,x); cl3=A(3,2,x); cl2=A(3,3,x); cl1=A(3,4,x); c0=A(3,5,x);
cr1=A(3,6,x); cr2=A(3,7,x); cr3=A(3,8,x); cr4=A(3,9,x);
dl4=A(4,1,x); dl3=A(4,2,x); dl2=A(4,3,x); dl1=A(4,4,x); d0=A(4,5,x);
dr1=A(4,6,x); dr2=A(4,7,x); dr3=A(4,8,x); dr4=A(4,9,x);
el4=A(5,1,x); el3=A(5,2,x); el2=A(5,3,x); el1=A(5,4,x); e0=A(5,5,x);
er1=A(5,6,x); er2=A(5,7,x); er3=A(5,8,x); er4=A(5,9,x);
fl4=A(6,1,x); fl3=A(6,2,x); fl2=A(6,3,x); fl1=A(6,4,x); f0=A(6,5,x);
fr1=A(6,6,x); fr2=A(6,7,x); fr3=A(6,8,x); fr4=A(6,9,x);
gl4=A(7,1,x); gl3=A(7,2,x); gl2=A(7,3,x); gl1=A(7,4,x); g0=A(7,5,x);
gr1=A(7,6,x); gr2=A(7,7,x); gr3=A(7,8,x); gr4=A(7,9,x);


AFA=al4*exp(1i*(k*4*d*cos((thetarad+dthlrada))+beta))
+al3*exp(1i*(k*3*d*cos((thetarad+dthlrada))+beta))+
al2*exp(1i*(k*2*d*cos((thetarad+dthlrada))+beta))+
al1*exp(1i*(k*d*cos((thetarad+dthlrada))+beta))+a0+ ar1*exp(-
1i*(k*d*cos((thetarad-dthrrada))-beta)) +ar2*exp(-
1i*(k*2*d*cos((thetarad-dthrrada))-beta)) +ar3*exp(-
1i*(k*3*d*cos((thetarad-dthrrada))-beta)) +ar4*exp(-
1i*(k*4*d*cos((thetarad-dthrrada))-beta));
AFB=bl4*exp(1i*(k*4*d*cos((thetarad+dthlradb))+beta))
+bl3*exp(1i*(k*3*d*cos((thetarad+dthlradb))+beta))+
bl2*exp(1i*(k*2*d*cos((thetarad+dthlradb))+beta))+
bl1*exp(1i*(k*d*cos((thetarad+dthlradb))+beta))+b0+ br1*exp(-
1i*(k*d*cos((thetarad-dthrradb))-beta)) +br2*exp(-
1i*(k*2*d*cos((thetarad-dthrradb))-beta)) +br3*exp(-
1i*(k*3*d*cos((thetarad-dthrradb))-beta)) +br4*exp(-
1i*(k*4*d*cos((thetarad-dthrradb))-beta));
AFC=cl4*exp(1i*(k*4*d*cos((thetarad+dthlradc))+beta))
+cl3*exp(1i*(k*3*d*cos((thetarad+dthlradc))+beta))+
cl2*exp(1i*(k*2*d*cos((thetarad+dthlradc))+beta))+
cl1*exp(1i*(k*d*cos((thetarad+dthlradc))+beta))+c0+ cr1*exp(-
1i*(k*d*cos((thetarad-dthrradc))-beta)) +cr2*exp(-
1i*(k*2*d*cos((thetarad-dthrradc))-beta)) +cr3*exp(-
1i*(k*3*d*cos((thetarad-dthrradc))-beta)) +cr4*exp(-
1i*(k*4*d*cos((thetarad-dthrradc))-beta));
AFd=dl4*exp(1i*(k*4*d*cos((thetarad+dthlradd))+beta))
+dl3*exp(1i*(k*3*d*cos((thetarad+dthlradd))+beta))+
dl2*exp(1i*(k*2*d*cos((thetarad+dthlradd))+beta))+
dl1*exp(1i*(k*d*cos((thetarad+dthlradd))+beta))+d0+ dr1*exp(-
1i*(k*d*cos((thetarad-dthrradd))-beta)) +dr2*exp(-
1i*(k*2*d*cos((thetarad-dthrradd))-beta)) +dr3*exp(-
1i*(k*3*d*cos((thetarad-dthrradd))-beta)) +dr4*exp(-
1i*(k*4*d*cos((thetarad-dthrradd))-beta));
```

F

```
AFe=el4*exp(1i*(k*4*d*cos((thetarad+dthlrade))+beta))
+el3*exp(1i*(k*3*d*cos((thetarad+dthlrade))+beta))+
el2*exp(1i*(k*2*d*cos((thetarad+dthlrade))+beta))+
el1*exp(1i*(k*d*cos((thetarad+dthlrade))+beta))+e0+ er1*exp(-
1i*(k*d*cos((thetarad-dthrrade))-beta)) +er2*exp(-
1i*(k*2*d*cos((thetarad-dthrrade))-beta)) +er3*exp(-
1i*(k*3*d*cos((thetarad-dthrrade))-beta)) +er4*exp(-
1i*(k*4*d*cos((thetarad-dthrrade))-beta));
AFf=fl4*exp(1i*(k*4*d*cos((thetarad+dthlradf))+beta))
+fl3*exp(1i*(k*3*d*cos((thetarad+dthlradf))+beta))+
fl2*exp(1i*(k*2*d*cos((thetarad+dthlradf))+beta))+
fl1*exp(1i*(k*d*cos((thetarad+dthlradf))+beta))+f0+ fr1*exp(-
1i*(k*d*cos((thetarad-dthrradf))-beta)) +fr2*exp(-
1i*(k*2*d*cos((thetarad-dthrradf))-beta)) +fr3*exp(-
1i*(k*3*d*cos((thetarad-dthrradf))-beta)) +fr4*exp(-
1i*(k*4*d*cos((thetarad-dthrradf))-beta));
AFg=gl4*exp(1i*(k*4*d*cos((thetarad+dthlradg))+beta))
+gl3*exp(1i*(k*3*d*cos((thetarad+dthlradg))+beta))+
gl2*exp(1i*(k*2*d*cos((thetarad+dthlradg))+beta))+
gl1*exp(1i*(k*d*cos((thetarad+dthlradg))+beta))+g0+ gr1*exp(-
1i*(k*d*cos((thetarad-dthrradg))-beta)) +gr2*exp(-
1i*(k*2*d*cos((thetarad-dthrradg))-beta)) +gr3*exp(-
1i*(k*3*d*cos((thetarad-dthrradg))-beta)) +gr4*exp(-
1i*(k*4*d*cos((thetarad-dthrradg))-beta));


AF1=AFA+AFB+AFC+AFd+AFe+AFf+AFg;



%AFnromalized=abs(AF)/(max(abs(AF)));
AFnromalized=abs((AF)/1);
%AFnromalizeddB=10*log10(AFnromalized.^2);
%AFnromalizeddB=AFnromalized.^2);
AFnromalizeddB=AFnromalized
% subplot(1,1,1);
% polar(thetarad,abs(AFnromalizeddB));



AFnromalized=abs((AF1)/1);
%AFnromalizeddB=10*log10(AFnromalized.^2);
%AFnromalizeddB=AFnromalized.^2);
AFnromalizeddB=AFnromalized
% hold on
% subplot(1,1,1);
% polar(thetarad,abs(AFnromalizeddB));
%polarpattern(thetadeg,AFnromalizeddB)



x=48:2:68;
y=abs(AF(x))
y2=abs(AF1(x))
subplot(2,1,1)
plot(y)
hold on
plot(y2)
y3=y-y2
subplot(2,1,2)
plot(y3)
```

# الملخص

في الآونة الأخيرة ، حظيت أنظمة تتبع المصدر الصوتي باهتمام واسع. وقد تم استخدام هذه الأنظمة في جميع التطبيقات التي يمكن أن تستفيد من الإشارة الصوتية لتحقيق التتبع ، مما يجعلها من أهم القضايا في مجال معالجة الإشارات والاتصالات. تعتمد أنظمة الاتصالات مؤخرًا على المسح الإلكتروني للفص المشع ، ويمكن القيام بذلك عن طريق نظام تشكيل حزمة مصفوفة من الميكروفونات.

في هذه الدراسة ، تم تصميم تقنية تتبع التبديل الفصي لتحقيق نظام تتبع صوتي. حيث يحتاج هذا النظام إلى نظام مسح شعاع إلكترونيا يعتمد على مصفوفة الميكروفونات ، وقد تم اقتراح توزيع معماري بتصميم نظام مسح اليكتروني لمصفوفة الميكروفونات باستخدام 57 ميكروفون موزعة بمسافات متساوية(سبع مجموعات من عناصر المصفوفة الخطية).

تم استخدام اسلوب تغذية الاتساع وبالاعتماد على تقنية التوزيع ذي الحدين لتحقيق نظام مسح الكتروني للفص الإشعاعي الذي لا يحتوي على الفصوص الجانبية, وقد حقق نظام المسح الشعاعي المقترح نطاق مسح يتراوح بين 30 إلى 150 درجة بفاصل درجتين وبواقع زاوية مسح بحدود 20 درجة في كل حالة.

لقد كان نظام المسح الشعاعي المقترح هذا جزءًا أساسيًا في تنفيذ نظام التتبع الصوتي باستخدام برنامج MATLAB الإصدار 2019.

حقق نظام التتبع الصوتي المقترح تتبعًا ، مع نسبة انحراف عن مركز منطقة المسح في حدود 0 إلى 5% ،وقد ظهر هذا الخطأ بسبب عدم وجود تناظر في شطري كل فص من فصوص المسح نتيجة استخدام تقنية إثارة السعة في تنفيذ نظام المسح الشعاعي.

وزارة التعليم العالي والبحث العلمي

جامعة نينوى

كلية هندسة الالكترونيات

قسم هندسة الاتصالات

# نظام تتبع صوتي يعتمد على تقنية مصفوفة الميكروفونات

رسالة تقدم بها

## عباس حيدر سليمان

إلى

مجلس كلية هندسة الالكترونيات

جامعة نينوى

كجزء من متطلبات نيل شهادة الماجستير

في

هندسة الاتصالات

بإشراف

## أ.م.د. محمود احمد محمود

1443 هـ

2022 م

# نظام تتبع صوتي يعتمد على تقنية مصفوفة الميكروفونات

## عباس حيدر سليمان

## رسالة ماجستير علوم في هندسة الاتصالات

## بإشراف

## أ.م.د محمود احمد محمود

1443 هـ          2022 م